

INCLUSION EVALUATION FOR CALCIUM TREATED STEEL IN INDUSTRY

MASc Thesis – L. Valladares; McMaster University – Materials Engineering

INCLUSION EVALUATION FOR CALCIUM TREATED STEEL AND ITS RELATION
TO CASTER BEHAVIOUR IN INDUSTRY

By LEWYN VALLADARES, B. Eng. – Materials

A Thesis Submitted to the School of Graduate Studies in Partial Fulfilment of the
Requirements for the Degree Master of Applied Science – Material Engineering

McMaster University © Copyright by Lewyn Valladares 2022

MASc Thesis – L. Valladares; McMaster University – Materials Engineering

McMaster University MASTER OF APPLIED SCIENCE IN ENGINEERING (2022)
Hamilton, Ontario (Materials)

TITLE: Inclusion Evaluation for Calcium Treated Steel and its Relation to Caster Behavior in Industry. AUTHOR: Lewyn Valladares, B. Eng. - Materials (McMaster University)
SUPERVISOR: Professor N. Dogan NUMBER OF PAGES: xiii, 134

Abstract

Undesirable solid oxides and sulphides, known as inclusions, are an inherent product of the steelmaking process that can clog the steel flow during casting. Caster operators can break up the clogged material to improve flow, but this reduces steel quality and yield. Modifying these inclusions using calcium treatment and its effects on industrial processing conditions are the focus of this study. To effectively improve calcium treatment, experimental and industrial data are required to develop models to predict inclusion behaviour. The advantage of experimental testing is that the precise control of chemistry, temperature, alloying elements, and sampling can help identify the effects of each variable. The difficulty, however, is correlating experimental results to real-time industrial processing, where these variables are difficult to control individually. In industry, indirect observations of caster behaviour may give an idea of the effectiveness of the treatment, but this is after the fact. In this study, liquid steel samples were taken at different processing steps without any modification to the process itself to ensure normal shop conditions. The inclusion analysis was conducted using an automated Scanning Electron Microscope (SEM) and AZtech feature analysis software to determine inclusion characteristics, including population, composition, and size. This study shows 8 sequential calcium-treated steel heats in an industrial setting and their associated clogging behaviour during a cast. The study indicated that a few heats with undermodified alumina inclusions immediately or subsequently affected the casting process leading to a severe clogging event.

Acknowledgements

Firstly, I would like to thank Stelco for the opportunity to pursue this thesis and expand my capabilities as a process researcher. I would like to thank my supervisors Dr. Neslihan Dogan and Chad Cathcart for their support and continuous guidance and knowledge. To Peter Badgley for providing me with the opportunity and encouraging me to pursue a higher education. To the steelmaking and caster operation managers and operators that provided me with process guidance and sampling. Their knowledge helped me connect and appreciate the differences between experimental research and industrial application.

Furthermore, I would like to especially thank Irina Melyashkevich at Stelco's Hamilton Lab for testing the samples and helping prepare and test the samples for analysis. Her fundamental knowledge of the SEM made for quicker troubleshooting and turnaround time. I appreciate her taking the time to teach me about the SEM and developing my abilities to use it.

Finally, I would like to thank my partner Lindsay for her continuous support and encouragement. Her guidance on grammatical and sentence structure helped me communicate my thoughts clearly through this thesis.

Table of Contents

Abstract	iii
Acknowledgements	iv
List of Figures	vii
List of Tables.....	xi
List of Abbreviations.....	xii
Declaration of Academic Achievement	xiii
1. Introduction	1
2. Literature Review.....	4
2.1 Steelmaking Process	4
2.1.1 BOF Steelmaking.....	5
2.1.2 Tapping Practices.....	8
2.1.3 BOF Slag Chemistry Control.....	9
2.1.4 Furnace Slag Carryover Control	10
2.1.5 Ruhrstahl Heraeus Oxygen Blow (RHOB) – Vacuum Degasser (VD)	12
2.1.6 Ladle Treatment Station (LTS) – Argon Stirrer (AS).....	14
2.2 Clean Steel Practices.....	15
2.2.1 Macro and Micro Inclusions	17
2.2.2 Inclusion Formation in Process.....	18
2.2.3 Influence of Slag Chemistry on Alumina Formation and Control.....	19
2.2.4 Thermodynamics of Alumina Inclusion Formation.....	24
2.2.5 Alumina Inclusion Morphology and Aggregation	30
2.3 Inclusion Assessment Techniques	32
2.3.2 Direct Inclusion Assessment.....	32
2.3.3 Indirect Inclusion Assessment	33
2.3.4 Caster Clogging Behaviour.....	37
2.4 Inclusion Removal Techniques/Methods	39
2.4.3 Inclusion Modification Process – Calcium Treatment	42
2.4.4 Fundamentals of Calcium Aluminate Inclusions	43
2.4.5 Fundamentals of Calcium Sulphide Inclusions.....	49
2.4.6 Application of Fundamentals in Industry – Modified Ca/Al Ratio	53
3. Gap Of Knowledge	57

4.	Project Methodology	58
4.1	Steel Chemistry Determination.....	59
4.2	Scanning Electron Microscope (SEM)	60
4.2.1	SEM System.....	60
4.2.2	Computer Controlled Scanning Electron Microscopy	63
4.3	Sample Analysis	64
4.3.1	Sample Collection	64
4.3.2	Sample Preparation Procedure for SEM Analysis	66
4.3.3	SEM Parameters/Procedure for Inclusion Analysis.....	68
4.4	Caster Behaviour Quantification	70
4.5	Ternary Diagram Quantification.....	70
5.	Results and Discussion.....	75
5.1	Determination of SEM Parameters.....	75
5.1.1	Effects of Accelerating Voltage on Inclusion Characteristics	75
5.1.2	Effects of Analysis Area on Inclusion Characteristics.....	77
5.2	Results from 8 Sequentially Casted Heats.....	79
5.2.1	Processing Parameters.....	80
5.2.2	Inclusion Population	82
5.2.3	Inclusion Population by Characteristic Type	84
5.2.4	Inclusion Area Fraction by Characteristic Type	86
5.2.5	Inclusion Density by Characteristic Type	88
5.2.6	Inclusions Size (ECD) – Equivalent Circular Diameter	90
5.2.7	Slag Sample Analysis.....	93
5.2.8	Modified Ca/Al Ratio Results.....	94
5.2.9	Correlating Population, Area Fraction, and Density to Clogging behaviour.....	97
6.	Summary and Conclusions.....	102
7.	Future Work	104
A.	Inclusion Type Population.....	106
B.	Inclusion Phase Area Fraction.....	110
C.	Inclusion Phase Density	114
D.	Inclusion Size (ECD) – Equivalent Circular Diameter	118
E.	Tundish 20 m Population, Density and Area Fraction v Rod Position	120
	References	123

List of Figures

Figure 2-1. Basic Oxygen Furnace process and inputs (Zeynep Yildirim & Prezzi, 2011).	6
Figure 2-2. Ellingham diagram showing the Gibbs free energy of formation of various elements in the steelmaking process (Gaskell, 2008).....	7
Figure 2-3. BOF tapping process showing the effectiveness of a vessel dam to help increase the steel height during tap. Left image is with a dam, right is without.	11
Figure 2-4. RH Degasser Process (Baochen et al., 2018)	13
Figure 2-5. Effect of slag FeO+MnO on total steel oxygen (Hille et al., 1991).	20
Figure 2-6. Effect of Slag FeO+MnO on Al fade (Ahlborg et al., 1993).....	21
Figure 2-7. Effect of FeO+MnO on the total oxygen in a tundish experiment (L. Zhang & Cai, 2001).	22
Figure 2-8. First and second order activity interaction coefficients (Hiroyasu et al., 1997; Yang, Duan, et al., 2013).....	25
Figure 2-9. The effect of interfacial tension on Al ₂ O ₃ nucleation (Yang, Duan, et al., 2013).....	27
Figure 2-10. Change in iron/alumina interfacial tension as a function of the alumina radius (Yang, Duan, et al., 2013).	29
Figure 2-11. Effect of nucleus radius on the nucleation of Al ₂ O ₃ (Yang, Duan, et al., 2013).....	29
Figure 2-12. Various observed morphologies of singular alumina particles after 1 min holding time. a) Spherical, b) Dendritic, c) Flower, d) Plate-like, e) Irregular (Faceted)(Yang, Duan, et al., 2013).	31
Figure 2-13. Inclusion growth mechanisms as a function of element supersaturation (Dekkers et al., 2002).	32
Figure 2-14. Empirical relations between oxygen EMF and celox® voltage (Turner, 2016).	34
Figure 2-15. OES-PDA techniques for determining inclusion population (Cathcart, 2018).	37
Figure 2-16. Various degrees of clogging in industry (Cathcart, 2018).....	38
Figure 2-17. Images taken from a CLSM. Shows agglomeration of three sets of alumina particles. a) t=0.0 s, b) t=1.0 s, c) t=2.0 s, d) t=3.0 s, e) t=4.0 s, f) t=5.0 s(Kang et al., 2011).....	40
Figure 2-18. CLSM experiment showing Spinel maintaining distance over time. b) t= 1.0 s, e) t=4.0 s(Kang et al., 2011)	41

Figure 2-19. Solid fraction of Slag A and B at 1530 C (1833K). a) Series of A slags, b) Series of B slags (da Rocha et al., 2017).....	42
Figure 2-20. Calcium aluminate inclusions composition after Ca treatment at 1600°C (Park et al., 2005).....	47
Figure 2-21. CaO- Al ₂ O ₃ phase diagram. Circled is the ideal zone for CA treatment to produce liquid inclusions at steelmaking temperatures (Abraham et al., 2013; Ahlborg et al., 2003).....	48
Figure 2-22. CA inclusions with varying ratios and liquidus temperatures (Park et al., 2005).....	49
Figure 2-23. Formation of CaS inclusions based on S levels (Story & Asfahani, 2013)...	51
Figure 2-24. Area fraction of CaS compared to quality and caster processing issues (Story & Asfahani, 2013).	53
Figure 2-25. Predicted vs the actual effects of S on the Ca/Al ratio for oxide inclusions (Story & Asfahani, 2013).	55
Figure 4-1. Project Methodology Steps.....	59
Figure 4-2. Schematic drawing of a typical SEM (Walock, 2012).	61
Figure 4-3. Sample location and nomenclature.	65
Figure 4-4. Lollipop sample dimensions	66
Figure 4-5. Polished and prepared sample. Including aluminum and copper tape for contrast and conductivity respectively.	67
Figure 4-6. Ca-Al-S ternary diagram illustrating liquid oxide boundary layers, CaS window and ideal zones for calcium aluminate inclusions (Kumar et al., 2019).....	71
Figure 4-7. Inclusion area fraction percentage for heat #1.....	74
Figure 4-8. Ca-S-Al ternary diagram for Heat#1 – After Ca sample. Circled area shows significant portion undermodified alumina inclusions.....	74
Figure 5-1. Inclusion count distribution for two samples. Circled are data points with significant discrepancies (Melyashkevich, 2021).	79
Figure 5-2. Inclusion population of production samples from all heats.....	83
Figure 5-3. Inclusion density% of production samples from all heats	84
Figure 5-4. Heat 1 inclusion phase population for all samples based on ternary quantification.....	86
Figure 5-5. Fraction of the number of each inclusion type for all samples in Heat 1	88
Figure 5-6. Area fraction of each inclusion type for all samples in Heat 1.....	88
Figure 5-7. The density of various inclusion types detected in Tundish 10m samples for all heats.....	90
Figure 5-8. Heat 1 ECD transformations for all samples. Showing a slow drop in inclusion size.....	92

Figure 5-9. Heat 2 ECD transformations for all samples. Shows a sharp drop in inclusion size at the Tundish 10m.....	92
Figure 5-10. Heat 3 ECD transformations for all samples. Shows an increase in small inclusions at the Tundish 10 and 20m.....	92
Figure 5-11. Heat 7 ECD transformations for all samples. Similar to Heat 2, it shows sharp drop in inclusions size at the Tundish 10m.....	93
Figure 5-12. Ladle slag FeO+MnO wt% transformation before and after Ca treatment. ..	94
Figure 5-13. Modified Ca/Al ratio for all heats after calcium treatment. Red dashed lines represent CxAx ratios.....	95
Figure 5-14. Relationship between Ca/Al ratio and the pre-Ca treatment S wt% for all heats.....	96
Figure 5-15. Tundish 10m inclusion phase population vs caster rod position for all heats.....	99
Figure 5-16. Tundish 10m inclusion phase density vs caster rod position for all heats...	100
Figure 5-17. Tundish 10m inclusion phase area fraction vs caster rod position for all heats.....	100
Figure A-1. Heat 2 inclusion phase population for all samples based on ternary quantification.....	106
Figure A-2. Heat 3 inclusion phase population for all samples based on ternary quantification.....	106
Figure A-3. Heat 4 inclusion phase population for all samples based on ternary quantification.....	107
Figure A-4. Heat 5 inclusion phase population for all samples based on ternary quantification.....	107
Figure A-5. Heat 6 inclusion phase population for all samples based on ternary quantification.....	108
Figure A-6. Heat 7 inclusion phase population for all samples based on ternary quantification.....	108
Figure A-7. Heat 8 inclusion phase population for all samples based on ternary quantification.....	109
Figure B-1. Area fraction of each inclusion type for all samples in Heat 2.....	110
Figure B-2. Area fraction of each inclusion type for all samples in Heat 3.....	110
Figure B-3. Area fraction of each inclusion type for all samples in Heat 4.....	111
Figure B-4. Area fraction of each inclusion type for all samples in Heat 5.....	111
Figure B-5. Area fraction of each inclusion type for all samples in Heat 6.....	112
Figure B-6. Area fraction of each inclusion type for all samples in Heat 7.....	112
Figure B-7. Area fraction of each inclusion type for all samples in Heat 8.....	113
Figure C-1. Density of each inclusion type for all sample in Heat 1.....	114

Figure C-2. Density of each inclusion type for all sample in Heat 2.	114
Figure C-3. Density of each inclusion type for all sample in Heat 3.	115
Figure C-4. Density of each inclusion type for all sample in Heat 4.	115
Figure C-5. Density of each inclusion type for all sample in Heat 5.	116
Figure C-6. Density of each inclusion type for all sample in Heat 6.	116
Figure C-7. Density of each inclusion type for all sample in Heat 7.	117
Figure C-8. Density of each inclusion type for all sample in Heat 8.	117
Figure D-1. Change in inclusion diameter for all samples for Heat 4.....	118
Figure D-2. Change in inclusion diameter for all samples for Heat 5.....	118
Figure D-3. Change in inclusion diameter for all samples for Heat 6.....	119
Figure D-4. Change in inclusion diameter for all samples for Heat 8.....	119
Figure E-1. Inclusion count v caster rod position for Tundish 20 m.....	120
Figure E-2. Inclusion density v caster rod position for Tundish 20 m.	121
Figure E-3. Inclusion area fraction v caster rod position for Tundish 20 m.	122

List of Tables

Table 2-1. Critical inclusion size guidelines for everyday products (Cathcart, 2018; L. Zhang, 2002).	18
Table 4-1. Grade chemistry aim (wt.%).	60
Table 5-1. The comparison of inclusion type and count with respect to KeV setting.	77
Table 5-2. Processing parameters for 8 heats studied	80

List of Abbreviations

AS	Argon Stirrer
ASCAT	Automated Steel Cleanliness Assessment Tool
BOF	Basic Oxygen Furnace
BOP	Basic Oxygen Process
BSE	Backscatter Electrons
CCEM	Computer Controlled Electron Microscopy
CLSM	Confocal Laser Scanning Microscopy
EAF	Electric Arc Furnace
ECD	Equivalent Circular Diameter
EDS	Energy Dispersive Spectroscopy
LECO	Laboratory Equipment Corporation TM
LTS	Ladle Trim Station (AS)
NMI	Non-Metallic Inclusion
OD	Outside Diameter
OES	Optical Emission Spectroscopy
PPM	Parts Per Million
RHOB	Ruhrstahl Heraeus Oxygen Blow (VD)
SE	Secondary Electrons
SEM	Scanning Electron Microscope
SEN	Submerged Entry Nozzle
TO	Total Oxygen
VD	Vacuum Degasser

Declaration of Academic Achievement

The author, Lewyn Valladares, is the author and main contributor of the written work included in this thesis with consultation from advisor Dr. Neslihan Dogan. There is no part of this work that has been published or submitted for publication or for a higher degree at another institution.

Research test work was completed by employees at Stelco's Lake Erie Works and Hamilton labs under guidance of Irina Melyashkevich.

1. Introduction

Steel is used in almost every facet of daily life for humans, from coffee makers to cooking utensils to vehicles used to travel and has been a critical aspect in the modernization and development of the world's cities, infrastructure, technology, and health care, and safety. It continues to be an integral part of human civilization, with a steady increase in world production at approximately 3% annually between 2015-2020 (*World Steel in Figures 2021*, 2021).

Steelmaking is one of the oldest processes in modern history. Over time science, engineering, and customer demand for improved quality control of steel have driven the need for continuous innovation. In simplest terms, steelmaking involves converting high carbon iron and scrap into steel using oxygen converters and refining stations before being cast. These steel grades are alloyed to achieve the desired mechanical properties such as formability, strength, and surface finish. An oxygen converter is primarily used to remove carbon and silicon along with undesirable elements such as phosphorus and sulphur. At the end of this process, steel is highly oxidized from the oxygen blow. This dissolved oxygen must be removed to prevent alloys from oxidizing and not meeting the chemistry specification. Oxidation of said alloys raises the production costs and time. For this purpose, adding a deoxidizing alloy such as aluminum as the steel is tapped into a ladle is the optimal method of removing dissolved oxygen. The downside of this practice is that it produces alumina (Al_2O_3). This is an impurity, or an undesirable product known as an inclusion. Alumina is one of many types of inclusions developed through the process of steelmaking. Therefore, the removal and/or modification of these inclusions will be the primary focus of this thesis.

After tapping the steel, it is then treated at a secondary steelmaking facility to further refine and finalize the steel chemistry. Other than the general alloy additions and temperature

adjustments, treatments can also involve removing or modifying inclusions. This type of treatment is known as clean steel practices or inclusion engineering.

The level of clean steel practices depends on the product quality and mechanical properties. Certain types of inclusions, such as MnS are detrimental to the formability of sheet steel while being beneficial to free machining steel (Cathcart, 2018). Inclusions can also affect the processing of the steel. For example, a buildup of solid Al_2O_3 inclusions in the submerged entry nozzle (SEN) at the caster can cause clogging by choking the amount of steel throughput per unit of time. To mitigate this, operators tend to blow oxygen up the SEN nozzle to burn/lance out the clog. The downside of this practice is that this introduction of oxygen to the liquid steel decreases the quality of the cast slabs and is therefore costly.

Calcium can be added to help modify the solid alumina inclusions into liquid or partially liquid calcium aluminates. Alumina inclusions are non-wetting in nature (Lindon & Billington, 1969). Calcium modifies the alumina into globular inclusion wetted by liquid steel (Abraham et al., 2013; Turkdogan, 1996). Therefore, the newly formed globular inclusion can pass through the SEN without adhering to the refractory walls thus preventing build up. Assuming the shape is maintained, these globular inclusions also prevent anisotropy in the final steel product. The concern with calcium treatment is understanding how much calcium is required to modify the alumina inclusions in the steel. Too little calcium causes unmodified alumina and partially modified calcium aluminates which can deposit and deter steel flow. Excessive Ca addition can cause overmodified calcium aluminate inclusions and the formation of calcium sulphides (CaS) which can cause refractory erosion (Story et al., 2003)

Inclusion assessments can be done in several ways, including analysis during steel production such as total oxygen calculations and caster clogging or postproduction analysis

such as computer-controlled electron microscopy (CCEM). Total oxygen measurement is an indirect method of understanding steel cleanliness by measuring the sum of the dissolved oxygen and the oxygen from the oxide inclusions. Dissolved oxygen in steel is relatively low (3-5ppm) and does not vary, so total oxygen can be a good quick method for operations to understand the relative levels of inclusion activity (Cathcart, 2018).

For detailed analysis, automated electron microscopy along with energy dispersive spectroscopy (EDS) can be used to understand the size, distribution, quantity, morphology, and chemistry of the inclusions. Although this is usually done after the fact, the analysis can help correlate how effective the treatment process is and optimize it for future operations.

The purpose of this study is to help understand the inclusion development in calcium-treated steel through post-processing analysis in an effort to correlate that data to the caster clogging behaviour. This study is done through a collaboration with an industrial partner and will develop recommendations for their processing techniques, inclusion modification, and further work to be conducted.

2. Literature Review

2.1 Steelmaking Process

There are two main routes to produce steel. They are namely Electric Arc Furnaces (EAF) and Basic Oxygen Furnaces (BOF). As the names suggest, an EAF primarily uses an electric arc to melt steel, while a BOF primarily uses a lance that blows oxygen at supersonic speeds into a bath of iron and scrap steel. This work will focus on the integrated steelmaking route used by the industrial partner that involves a Blast Furnace to produce liquid iron, Basic Oxygen Furnace, Secondary Steelmaking facilities such as an argon stirrer, vacuum degasser, and a caster.

In the simplest terms, BOF steelmaking involves charging hot metal cast from a blast furnace along with scrap into an additional furnace where oxygen is blown at high velocity. This oxygen achieves three main goals: melt the scrap, decarburize the bath to a set point and reach the aim steel temperature for the designated steel grade. Fluxes such as burnt lime and dolomitic lime are added to maintain “basic” slag chemistry to balance acidic slag components generated such as SiO_2 . Once the three criteria are met, the steel is ready to be tapped into a steel ladle. During the tap, alloying elements and synthetic fluxes can be added to achieve the desired steel grade chemistry and ladle slag conditions.

Post tap, the steel travels to the secondary stations for the final refining steps. This involves further decarburization, if necessary, micro-alloy additions, temperature modifications, and calcium treatment. At the industrial partner’s facility, there are two primary secondary refining stations, a degasser (RHOB) that conducts steel treatment in a vacuum and an argon stir station (LTS) that uses a top-down lance to stir the steel. Calcium treatment is performed only at the LTS in the form of Ca-Sil wire. Post-secondary treatment, the steel is transferred to the caster, where the ladle opens into a tundish that is a reservoir for steel

before being cast into molds. A brief description of each process is provided in the following sections.

2.1.1 BOF Steelmaking

The first commercial use of a top blowing oxygen lance in a furnace was conducted in the 1950s at two facilities, one in Linz and one in Donawitz, Austria. Oxygen steelmaking began being known as the Linz-Donawitz or LD process and was adopted by several countries worldwide (Schober, 2013). A schematic diagram of a typical BOF and its inputs is shown in Figure 2-1 (Zeynep Yildirim & Prezzi, 2011).

North American producers named it the BOP (Basic Oxygen Process) or BOF (Basic Oxygen Furnace). Later in the 1970s, the bottom blowing oxygen steelmaking process was developed in Canada and Germany, known as OBM or Q-BOP (Turkdogan, 1996). These facilities mounted tuyeres in the bottom of the furnaces to blow oxygen and carry fluxes. To help protect the tuyeres from damage, propane or some hydrocarbon gaseous mixture is blown around the tuyere. Once the gas contacts the hot iron, it dissociates into carbon and hydrogen. The dissociation reaction is endothermic and therefore cools the tuyere (Turkdogan, 1996). Improvements in steelmaking technology have allowed for furnaces to combine top and bottom blowing capabilities (Turkdogan, 1996).

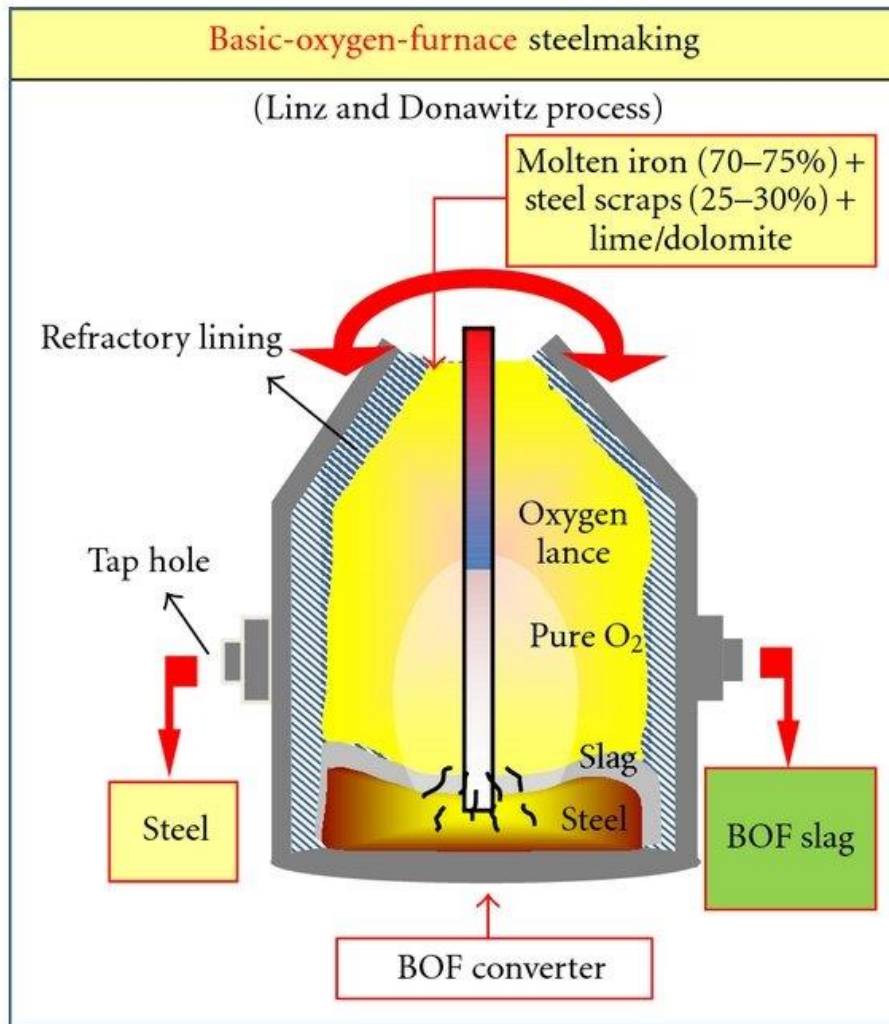


Figure 2-1. Basic Oxygen Furnace process and inputs (Zeynep Yildirim & Prezzi, 2011).

The industrial partner's BOF uses a top oxygen lance for primary decarburization and desiliconization which ultimately increases the steel temperature. After molten iron and steel scrap are charged into the furnace, the oxygen lance is lowered to certain setpoints determined by different blowing profiles, and then the pure O₂ blow begins. As the name suggests, the steel is refined in an oxidizing environment where most elements are oxidized at varying rates due to unique oxygen affinities which can be described by an Ellingham Diagram show in Figure 2-2 (Gaskell, 2008). The primary energy sources are the

exothermic reactions of oxygen with carbon and silicon, as well as the physical temperature of the incoming iron. Carbon and silicon predominantly come from hot metal, with trace amounts from steel scrap.

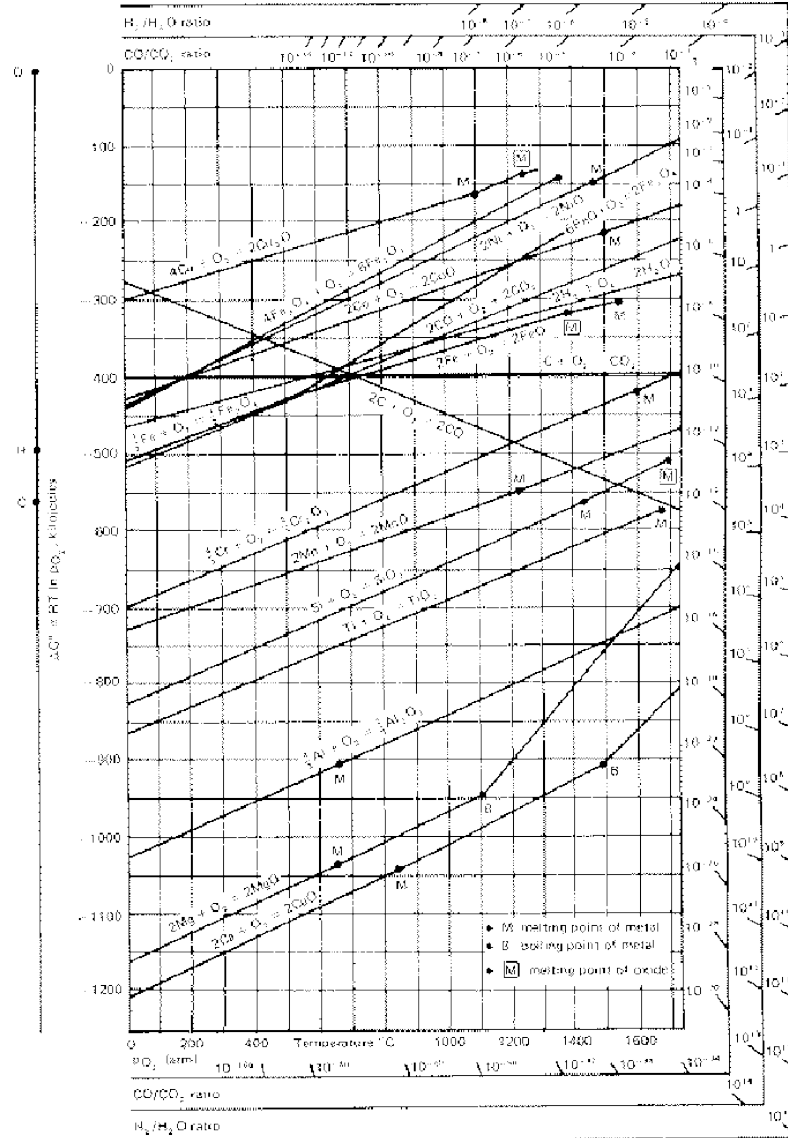


Figure 2-2. Ellingham diagram showing the Gibbs free energy of formation of various elements in the steelmaking process (Gaskell, 2008).

Along with oxygen, fluxes such as Burnt Lime (~98% CaO) and Dolomitic Lime (~60%CaO/40%MgO) are added to form a slag to absorb the oxidized elements and assist with desulphurization as well. Oxidation products such as SiO₂ are acidic in nature and need to be balanced to prevent refractory lining damage. Therefore, the bulk slag is basic to help protect the vessel's refractory, which is also basic, hence the name Basic Oxygen Furnace. This is monitored with the help of a V-Ratio (wt% CaO/wt%SiO₂), which is usually kept between 2.5 to 4.0.

Slag components such as FeO and MnO play a part in the efficiency of inclusion removal in the secondary refining of steel (Ji et al., 2018; R. Wang et al., 2017). During the tapping process, care is taken to avoid too much furnace slag from being carried over, but this is not easily controllable. Synthetic slag materials are added during the tap to help further refine and dilute slag carried over from the furnace. This fluxing also reduces air exposure and temperature loss during processing and ladle transit. These processes are briefly described in the following sections.

2.1.2 Tapping Practices

Once the BOF has reached the end of the blow, the liquid steel is prepared for tapping into a ladle. Determining the end point of the blow is done using off-gas analyzers along with temperature/oxygen probes that are dropped into the bath, or, in some cases, a physical steel sample taken from the furnace directly. Using the steel grade card aims as a guide and the calculated temperature from the bombs, the vessel operator decides when to start tapping the heat. At this point, the steel would have between 600-800 ppm of dissolved oxygen along with oxides residing in the slag (C. Bell et al., personal communication, 2021).

During the tap, the bulk of the alloys required for the steel chemistry are added. Since most alloy additions would be oxidized by the dissolved oxygen, a deoxidizer needs to be added prior to the additions to increase the recovery of the desired alloying elements. Deoxidizers such as Mn and Si can be added and effectively reduce the oxygen content to ~50 ppm (Turkdogan, 1996). However, aluminum is the primary deoxidizer for most steel grades produced by the industrial partner. Aluminum effectively brings the dissolved oxygen down to under 5 ppm (Turkdogan, 1996).

The BOF/tapping process is the earliest point for forming alumina (and other) inclusions. Therefore, it's vital to ensure that the desired temperature and chemistry levels are met as this avoids reintroducing of aluminum and oxygen later in the process through reheating, cooling or deoxidation.

Along with alloys, ladle fluxes are added to the steel bath to help desulphurization, temperature control, and dilution of the vessel slag carried over during the tapping process.

2.1.3 BOF Slag Chemistry Control

BOF Slag is highly oxidized with oxides such as FeO and MnO, which affect the inclusion removal capability explained later in [Chapter 2.2.3](#) (Ji et al., 2018; R. Wang et al., 2017). These oxides are inherent products of the oxygen blowing process. MnO is influenced by the amount of Mn added into the furnace in the form of molten iron and steel scrap blend. Manganese is oxidized to roughly 0.15 wt% in the steel before reaching equilibrium at the industrial partner's BOF.

Precise control of FeO content in the slag is complex, but there are methods to avoid creating too much or too little FeO. Assuming a set carbon aim, industrial aims for slag FeO depend on the processing methods (top vs. bottom blowing) and the efficiencies of

each plant. A thermodynamic model is used to estimate the required oxygen needed to “blow” the heat and achieve the aim carbon and aim temperature based on the inputs. These values are a guideline, and lower or higher values do not necessarily mean that the heat is over or under blown. Under blown heats have lower FeO%, while over-blown heats have higher FeO%. Variables that affect the blowing practice of the heat include, but are not limited to, incorrect iron or scrap chemistry, input weights, total flux addition, iron ore addition and final temperatures (C. Bell et al., personal communication, 2021). Details regarding the effects of FeO and MnO on inclusion development and control will be discussed later

2.1.4 Furnace Slag Carryover Control

As mentioned in the previous chapter, furnace slag is a source of FeO and MnO which can be detrimental to inclusion control later in the process. Therefore, it is important to avoid too much vessel slag being carried over into the steel ladle. There are a few key factors that affect the operators control of slag carryover i.e., tap hole diameter, vessel tilt speed, vessel refractory profile and a vessel dam (C. Bell et al., personal communication, 2021). Slag, being less dense than steel, naturally floats on top of the steel if the bath is not significantly disturbed. As the vessel is tilted to begin tapping, it is necessary to maintain a good height of the steel layer over the tap hole. As the steel flows through the tap hole, it naturally creates a vortex on the top layer of steel, similar to most liquids tapped from the bottom of a container. As the height of the steel layer over the tap hole increases, the size of the vortex decreases. If this vortex is large enough, it will begin to entrain the slag from the surface layer through the tap hole and into the ladle below. Figure 2-3 depicts a cross section of the BOF during tap. Certain aspects such as the “slag level”, “vortexing”, “vessel dam” mentioned in this section are exaggerated in the image to improve the visuals.

Tap hole diameter is affected by the total minutes of use on it. The diameter wears out over time and therefore increases the flow rate of the steel which effectively increases the chances for vortexing slag.

Vessel tilt speed is important in slag carryover towards the end of the tap. Once the steel is fully tapped, slag will start pouring into the ladle, and it is important for operators to quickly tilt the vessel and stop the tap. A vessel dam is a layer of spray refractory created near the lip of the vessel on the tap side. This layer is created to help hold more steel above the tap hole while tapping the heat. It acts as a barrier to prevent steel coming out the mouth of the vessel as its tilted down. This effect is shown in Figure 2-3. The left image shows the ability to create a large steel height reducing the ability to vortex slag. The image on the right shows the opposite effect where a dam is not present. A combination of these components helps improve control of the slag carryover into the ladle and therefore its important that they are maintained for consistency (C. Bell et al., personal communication, 2021).

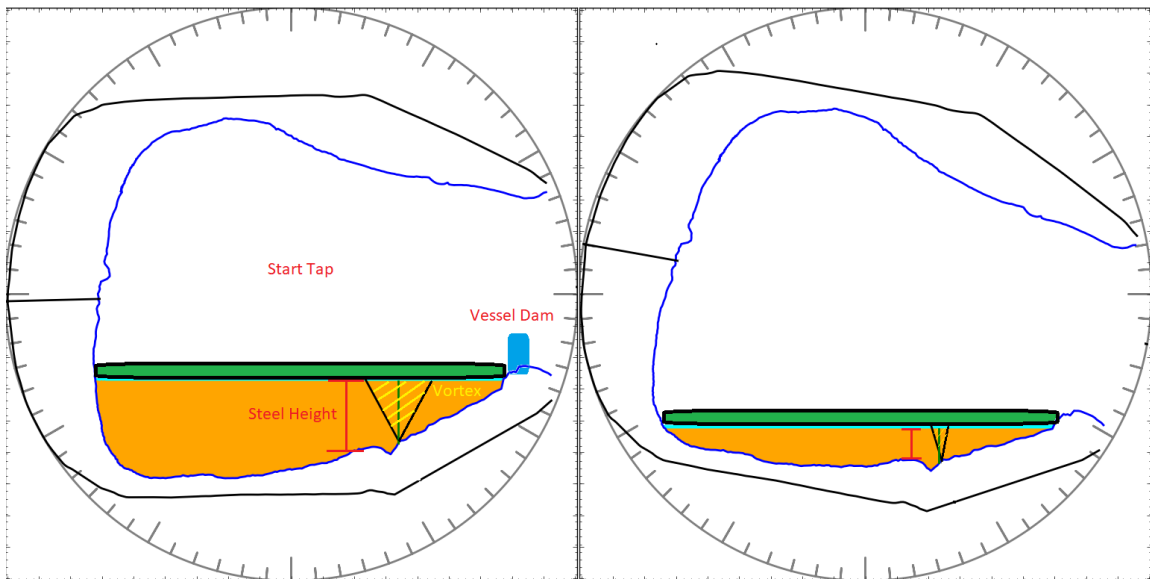


Figure 2-3. BOF tapping process showing the effectiveness of a vessel dam to help increase the steel height during tap. Left image is with a dam, right is without.

2.1.5 Ruhrstahl Heraeus Oxygen Blow (RHOB) – Vacuum Degasser (VD)

A degasser is used as a secondary treatment facility to refine steel to meet the required specifications. An RHOB degasser has two snorkels that are dipped into the steel ladle. The snorkels have argon tuyeres to aid steel moving from one snorkel into the chamber, then out the second snorkel as seen in Figure 2-4 (Baochen et al., 2018). The main vessel is evacuated to low atmospheric pressure of 1 to 60 torr, allowing the steel to be treated in a vacuum environment. This environment is crucial for decarburization to produce ultra-low carbon grades (<0.003 wt% C) where the aim carbon is not achievable only through blowing oxygen at the BOF. Alloys can also be directly added to the steel, preventing possible oxidation from the atmosphere (minimum) and the slag.

Degassers also allow for negligible slag-steel interaction during the processing of the steel. As the snorkel enters the steel in the ladle, a small amount of the slag enters the chamber, but the majority of the slag is left outside the snorkels floating on top of the ladle. Care is taken to avoid slag entering the vessel due to the potential damage caused by oxidized elements entering an evacuated environment.

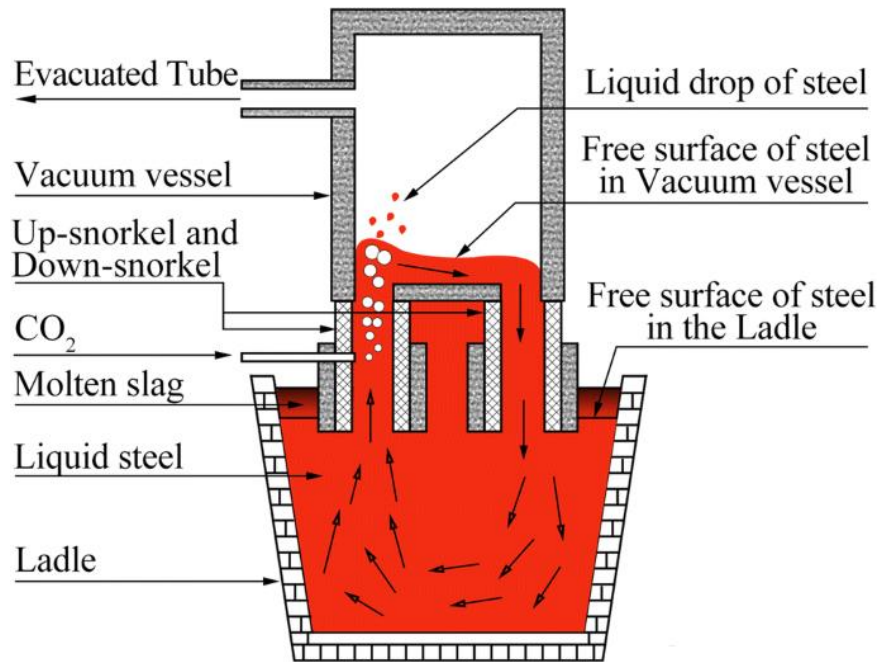


Figure 2-4. RH Degasser Process (Baochen et al., 2018)

The RHOB circulation rate makes an ideal way to remove/float inclusions into the slag (X. Wang et al., 2012; Zheng & Zhu, 2016). Zheng et al. (Zheng & Zhu, 2016) studied the effects of the circulation rate on the removal of inclusions. Using a 1:7 scale model of a 145-ton RH degasser, their work showed that a low circulation rate promoted inclusion removal primarily through Stokes floatation. Stokes floatation is the natural ability for a sphere to float in a given liquid medium which in-production may be time consuming and ineffective. Similar work conducted by Wang et al. on the impact on steel cleanliness showed that degassing, at the RH, resulted in a 40% decrease in the number of inclusions (X. Wang et al., 2012). According to Zheng et al. (Zheng & Zhu, 2016), to help improve the effectiveness of Stokes floatation, an increase in flow rate created more chance for collisions and therefore aggregation to form larger particles which are easier to float out.

At the industrial partner's facility, the RHOB, other than microalloying, is also used for cooling, reheating, and desulphurization practices. Temperature control is an important

facet for maintaining consistent production rates. At this facility cooling is done through use of chill scrap which are small pieces of clean scrap. Approximately 1000 kg will cool 10 degrees Celsius. To reheat chemically, solid aluminum cones/pieces are added along with gaseous oxygen to force an exothermic reaction producing heat shown in (2-1). Aluminum is also used to reduce the oxygen level in the steel or as an alloy to meet the aim specifications.



Although the RHOB is an efficient stirrer for inclusion removal, its use is limited due to the added production time and cost compared to the Argon stirrer. The degasser accounts for 30-35% of total yearly production due to this. This is an important aspect in the realities of steel processing in industry.

2.1.6 Ladle Treatment Station (LTS) – Argon Stirrer (AS)

The ladle treatment station is an argon stirring station for macro and micro alloy additions and calcium treatment. The station uses a top lance to inject argon into the ladle to initiate stirring. It is important to note that in contrast to the vacuum degasser, slag and steel interaction during stirring are more prevalent at this station. This treatment method can have a negative impact on inclusion behaviour through reoxidation. Karoly et al, denoted significant reoxidation through top lance stirring compared to porous plugs (Karoly et al., 2012) while Kaushik et al. showed extensive pickup of Ca from the slag resulting in unwanted CaS inclusions (Kaushik & Yin, 2012).

The key aspect of the LTS is the ability to use bulk and wire additions. Wire additions are ideal for achieving element specifications with constricted ranges as small amounts can be added with precise control. Additionally, they penetrate deeper into the steel bath

preventing interactions with the slag that can occur with bulk alloys. Cooling and reheating can also be done at LTS, similar to the RHOB, with the only difference being that Al wire is used instead of bulk alloy additions.

Due to its wire capabilities, the LTS station is used for calcium addition to ensure an accurate amount of calcium added per heat. Post calcium addition, the heat is stirred for approximately 5 mins to allow time for the calcium to modify the inclusions and ensure a smooth cast. Stirring also enables the inclusions to float up to the slag.

This station accounts for the bulk of production at the partner's facility due to its capability to begin treatment immediately as it does not require a chamber or vessel to be evacuated.

2.2 Clean Steel Practices

The practice of steel cleanliness refers to the production of steel that has low levels of solutes such as sulphur and phosphorus while maintaining minimal non-metallic inclusions such as oxides and sulphides. Oxides and sulphides are considered the primary types of inclusions in steelmaking practices as their solubility in liquid steel reduces as the temperature decreases (Cathcart, 2018; A. L. V. da Costa e Silva, 2018). Oxygen is used as a refining agent in steelmaking production and sulphur is sourced from inputs such as scrap, coke, and iron.

As mentioned previously, there are deoxidizers that have a high affinity for oxygen such as manganese, aluminum, and silicon. These alloys can be used as part of the treatment process but as a result of the reaction produce non-metallic inclusions (NMI) (A. L. V. da Costa e Silva, 2018). Alumina is the primary inclusion developed at the industrial partners facilities. The level of dissolved sulphur is important to control as it has a high affinity for calcium. Therefore, care must be taken during the calcium treatment process to ensure that

sulphur is low enough prevent hindering the calcium modification of other non-metallic inclusions such as alumina (A. L. V. da Costa e Silva, 2018).

For this study, clean steel will only refer to steel being produced with low levels of non-metallic inclusions as described by (Cramb, 1998). The production of clean steel is to prevent the development of these inclusions through careful steel processing or using techniques such as stir practice, optimized slag chemistry, or calcium treatment to float or modify these inclusions, respectively, after the fact.

Inclusions can play a detrimental role in processing and the final product quality of the steel. They can cause clogging at the caster, which causes a reduction in steel quality, production output, and yield. Inclusions can also affect the mechanical properties of steel (formability, strength) and surface quality/finish. Since this varies based on the application of the steel being produced, the focus of the types, sizes or the number of inclusions will greatly depend on the final product (Cathcart, 2018). While all steel products have some level of inclusion development, especially at large scale mills, not all inclusions are harmful to steel properties. If distributed evenly, smaller inclusions (<4 μm) would not cause too much of a problem (product dependent). Inclusions that are larger, caused by agglomeration or external factors (slag entrapment) could affect the capabilities of that product (Pretorius et al., 2015). Types of inclusions such as MnS may not be desirable for formability but are needed for free machining steel (Cathcart, 2018). The need for clean steel practices is primarily product and customer dependent, but the driver could also be for an increase in production output.

2.2.1 Macro and Micro Inclusions

Inclusions can be classified into a few categories with primary inclusions that are formed before the solidification of steel (caster) and secondary inclusions that are formed during the solidification of steel (A. L. V. da Costa e Silva, 2018). Keissling proposed that an inclusion is considered macro if it is large enough to cause immediate failure while in use (Keissling, 1968). Since this work does not involve solid steel, mechanical failure, or morphological analysis as part of the scope, macro inclusions will not be designated by a specific diameter. Micro inclusions should be prevented, reduced, or modified earlier in the process to promote agglomeration and the formation of macro-inclusions which are easier to float out. Macro inclusions may be more difficult to remove further down the processing line and are the most detrimental to the mechanical properties of steel product. Several researchers (Cathcart, 2018; Pretorius et al., 2015; L. Zhang, 2002) have issued guidelines on the critical sizing of the inclusion relative to various steel products. These guidelines are generalized and so can vary based on the specific customer requirements. Table 2-1 displays some of the guidelines which help understand the influence of inclusions in certain everyday products (Cathcart, 2018; L. Zhang, 2002).

For these examples, larger critical inclusion sizes are allowed for home appliances and furniture. Critical structural failure for these products is rare and negligible compared to ball bearings. Critical failure for bearings may result in inconsistent friction reduction which can cause a significant machine failure.

Table 2-1. Critical inclusion size guidelines for everyday products (Cathcart, 2018; L. Zhang, 2002).

Steel Product	Application	Critical Inclusion Size (um)
Cold Rolled Steel	Multiple applications – home appliances, furniture, etc.	240
Cold Forgings	Parts with complicated shapes – gears, engine parts, etc.	100
Wire	Multiple applications - machinery, electrical wiring, structural, etc.	20
Ball Bearings	Machinery – friction reduction	15
Shadow Mask - CRT	Cathode Ray Tube televisions	5

2.2.2 Inclusion Formation in Process

Inclusions formed through the processing of steel can be classified in two ways: exogenous and indigenous. Exogenous inclusions are developed through external factors such as interactions with ladle/tundish slag, refractory wear, and reoxidation process. These inclusions are inherent and can be minimized through process optimization (Wilson, 1984). Modern steelmaking has significantly reduced the formation of these inclusions through ladle slag control and improved refractory brick chemistry.

Indigenous inclusions are developed due to alloying products used in the steel production. These inclusions cannot be eliminated as they are the product of refining techniques in steelmaking. Oxides and sulphides are the primary types of inclusion formed in the process (A. L. V. da Costa e Silva, 2018) and will be the focus of this study. The formation reaction of alumina is illustrated by Equation (2-1).

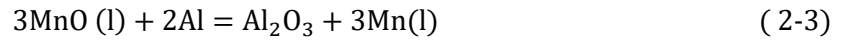
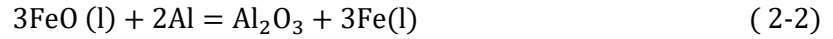
Sulphur is an impurity sourced from liquid iron as a reaction product of iron ore with carbon and scrap commodities charged into the furnace. Sulphur from liquid iron can be reduced prior to the charging into the furnace, but the amount of desulphurization required is dependent on the maximum sulphur for each individual grade. The stable sulphide in liquid steel is CaS which is formed primarily in two ways. A reaction with CaO from the BOF slag or ladle fluxing and formation from calcium treatment where Ca reacts with alumina to form liquid or partially liquid calcium aluminates or form CaS. CaS inclusions are solid at steelmaking temperatures (~1600°C) and can be detrimental to castability (Behrens & Webster, 2018).

Classifying inclusions as exogenous and indigenous can be convoluted in some cases. If the exogenous class includes inclusions that were formed by steel contact with air or entrained slag, the range of these inclusions expands significantly. It is best to classify inclusions based on their specific composition and their size (A. L. V. da Costa e Silva, 2018).

The fundamental chemical equations that form these inclusions along with techniques used to control them, will be discussed later.

2.2.3 Influence of Slag Chemistry on Alumina Formation and Control

As discussed previously, FeO and MnO are an inherent product of the BOF steelmaking process as they are created in the vessel during oxygen blowing and compose a significant weight percent of vessel slag (predominantly FeO). Furthermore, even with proper procedures as noted in [Chapter 2.1.4](#), vessel slag is carried over and becomes part of the ladle slag. Thermodynamically these oxides are favourable to react with dissolved aluminum creating alumina particles later in the process. The reactions are shown in (2-2),(2-3) (Tapia et al., 1996):



The higher the total FeO and MnO percentages in the slag, the greater the potential for reoxidation of the steel and therefore an increase in alumina generation. Several publications have traced quality defects such as slivers to reoxidation product from high FeO in ladle slag (Chakraborty & Hill, 1994; Hille et al., 1991; Tsai et al., 1990; L. Zhang, 2002). Figure 2-5 (Hille et al., 1991) and Figure 2-6 (Ahlborg et al., 1993) depict the effects of slag FeO and MnO on total oxygen in the steel and aluminum fade respectively. In both cases, higher slag FeO + MnO tends to increase the oxygen level in the steel leading to greater aluminum loss and subsequently alumina formation.

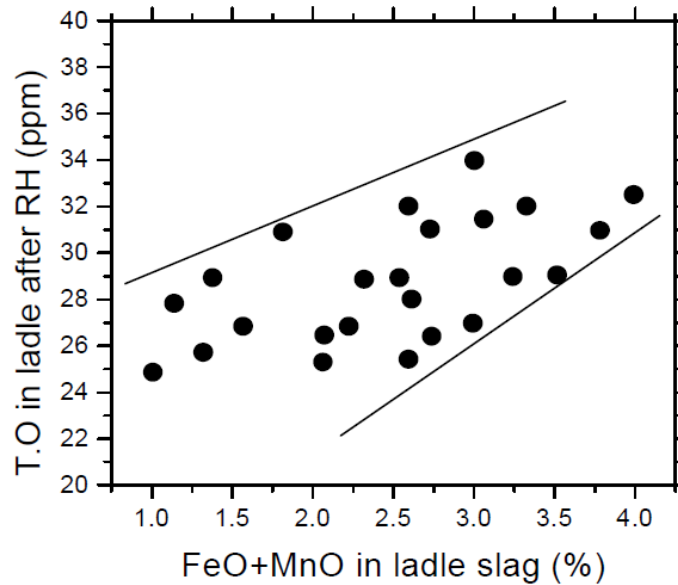


Figure 2-5. Effect of slag FeO+MnO on total steel oxygen (Hille et al., 1991).

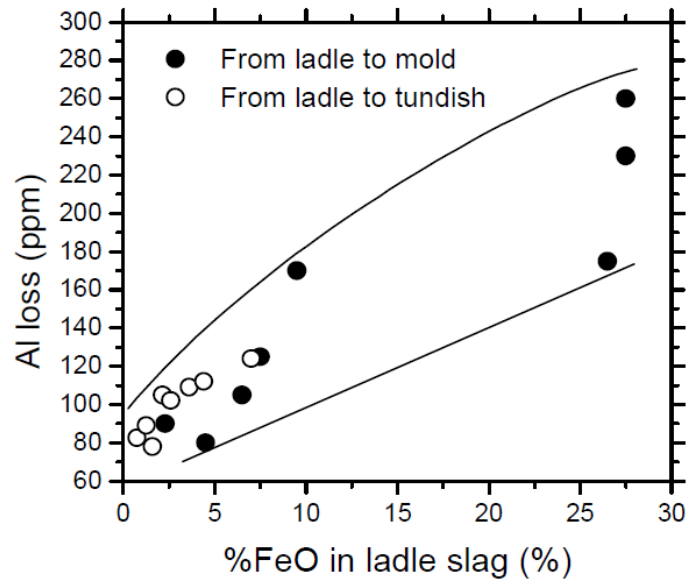


Figure 2-6. Effect of Slag FeO+MnO on Al fade (Ahlborg et al., 1993).

Furthermore, the effect of FeO and MnO on the casting performance is shown on Figure 2-7 (L. Zhang & Cai, 2001). The TO primarily represents oxides in the steel. A reduction in the total oxygen, over the course of casting, indicate oxides floating to the slag. As seen in this graph, higher FeO + MnO in the slag impedes this.

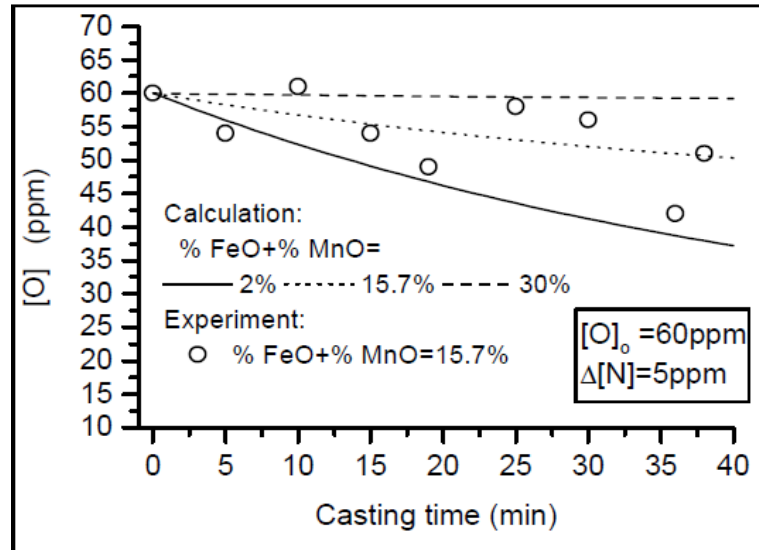


Figure 2-7. Effect of FeO+MnO on the total oxygen in a tundish experiment (L. Zhang & Cai, 2001).

Some of the predominant ways of minimizing FeO and MnO during processing are as follows:

- Increasing the final carbon aim at the BOF and reducing overblowing. This effectively serves two purposes, lowering the total dissolved oxygen and reducing the production of FeO from overblowing (Tsai et al., 1990).
- Using sub lance technology to prevent the steel from being re-blown after the main blow is completed. Sub lances can be used to accurately determine the steel carbon during the blowing process. This along with off-gas analysis, can improve the predictability of final carbon and temperature (Tsai et al., 1990).
- Mechanical stoppers have also been implemented to plug the tap hole, from inside or outside the vessel. This can be a type of dart that floats in steel but sinks in slag or a mechanical stopper arm affixed to the vessel shell. These are effective in BOF

shops with slow vessel tilting speeds that make it difficult to stop the tap quickly (Emi, 1994; Tsai et al., 1990).

- Slag conditioners with high aluminum content can be used to deoxidize the slag therein reducing the total FeO + MnO (L. Zhang, 2002).

The ideal aim for total FeO and MnO is as low as feasibly possible and may depend on the process and capabilities in the individual steel shop.

Dilution of FeO and MnO can be achieved by increasing the total synthetic ladle flux additions (Pretorius et al., 2015). However, since the tapping process is conducted manually, it is difficult to predict the total volume of slag carryover and therefore the total amount of synthetic slag required to achieve sufficient dilution. Steel grades have set amounts of synthetic slag material added which are primarily based on the sulphur maximums of the steel. The two types of synthetic slag available at the industrial partner are Ladle Flux 1 and Ladle Flux 2. These are a blend of CaO-MgO-CaF₂ with Ladle Flux 2 having a higher wt% CaF₂ relative to Ladle Flux 1. A combination of these synthetic slags is added to the ladle during the tapping process which helps with desulphurization.

Past the tapping phase, slag chemistry improvements are difficult to conduct due to physical restrictions. Slag modifiers can be added; however, these materials are expensive and can cause refractory damage.

Therefore, it is imperative that furnace slag carryover is controlled well, and the formation of alumina is done as early in the process as possible.

2.2.4 Thermodynamics of Alumina Inclusion Formation

For the purposes of this thesis, the thermodynamics of indigenous or in process inclusions will be discussed. Exogenous inclusions are considered out of scope and will be a discussion for future projects. The focus will be primarily on alumina inclusions and their morphology. Calcium based inclusions, such as calcium aluminates (C_xA_x) and calcium sulphides (CaS) will be discussed later.

Thermodynamics states that alumina (or any oxide) formation occurs at equilibrium where the net generated Gibbs free energy equals zero. However, due to the increasing interfacial energy of the new phase and liquid steel, additional energy is required for the precipitation of the inclusion (Yang, Duan, et al., 2013).

The formation of alumina can be described by the following reactions (Hiroyasu et al., 1997; Yang, Duan, et al., 2013):



$$\log K = 11.62 - \frac{45300}{T} \quad (2-5)$$

$$K = \frac{a_{Al}^2 a_O^2}{a_{Al_2O_3}} \quad (2-6)$$

$$\log K = 2 \log f_{Al} + 2 \log [\%Al] + 3 \log f_O + 3 \log [\%O] + \log a_{Al_2O_3} \quad (2-7)$$

Where K , a_{Al} , a_O , $a_{Al_2O_3}$, are the equilibrium constant and activities of aluminum, oxygen, and alumina respectively. The square brackets represent species dissolved in iron while round brackets represent solid species. Al and O standard state activities are represented as part of the melt and Al_2O_3 is considered a pure solid. The [%i] represents the weight percent of each element. The activity coefficient of individual elements i based on a 1%

mass fraction of standard state is represented by f_i . Therefore, f_i can be calculated using the first and second order equations described in the work by (Hiroyasu et al., 1997) in Figure 2-8 (Hiroyasu et al., 1997; Yang, Duan, et al., 2013).

First order	Second order
$e_{\text{O}}^{\text{O}} = 0.76 - 1750/T$	$r_{\text{Al}}^{\text{O}} = -107 + 275,000/T$
$e_{\text{Al}}^{\text{Al}} = 80.5/T$	$r_{\text{O}}^{\text{Al}} = 0.0033 - 25.0/T$
$e_{\text{Al}}^{\text{O}} = 3.21 - 9720/T$	$r_{\text{Al}}^{\text{Al}_2\text{O}_3} = -0.021 - 13.78/T$
$e_{\text{O}}^{\text{Al}} = 1.90 - 5750/T$	$r_{\text{O}}^{\text{Al}_2\text{O}_3} = 127.3 + 327,300/T$

Figure 2-8. First and second order activity interaction coefficients (Hiroyasu et al., 1997; Yang, Duan, et al., 2013).

Using the first and second order activity interaction coefficients and substituted into Equation (2-7) the final equation is described by the following (Hiroyasu et al., 1997; Yang, Duan, et al., 2013).

$$\log K = 2(2e_{\text{Al}}^{\text{Al}} + 3e_{\text{O}}^{\text{Al}})[\% \text{Al}] + (2e_{\text{Al}}^{\text{O}} + 3e_{\text{O}}^{\text{O}})[\% \text{O}] + 2\log[\% \text{Al}] + 3\log[\% \text{O}] \quad (2-8)$$

$$+ 2r_{\text{Al}}^{\text{O}}[\% \text{O}]^2 + 3r_{\text{O}}^{\text{Al}}[\% \text{Al}]^2 + (2r_{\text{Al}}^{\text{Al}_2\text{O}_3} + 3r_{\text{O}}^{\text{Al}_2\text{O}_3})[\% \text{Al}][\% \text{O}]$$

Where e_i^i and r_i^i are first and second order activity interaction coefficients, respectively. This equation does not consider the interfacial tension on nucleation of Al_2O_3 or at $\sigma=0$. When the effect of interfacial tension on the nucleation is considered, the work conducted by Turpin (Turpin & Elliott, 1966) note that the required Gibbs free energy change for nucleation can be described using the following simplified equation (assuming constant aluminium concentration) (Turpin & Elliott, 1966).

$$\Delta G_{\text{hom}}^{\text{crit}} = -2.303RT\left\{\left[\left(2e_{\text{Al}}^{\text{O}} + 2e_{\text{O}}^{\text{O}}\right)\left([\%O] - [\%O]_{\text{eq}}\right)\right] + 3\left(\log[\%O] - \log[\%O]_{\text{eq}}\right) + 2r_{\text{Al}}^{\text{O}}\left([\%O]^2 - [\%O]_{\text{eq}}^2\right) + \left(2r_{\text{Al}}^{\text{Al}_2\text{O}_3} + 3r_{\text{O}}^{\text{Al}_2\text{O}_3}\right)[\%Al][\%O] - [\%O]_{\text{eq}}\right\} \quad (2-9)$$

The critical supersaturation in terms of free energy for homogenous nucleation can be described by (Turpin & Elliott, 1966):

$$\Delta G_{\text{hom}}^{\text{crit}} = -2.7V\left(\frac{\sigma^3}{kT\log A}\right)^{\frac{1}{2}} \quad (2-10)$$

Where $\Delta G_{\text{hom}}^{\text{crit}}$ is the critical super saturation for homogenous nucleation; V is the molar volume for the new phase (approximately $25.6 \times 10^{-6} \text{ m}^3/\text{mol}$); σ is the interfacial tension between the steel matrix and the new phase; k is the Boltzmann constant; T is temperature in kelvin and A is the frequency factor valued at a constant 10 for Al_2O_3 (Turpin & Elliott, 1966; Wasai & Mukai, 2002b).

Yang et al. graphed the predicted equations along with experimental data from multiple researchers. The equations were plotted at different interfacial tensions (σ) shown in Figure 2-9 (Yang, Duan, et al., 2013). The consensus of the data indicate that higher interfacial tension makes nucleation more difficult to proceed as higher oxygen content is needed for nucleation to occur. Additionally, when comparing to experimental data, it confirms that supersaturation is needed for nucleation. Given that experimental results showed that the interfacial tension between Al_2O_3 and liquid iron is between 0.5-1.5 N/m, it is ideal to keep oxygen levels low and aluminum levels steady during treatment to avoid homogenous nucleation of alumina particles (Yang, Duan, et al., 2013).

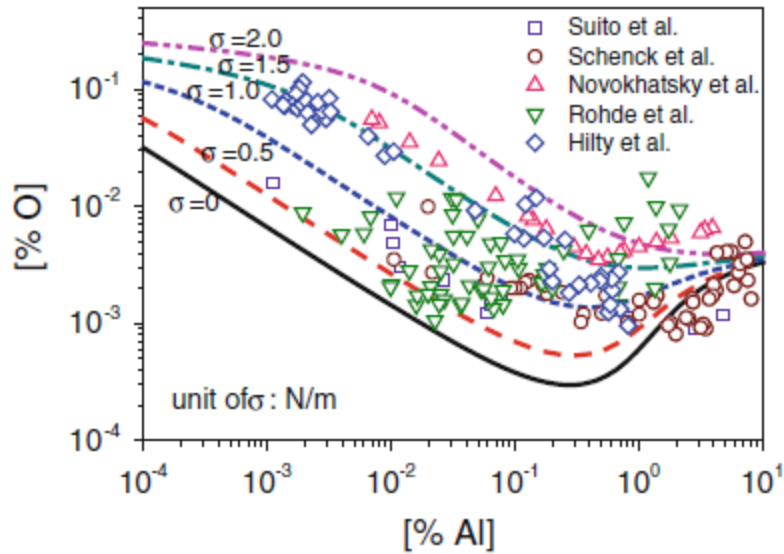


Figure 2-9. The effect of interfacial tension on Al_2O_3 nucleation (Yang, Duan, et al., 2013).

Additionally, Wasai and Mukai investigated the effect of the nucleus radius on the precipitation of Al_2O_3 in steel (Wasai & Kusuhiro, 1999; Wasai & Mukai, 2002b). The following relationship between the interfacial tension (Al_2O_3 and Iron) and the nucleus size of Al_2O_3 , was determined (Wasai & Kusuhiro, 1999; Wasai & Mukai, 2002b).

$$\frac{\sigma_0}{\sigma} = \frac{\frac{1}{\bar{V}}}{\left(\frac{2\Gamma}{r} + \frac{1}{\bar{V}}\right)} \quad (2-11)$$

Where σ_0 is the interfacial tension of alumina with particle radius r , σ is the interfacial tension of alumina the interfacial tension of alumina when r is infinity, \bar{V} is the molar volume of alumina and Γ is the surface excess which is determined by the following equation (Yang, Duan, et al., 2013).

$$\Gamma = N(\text{Avogadro's number})^{-\frac{1}{3}} \bar{V}^{-\frac{2}{3}} \quad (2-12)$$

Figure 2-10 (Yang, Duan, et al., 2013) shows the relationship and indicates that interfacial tension decreases with decreasing radius. Similar to the effect of interfacial tension, Yang et al graphed Figure 2-11 (Yang, Duan, et al., 2013) the effects of different nucleus radii on the nucleation of Al_2O_3 alongside experimental data from multiple researchers. In general, when the radius required for nucleation is larger, the total aluminum and oxygen concentration required is greater. Consequently, knowing the steel oxygen and aluminum concentration can help industry determine the ease of alumina formation in the melt and therefore improve processing control (Yang, Duan, et al., 2013).

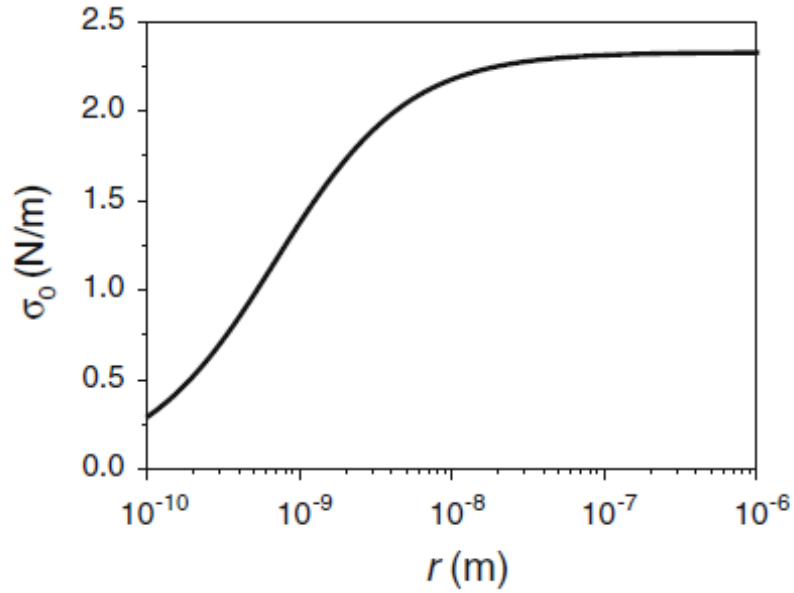


Figure 2-10. Change in iron/alumina interfacial tension as a function of the alumina radius (Yang, Duan, et al., 2013).

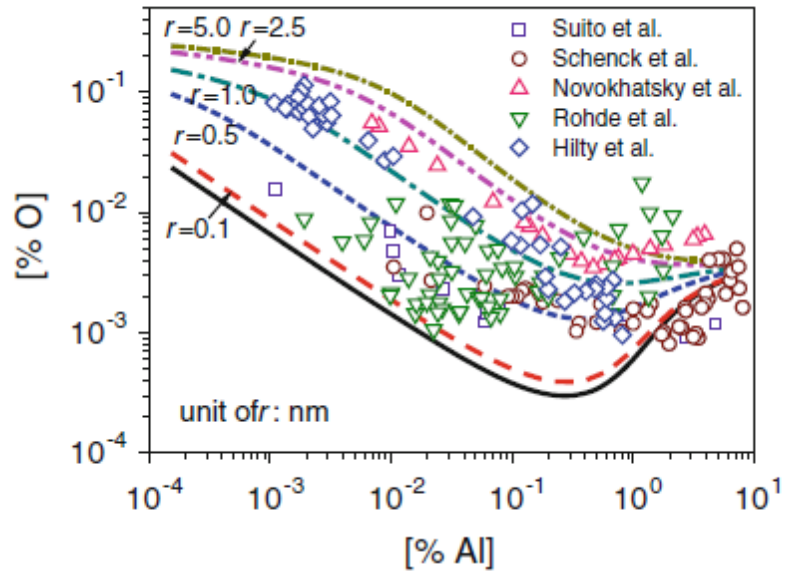


Figure 2-11. Effect of nucleus radius on the nucleation of Al_2O_3 (Yang, Duan, et al., 2013).

2.2.5 Alumina Inclusion Morphology and Aggregation

Alumina inclusions develop different morphologies as they grow after nucleation is achieved. Once nucleation occurs, the nucleus grows by Ostwald ripening and Brownian diffusion. Yang et al. investigated the morphology of alumina inclusions during the deoxidation process experimentally. They collected samples approximately 1 min after Al deoxidation that were then observed using an SEM. They suggested that the morphology of an alumina inclusion is dependent on the supersaturation of the deoxidizing elements. Equation (2-13) (Yang, Duan, et al., 2013) describes this relationship (Yang, Duan, et al., 2013).

$$S = \frac{a_{\text{O}}^3 * a_{\text{Al}}^2}{(a_{\text{O}}^3 * a_{\text{Al}}^2)_{\text{eq}}} = \frac{a_{\text{O}}^3 * a_{\text{Al}}^2}{K_{\text{Al}_2\text{O}_3}} \quad (2-13)$$

Where S is the supersaturation degree. When deoxidization occurs, it causes a decrease in supersaturation. This along with the diffusion of aluminum cause alumina to develop in the following manner as suggested by Yang et al. First spherical shapes were the dominant and smallest (<2 um) and they were then transformed into other shapes such as dendritic, flower, plate like and irregular (faceted, polyhedral etc.). Dendritic shapes show nucleation sites and have distinct growth directions. Some grow in one direction while others grow in multiple. Flower shapes, like dendrites, have distinct growth directions and nuclei. The dissimilarity comes with the shape of the arms which are flatter, less uniform, and smaller plate like inclusions were semi-transparent and large. These types of morphologies are shown in Figure 2-12 (Yang, Duan, et al., 2013) and have been observed in previous works (Dekkers et al., 2003b, 2003a; Van Ende et al., 2009; Wasai & Mukai, 2002a).

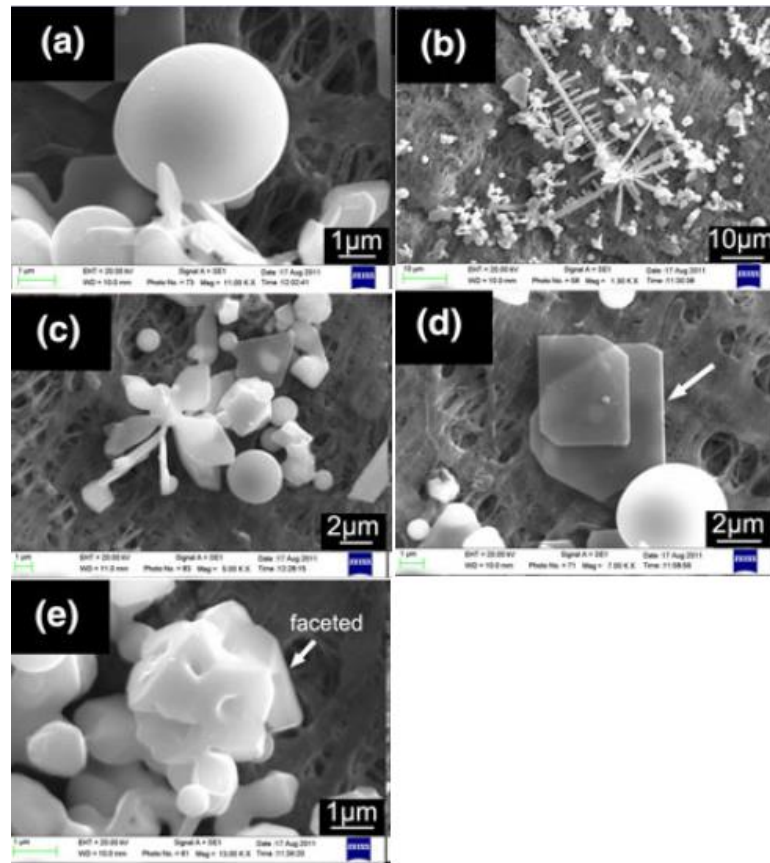


Figure 2-12. Various observed morphologies of singular alumina particles after 1 min holding time. a) Spherical, b) Dendritic, c) Flower, d) Plate-like, e) Irregular (Faceted)(Yang, Duan, et al., 2013).

In summary, the three main factors that affect the morphology of an inclusion from a grain growth perspective are the supersaturation of the dissolved elements, grain surface roughness, and any impurity particles (Dekkers et al., 2003b). This summary is shown in Figure 2-13 (Dekkers et al., 2002) which describes the effects of element concentrations on the growth rate and therefore morphology of the inclusions (Dekkers et al., 2002; Yang, Duan, et al., 2013).

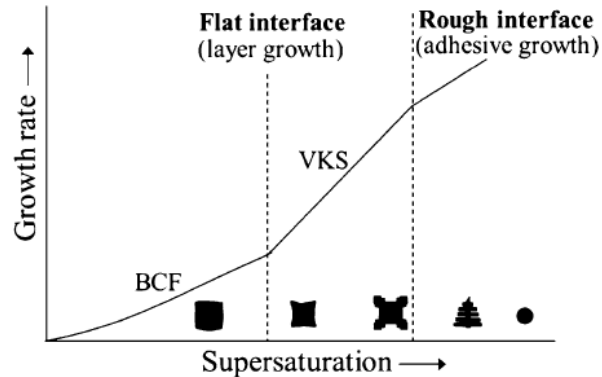


Figure 2-13. Inclusion growth mechanisms as a function of element supersaturation (Dekkers et al., 2002).

2.3 Inclusion Assessment Techniques

2.3.2 Direct Inclusion Assessment

Direct inclusion analysis, which relates to analyzing inclusions at the micro level, can be done in several ways and can provide quantitative information such as size, chemical composition, structure, and distribution. A guideline describing the advantages and disadvantages of the different methods is illustrated in published works by Zhang et al (L. Zhang & Thomas, 2003).

For the purposes of this thesis, the methods available and used at the industrial partner's facility will be described below:

Optical Microscopy – This is a traditional method of observing inclusions in 2-dimensional form using the human eye for quantification purposes (L. Zhang, 2002). Complex inclusions are difficult to interpret using this method and can be mistakenly identified. Additionally, counting smaller inclusions is time consuming as large inclusions are rare particularly in liquid steel samples (Cathcart, 2018). . This method is preferable

for final steel product, such as sheet metal or tubular, as it can identify large inclusions or clusters of smaller inclusions. This can be used to preface further in-depth inclusion analysis.

Automated Scanning Electron Microscopy (SEM) – Electron microscopy can reveal 3-dimensional morphology when analyzing individual inclusions, however, for automated analysis a 2-dimensional image is enough to determine size, quantity, and chemistry. For steel samples, this method along with an EDS detector and automated inclusion program software, can provide a quantitative analysis of the inclusion characteristics for a sample of steel. This automated method can be used to run multiple production steel samples at one time, providing large quantities of inclusion behavioural data for future process modifications. By collecting and analysing this data, steel manufacturers can track their steel cleanness and model the behaviour for future production.

2.3.3 Indirect Inclusion Assessment

Indirect assessments develop quicker in-production inclusion assessments so that issues can be rapidly identified and modified in processes such as optimizing the calcium addition (Smith et al., 2004). Therefore, they are usually the industrial method of understanding inclusion development in the steel. Indirect assessments involve using total oxygen measurements, nitrogen pickup, caster clogging behaviour, and calcium fade (in Ca-treated steels).

Total Oxygen (TO) - This measurement is the summation (ppm) of the total dissolved or free or non bonded oxygen in the steel and the oxygen that is combined with the non-metallic inclusions. Dissolved oxygen is relatively easy to measure in a process using a CELOX®. This instrument calculates the dissolved oxygen in the steel using the steel temperature and oxygen emf. The relationship between EMF, oxygen activity ($a(O)$) and

temperature is shown in the Figure 2-14 (Turner, 2016). Assuming that the steel is deoxidized, and no heating or cooling is done, dissolved oxygen remains relatively steady. Therefore, total oxygen can be used to focus on the oxygen in the non-metallic inclusions. Although larger inclusions can skew the assumptions, their population is typically small in liquid samples. Therefore, it can be assumed that the total oxygen value is representative of oxidized micro-inclusions (Abraham et al., 2013; Cathcart, 2018).

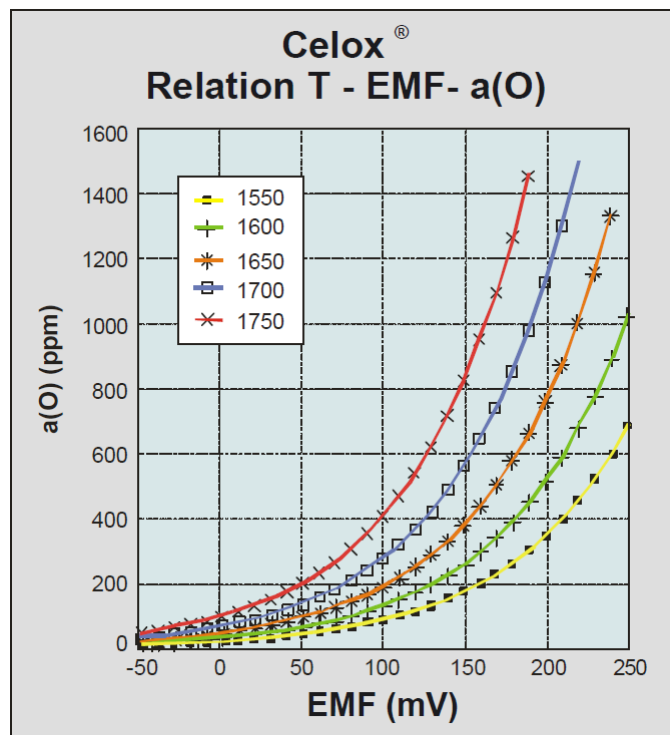


Figure 2-14. Empirical relations between oxygen EMF and celox® voltage (Turner, 2016).

Aluminum Fade - Aluminum loss in general, is an indication of reoxidation, however, Al can also be oxidized by slag and is not a good representation of inclusion development in the steel. Aluminum fade can be determined by the change in steel bulk chemistry between processing steps such as observing samples taken from AS to caster. Between these two points, alloys cannot be added and therefore any loss in Al is an indication of oxidation. The steel bulk chemistry is measured using OES for steel samples taken during the process.

Nitrogen Pickup - Nitrogen is measured as part of the standard steel sampling process using an OES. This measurement is crude but needs to be performed when looking at all factors that cause reoxidation of the steel and therefore the formation of inclusions (L. Zhang, 2002). Nitrogen pickup is a good indicator of air entrapment during the processing of the steel. The easiest way for air entrapment is during a transfer of steel from one vessel to another through pouring. The main concern for air entrapment occurs during the transfer of steel from the ladle to the tundish. This transfer is typically done through a ceramic ladle shroud and the joint is flooded with argon, which protects the steel from the air. Nitrogen pickup can be used to determine if the shroud is misaligned or if the gasket is properly maintained or if a crack causes a leak. Therefore, controlling nitrogen includes after tap practices, ladle and tundish fluxing, and argon flow at the caster.

Sulphur Print – This method is popular and inexpensive as it uses an acid to etch sulphur rich areas of a slab piece. The etched slab is then compared to set of standard etches with numerical ratings such as the Mannesmann rating (SMS Siemag Standards Office, 2011). Although this method is quick the analysis is qualitative and can be subjective to the person analyzing the sample.

Calcium/Aluminum Ratio - This ratio is calculated by dividing the total weight percent of calcium and aluminum derived from OES steel chemistry analysis taken during the process.

Post calcium treatment, a calcium/aluminum ratio, of the bulk chemistry, may be used to verify the effectiveness of Ca treatment. However, as mentioned by Turkdogan, this simple ratio is an inaccurate and misleading indicator of the calcium-aluminate state (Turkdogan, 1984). According to Turkdogan, in most cases, 90% of the aluminum is dissolved in steel and not part of an inclusion but rather the bulk steel. This inadvertently makes the simplified Ca/Al ratio impractical. Moreover, calcium is not regarded as an alloying

element but more for the benefit of inclusion modification. Most of the calcium added either evaporates as a fume loss or reacts to form an oxide or sulfide which either remains in liquid steel as part of the steel chemistry or floats into the slag (Story & Asfahani, 2013).

Calcium/Total Oxygen Ratio - Using the bulk weight percent of calcium in the melt along with the total oxygen can provide a “meaningful measure of the steel castability” for calcium treated grades (Turkdogan, 1984). Based on studies conducted by Kor et.al, when the $C_{\text{tot}}/O_{\text{tot}}(\text{TO})$ ratio reaches 0.6, conditions for the clean steel development become favorable (Abdelaziz et al., 2009; Kor & Glaws, 1998). The downside of using this ratio is that the TO will also include oxides developed from exogenous inclusions such as mold flux that can skew the data. This can sometimes cause the ratio to inaccurately predict that inclusions are under modified (i.e. Al_2O_3) (Story & Asfahani, 2013).

OES-PDA (Pulse Discrimination Analysis) – This method has shown to provide a method of quickly detecting inclusions in a steel sample (Ruby-Meyer & Willay, 1997). OES spark data displays intensities of identifiable elements. PDA identifies individual sparks with intensities much higher (high elemental concentration) relative to other individual sparks that come from dissolved elements. These high intensity sparks are indicative of an inclusion. This analysis is shown in Figure 2-15 (Cathcart, 2018). This method helps provide an estimated quantity of inclusions but does not provide additional information such as shape or size. This method is still developing real-time Ca treatment effectiveness with work by Oltmann et al. (Oltmann et al., 2015).

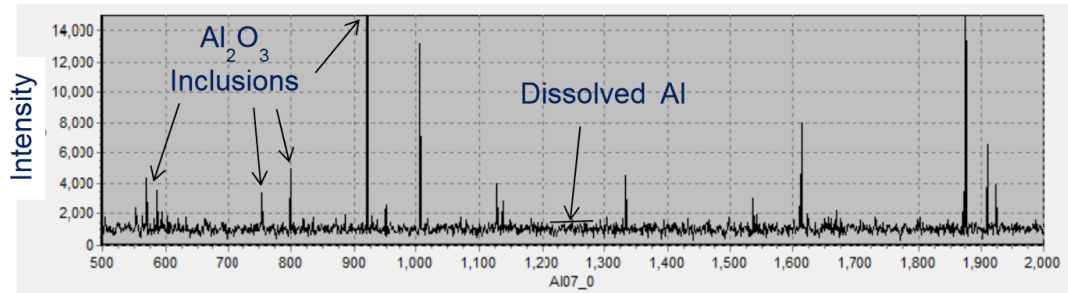


Figure 2-15. OES-PDA techniques for determining inclusion population (Cathcart, 2018).

2.3.4 Caster Clogging Behaviour

During casting, the position of the stopper rod, which controls steel flow, is used as an indicator of clogging. The automated system tries to maintain a setpoint mould level by controlling the steel flow rate into the Submerged Entry Nozzle (SEN) by lowering or raising the stopper rod (Cathcart, 2018; Torga et al., 2011).

Figure 2-16 (a) (Cathcart, 2018) is an indication of no clogging, mould level (maroon trend) and cast speed is maintained and consistent through the entire heat. The Y axis indicates the mould level height while the X axis is the progress in time. Figure 2-16 (b) (Cathcart, 2018) shows moderate clogging where the stopper rod is rising to compensate for lower steel flow rate through the SEN. Because of this automatic compensation, the mould level and cast speed are maintained. Figure 2-16 (c) (Cathcart, 2018) shows severe clogging where the stopper rod positioning is not steady and spikes up and down consistently. This is most likely due to build up and release of clogging material within the SEN. This rapid change causes the mould level to spike. The operators begin to slow down the speed of the caster to help with this issue. Figure 2-16 (d) (Cathcart, 2018) shows catastrophic clogging as the stopper rod is making large adjustments constantly to help control the mould level. Additionally, there are multiple speed changes to help accommodate this issue.



Figure 2-16. Various degrees of clogging in industry (Cathcart, 2018).

It is important to note that these are observations that are based on opinions are therefore subject to interpretations. Moreover, it is difficult to interpret smaller changes in clogging behaviour when observing these graphs.

In practice, caster operators may not notice mild to moderate clogging as mould sensors automatically adjust the steel flow at small increments. In some cases, the system can automatically try to flush the clogged material by raising the stopper rod quickly to rapidly increase the steel flow with the notion of breaking up or “flushing” the clogged area. Severe or catastrophic clogging may require intervention by operators to break down the clogged material. This involves the use of an oxygen lance into the tundish through the SEN and lancing or burning out the clogged material. Other than a delay in process, due to slower cast speed, the major downside to this procedure is introducing oxygen into the liquid steel.

This reduces the quality of the slab at the point of oxygen blow. This slab may need to be cropped to remove the affected area or scrapped altogether, resulting in yield loss.

2.4 Inclusion Removal Techniques/Methods

Inclusion removal takes place in the ladle or in the tundish and mould at the caster. This is done through three main steps; (1) inclusion floatation from bulk steel to the slag/steel interface, (2) separation at the interface and (3) dissolution by the slag (da Rocha et al., 2017). Having a set stir or rinse practice after final alloy addition, heating or cooling is recommended to float the inclusions out and into the slag. For this to be effective, it is necessary to have a good slag chemistry as mentioned in [Chapter 2.2.3](#) and below. The ability for inclusions to float can be evaluated by Stokes' Law which describes the drag forces acting on a spherical object in a fluid medium. Inclusions with small diameters will have limited floatation velocities (Costa e Silva, 2018). Convective current in the steel can help these smaller inclusions float but would require a long processing time. In practice, longer stir times could have the opposite effect on the cleanliness of steel. Longer stir times means increased temperature loss and therefore reheating is required, and this can lead to alumina inclusion generation.

Agglomeration of inclusions is the best possible way to improve the floatation mechanics. Work done by (Braun et al., 1979; Kang et al., 2011) proved that alumina readily clusters together with minimal stirring rates. The work done by (Braun et al., 1979) also proved that too high of a stirring rate may break up larger clusters of alumina. However, in-situ observations conducted by (Kang et al., 2011) clearly showed the readiness of alumina to cluster, while inclusions such as spinel and calcium aluminate did not cluster. This readiness for alumina to cluster is described in Figure 2-17 (Kang et al., 2011). Kang et al. (Kang et al., 2011) used a Confocal Laser Scanning Microscope (CLSM) to observe, in liquid steel, three sets of alumina particles (A,B,C) cluster together over time. A similar experiment, shown in Figure 2-18 (Kang et al., 2011), was conducted for spinel where it

was clear that these inclusions did not readily cluster. Furthermore, in-situ observational work by Mu et al. (Mu et al., 2017) indicated that alumina particles displayed an attractive force between themselves. Their observations indicated smaller alumina particles accelerate as they approached much larger alumina clusters. If the particles are only influenced by a constant liquid steel flow, acceleration of these particles should not occur.

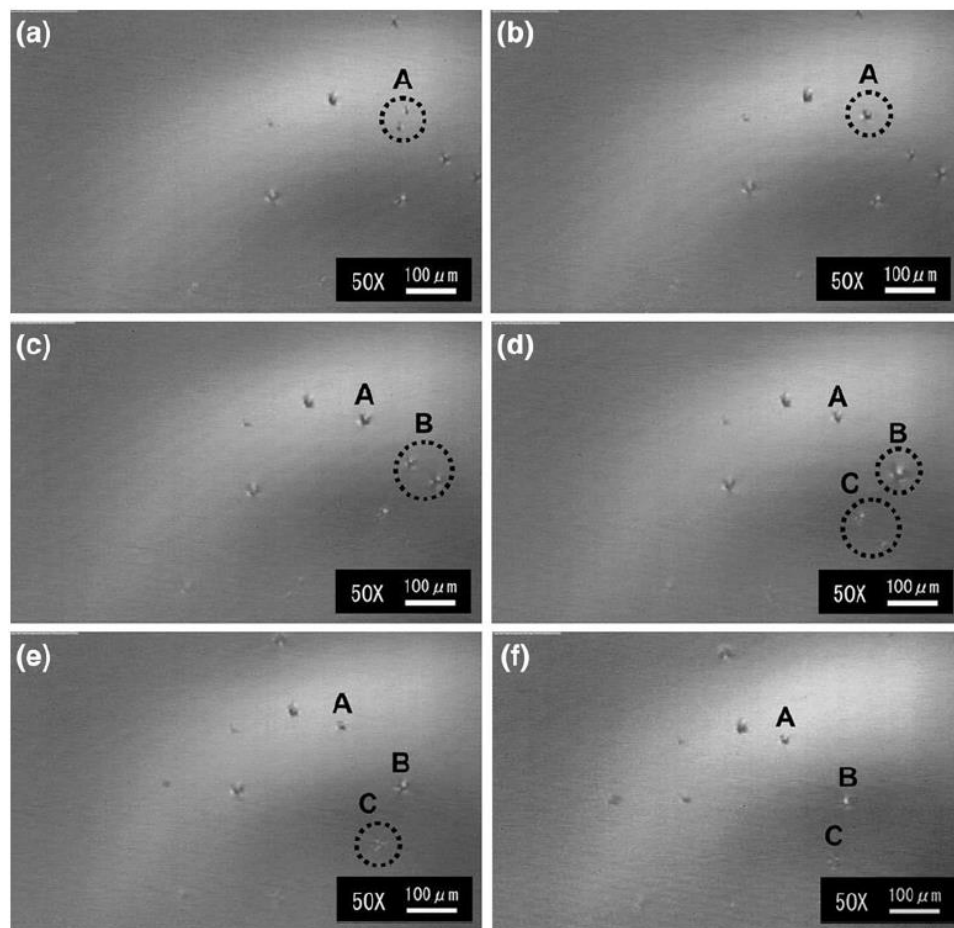


Figure 2-17. Images taken from a CLSM. Shows agglomeration of three sets of alumina particles. a) $t=0.0$ s, b) $t=1.0$ s, c) $t=2.0$ s, d) $t=3.0$ s, e) $t=4.0$ s, f) $t=5.0$ s (Kang et al., 2011).

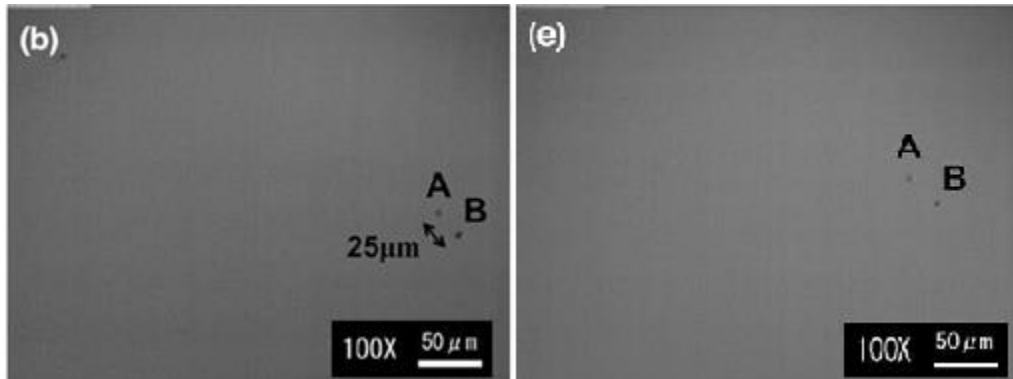


Figure 2-18. CLSM experiment showing Spinel maintaining distance over time. b) $t= 1.0\text{ s}$, e) $t=4.0\text{ s}$ (Kang et al., 2011)

For effective inclusion removal, it is necessary to have a good slag chemistry as mentioned in [Chapter 2.2.3](#).

The intention of stirring is to float inclusions from the liquid steel to the slag. Therefore, it is imperative that the components of the slag enable it to hold inclusion particles effectively. De Rocha et al (da Rocha et al., 2017) used ASPEX and computational thermodynamic software such as FACTSage to analyze two kinds of slag sampled from an industrial facility. To help improve the steel makers processing and products, this analysis compared the slag chemistry to quality parameters such as inclusion population, chemical composition, and solid/liquid fractions. Slag A was a CaO-SiO₂-MgO-Al₂O₃ system. Slag B was based on the same system with added CaF₂ (Fluorite or Fluorspar). Minor oxides were ignored for the purposes of this study. Slag B is similar to the industrial partner's ladle flux blend. CaF₂ lowers the liquidus temperature of the slag, therefore fluidizing it or decreasing the viscosity (da Rocha et al., 2017; Wu, 2011). Slag B showed lower solid fraction values, averaging 0.35 compared to Slag A with solid fractions up to 0.66 at a given temperature of 1520 C and varying MgO% as described by Figure 2-19 (da Rocha et al., 2017).

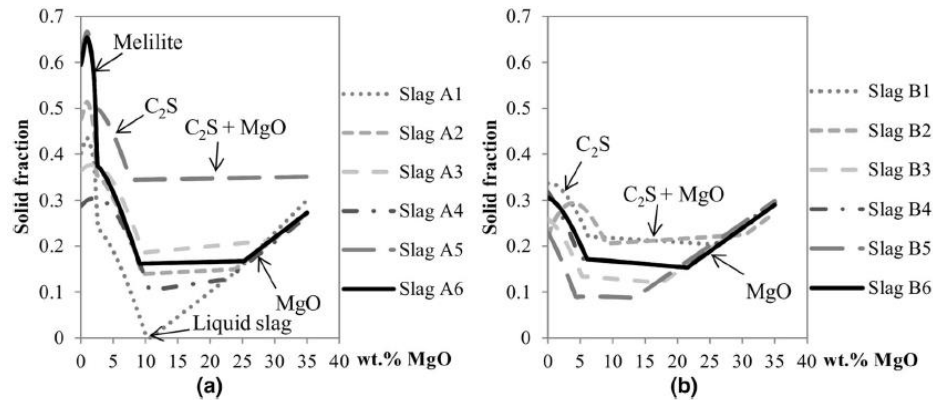


Figure 2-19. Solid fraction of Slag A and B at 1530 C (1833K). a) Series of A slags, b) Series of B slags (da Rocha et al., 2017).

One key factor that impacts the ability to absorb or allow inclusions to mix with the slag is the binary basicity factor. This is the ratio of CaO/SiO₂. A larger basicity factor of the liquid fraction of the slag improves the dissolution of steelmaking's primary inclusion; alumina (Yang, Zhang, et al., 2013). This is because of the effective driving force of CaO saturation that helps drive the dissolution of inclusions into the slag (Valdez et al., 2006). Da Rocha's observation confirms this theory as one slag type with the highest CaO content (53.08% CaO) had the lowest inclusion density in the liquid steel at <0.22 inclusions/mm². Consequentially, the highest inclusion density in the liquid steel, at >0.75 inclusions/mm² was observed in the slag with low CaO content (48.19%) (da Rocha et al., 2017).

2.4.3 Inclusion Modification Process – Calcium Treatment

Calcium treatment at the industrial partner facility takes place at the Ladle Treatment Station only. Calcium is added in the form of Calcium-Silicon (CaSi) wire. Wire, specifically, is used for a few reasons: (1) Greater control on the amount of material added, bulk additions can have in-process issues such as lodging themselves in the transfer system, leading to an incorrect amount of calcium addition; (2) Better penetration of the alloy through the slag and into the bath. It is vital that the calcium reach deeper into the steel

bath before reacting as calcium's melting and boiling points are 839°C and 1500°C, respectively well below steelmaking temperature (1600°C) (Turkdogan, 1996)..

Calcium treatment is commonly performed at the very end of the treatment process. In other words, any alloying, reheating, or cooling (using chill scrap) is conducted prior to the calcium treatment to ensure its effectiveness. Operators are aware of the calcium treatment time and therefore understand the associated temperature changes. Ideally, the temperature coming from the BOF is enough to prevent any temperature adjustments at the secondary station (LTS Level 1 Manual).

For the industrial partners process, the average calcium level at the secondary station following CaSi addition is ~ 25 ppm. The industry partners practice is to introduce the same amount of Ca even though there may be a change in the amount of steel weight. During calcium treatment, the argon flow rate of the stirring lance is reduced from ~15 Nm³/hr to between 6-8 Nm³/hr. The addition of the wire takes ~5 min, and then a rinse stir is performed for ~3 mins. Finally, a steel sample is taken before being sent to the caster (LTS Level 1 Manual).

2.4.4 Fundamentals of Calcium Aluminate Inclusions

Calcium reacts with alumina to form molten calcium aluminates which are globular in shape due to the surface tension effect (Turkdogan, 1996). There are multiple advantages to calcium treatment or morphology modifications of oxides and/or sulphides that include processing and final product quality and functionality. Some of the benefits are listed below:

- Improved steel castability through minimization of clogging at the SEN.

- Reduction in steel cracking under reheating, especially when welding (Heat Affected Zone).
- To improve axisymmetric tensile ductility and impact energy in steel with tensile strength below 1400 MPa (Turkdogan, 1996).

From an industrial perspective, there are disadvantages to calcium treating. Some of the reasoning's are listed below:

- Increased alloying costs – Calcium wire.
- Increased rinse and stirring time can reduce daily production rates.
- Increased cost and time to achieve required sulphur levels.
- Increased number of inclusions which can be detrimental if not processed properly after calcium treatment.

After calcium is injected into the bath, a series of reactions occur. Calcium is exceedingly reactive when added to liquid steel. It can vaporize, react with oxygen, sulphur, and modify inclusions (Ahlborg et al., 2003; Park et al., 2005). The equations are listed below but note that these reactions do not all occur equally. The rate at which each reaction proceeds depends on metal chemistry and the process variables (Turkdogan, 1996).

Equation (2-14) describes the vaporization of Ca when added to liquid steel.

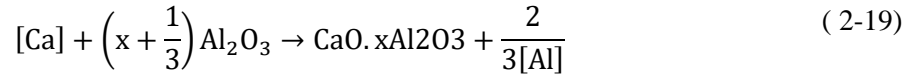
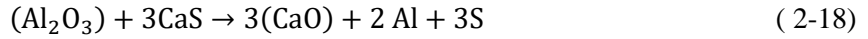
Equation (2-15) describes the transformation of gaseous Ca to Ca dissolved in the steel (Abdelaziz et al., 2009; Story & Asfahani, 2013).

Equation (2-16) shows the dissolved Ca reacting with dissolved oxygen and forming CaO. For calcium treatment purposes, CaO forms as part of a transient phase before modifying with alumina. Experiments have shown that CaO is primarily the transient phase in low S steel (<7ppm S) (Verma et al., 2011b) .

Equation (2-17) is the formation of CaS inclusions. Early onset formation of CaS inclusions occurs at S levels >0.01 wt% (Story & Asfahani, 2013). The intricacy of this formation is discussed in the next section.

Equation (2-18) can be used to determine how effectively Al_2O_3 inclusions are modified and if CaS inclusions are formed (Ahlborg et al., 2003). If the dissolved S is less than 300 ppm at 1600°C , CaS is not considered stable when in contact with an unmodified or Ca saturated C_xA_x type inclusion in aluminum killed steel (Verma et al., 2011a). CaS inclusions in contact with unmodified alumina were observed in experiments conducted by Verma et al, leading to the proposed transient CaS that can form prior to reacting with Al_2O_3 according to Equation (2-18) (Ahlborg et al., 2003; Higuchi et al., 1996; Lu et al., 1988; Tiekink et al., 2008; Verma et al., 2011a). There are three known ways in which CaS co-exists with oxide inclusions: Over modification from Ca treatment (Equation (2-17)) (Geldenhuis & Pistorius, 2000; Kor, 1990), a ring of CaS formed around a C_xA_x during solidification as a result of sulphur enrichment (Y. Wang et al., 2002) and the aforementioned formation of transient CaS.

Equation (2-19) (Tabatabaei et al., 2018b; Verma et al., 2011a) and Equation (2-20) describe the formation of calcium aluminates through pure calcium reacting with alumina directly or transiently through CaO (Verma et al., 2011b).



Oxygen activity in the steel plays a significant part in the effectiveness of calcium treatment. Therefore, it is important to base the formation of calcium aluminates on the thermodynamic equilibrium of calcium, aluminum, and oxygen. The inclusion compositions can be determined using the following equation (Park et al., 2005):

$$\log \left[\frac{X_{\text{CaO}}}{X_{\text{Al}_2\text{O}_3}} \right] = \log \left[\frac{a_{\text{Ca}}}{a_{\text{Al}}^2 a_{\text{O}}^3} \right] - \log \left[\frac{Y_{\text{CaO}}}{Y_{\text{Al}_2\text{O}_3}} \right] + \log \left[\frac{K_{\text{Al}}}{K_{\text{Ca}}} \right] \quad (2-21)$$

Calcium aluminates form multiple phases after post-treatment. For simplification purposes, these phases are designated as C_xA_x where "C" means CaO, and "A" means Al_2O_3 . Based on the above equations, it can be said that the CaO to Al_2O_3 ratio ($\log \left[\frac{X_{\text{CaO}}}{X_{\text{Al}_2\text{O}_3}} \right]$) is linearly related to $\log \left[\frac{a_{\text{Ca}}}{a_{\text{Al}}^2 a_{\text{O}}^3} \right]$, assuming the activity coefficient is not greatly affected by the composition of the steel. The ratio $\left[\frac{X_{\text{CaO}}}{X_{\text{Al}_2\text{O}_3}} \right]$ or C_xA_x inclusion type is shown as a function of activity of Ca to Al and O levels (Park et al., 2005). Park et al. indicates that the slope of the linear relationship is close to unity or a 1 to 1 stepwise increase with high Ca and low Al which is shown in Figure 2-20 (Park et al., 2005). The slope is much less than 1

when low Ca and high Al is present. This means that the ratio of γCaO to $\gamma\text{Al}_2\text{O}_3$ would increase by increasing the activity of Ca (Park et al., 2005).

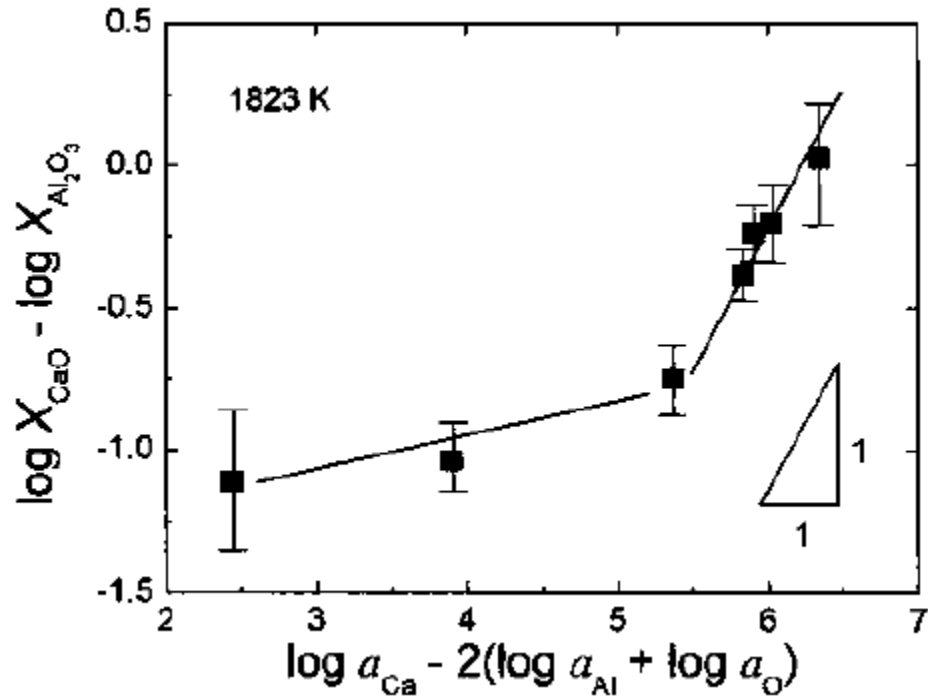


Figure 2-20. Calcium aluminate inclusions composition after Ca treatment at 1600° C (Park et al., 2005).

Research from (Kohatsu & Brindley, 1968) using sintered pellets of CaO and Al₂O₃ shows all known compounds of the CaO-Al₂O₃ system. These compounds included C₃A, C₁₂A₇, CA, CA₂, CA₆ where C₁₂A₇ was quantitatively the major compound formed in these experiments. Most of these phases matched with the phase diagram seen in Figure 2-21 (Abraham et al., 2013; Ahlborg et al., 2003).

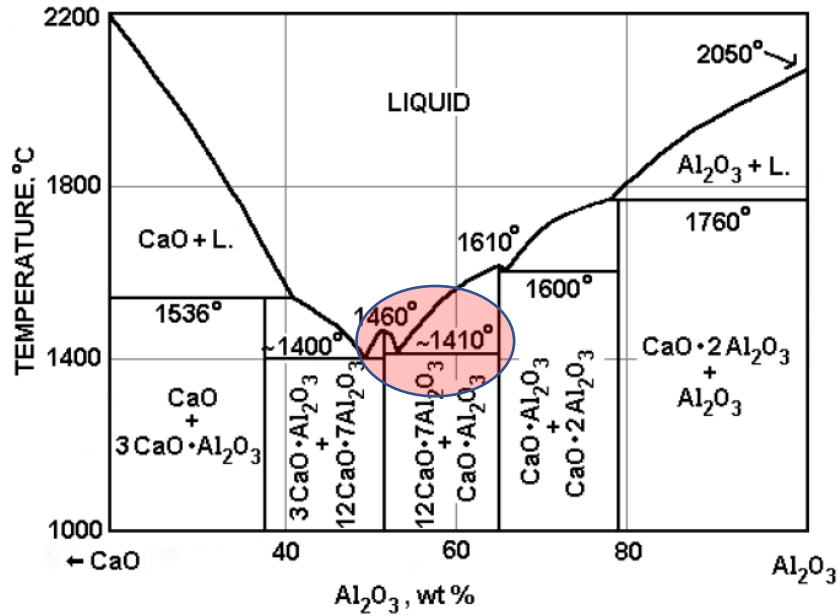


Figure 2-21. CaO- Al₂O₃ phase diagram. Circled is the ideal zone for CA treatment to produce liquid inclusions at steelmaking temperatures (Abraham et al., 2013; Ahlborg et al., 2003).

According to Figure 2-21, the melting points of CA, C₁₂A₇ and C₃A are below typical steelmaking temperatures (~1600°C) (Abraham et al., 2013; Ahlborg et al., 2003). They are therefore desirable to ensure the inclusions formed are mostly, if not all, liquid in practice. These liquid inclusions are less likely to adhere to the refractory surfaces, such as the SEN, and cause clogging. Additionally, these inclusions can absorb sulphur and form duplex inclusions. Images of CA inclusions with varying CA ratio along with their corresponding liquidus temperature is shown in Figure 2-22 (Park et al., 2005).

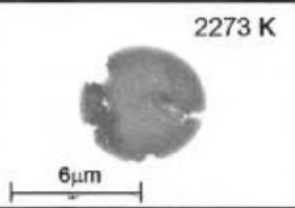
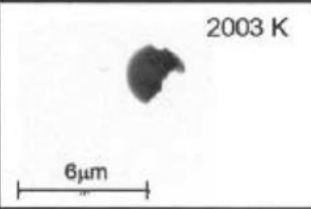
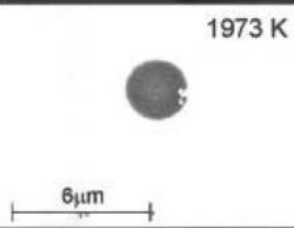
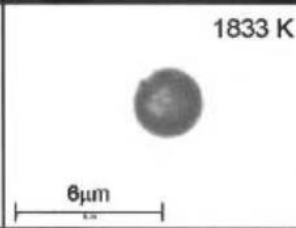
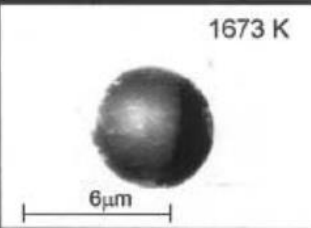
(pct CaO)/(pct Al ₂ O ₃)	0.02	0.25	
SEM image of inclusions	2273 K 	2003 K 	
	0.42	0.66	0.87
	1973 K 	1833 K 	1673 K 

Figure 2-22. CA inclusions with varying ratios and liquidus temperatures (Park et al., 2005).

It is difficult to completely modify every inclusion to the desired chemistry due to the short reaction time, and slow Ca mass transfer in the inclusion, reaction with refractories, Ca evaporation, and slag entrapment (Ahlborg et al., 2003; Tabatabaei et al., 2018a). The degree of control is further lowered when certain processing variables are inconsistent such as they are in an industrial environment. Dissolved aluminum, oxygen, calcium, and sulphur can all be affected by slag conditions, steel temperature adjustments, refractory conditions, and alloy inputs. The effects of calcium must be observed from a macro scale and modeled according to shop conditions. For this purpose, a large amount of inclusion data from multiple heats and conditions are required.

2.4.5 Fundamentals of Calcium Sulphide Inclusions

Residual sulphur has shown to cause pitting corrosion, steel embrittlement, anisotropy and stress cracking (Xiao et al., 2011). Most steel grades, at the partners facility, have a designated maximum concentration of sulphur but not an aim. Tolerable sulphur concentrations are set by customer or processing requirements.

Over addition of calcium can lead to the formation of solid CaS inclusions which are detrimental to the castability of steel. Additionally, excess calcium can react with the alumina contained within slag and refractory, increasing the number of inclusions formed in the steel and reducing the cleanliness. Figure 2-23 (Story & Asfahani, 2013) depicts the favourability for CaS inclusions to form a starting point of a pure Al₂O₃ inclusion (Point A). These points were developed using the following activity equation for CaS (Story & Asfahani, 2013).

$$a_{\text{CaS}} = \left(\frac{f_{\text{Al}}^2 [\% \text{Al}]^2 f_{\text{S}}^3 [\% \text{S}]^3 a_{\text{CaO}}^3}{K_{\text{eq}} a_{\text{Al}_2\text{O}_3}} \right)^{\frac{1}{3}} \quad (2-22)$$

Where [%Al], [%S] are the concentrations of dissolved Al and S respectively (Story & Asfahani, 2013).

Points B and C are critical points of CaO at which the onset of CaS formation begins. For S > 0.01 wt%, the critical point is B, while at low S (0.003-0.006 wt%), the critical point is C. At lower S level, Ca can modify more alumina inclusions before the onset of CaS formation occurs (Story & Asfahani, 2013).

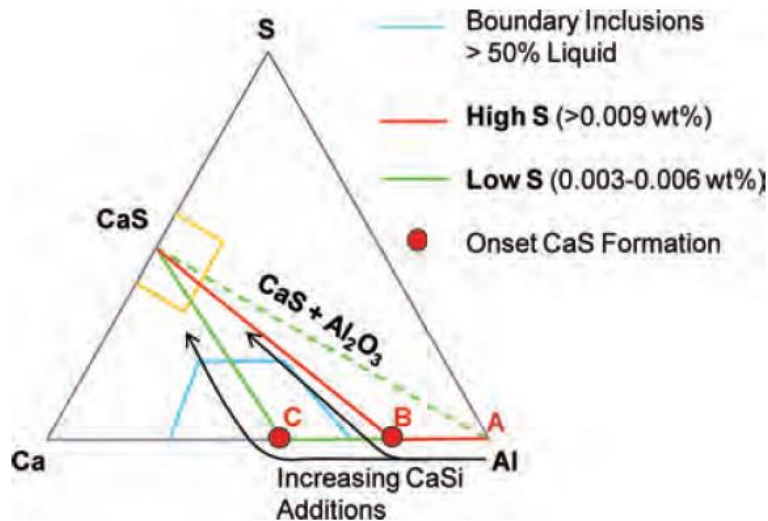
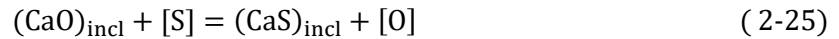
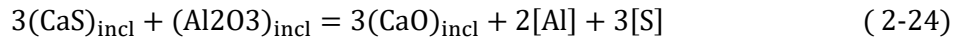


Figure 2-23. Formation of CaS inclusions based on S levels (Story & Asfahani, 2013).

As more CaS inclusions are formed, it reduces the chance for Ca to modify alumina inclusions, as noted by (Lu & Irons, 1994). However, Verma et al. explains the formation of transient CaS can be useful as it helps capture Ca to subsequently react with alumina through Equation (2-24) (Verma et al., 2011b).

The general consensus on the formation and evolution mechanics of CaS inclusions after Ca injection in the melt is summarized by Liu et al (Liu et al., 2018). (1) CaS inclusions are generated immediately as a transient phase once the calcium is injected, then decompose as the calcium evaporates (Lu & Irons, 1994; Ren et al., 2014; Verma et al., 2011a). (2) Transient CaS inclusions react with alumina to form modified inclusions Equation (2-24) (Ren et al., 2014; Verma et al., 2011a, 2011b, 2012). (3) CaO-Al₂O₃-CaS inclusions that formed first get converted to CaS-Al₂O₃ inclusion with low T.O and high dissolved sulphur due to Equation (2-25) (Xu et al., 2016). (4) CaS inclusions precipitate in CaO-Al₂O₃-CaS due to the reverse of Equation (2-24) (Liu et al., 2018; Y. Wang et al., 2002; T. Zhang et al., 2018).



After the formation of CaS in the melt, it can form as multiple types of inclusions as follows: (1) In contact with an oxide type inclusion (Guo et al., 2016; Tiekink et al., 2008; Verma et al., 2010), (2) Surrounding an oxide inclusion as a ring (Choudhary & Ghosh, 2008; Guozhu et al., 1996; Y. Wang et al., 2002), (3) Distributed within an oxide (Yang, Zhang, et al., 2013), (4) Pure CaS inclusion (Geldenhuis & Pistorius, 2000; Verma et al., 2011a) and (5) Part of a Ca-Mn complex inclusion (Guo et al., 2016; Lu et al., 1991).

The first three types are complex inclusions caused by the transient formation, precipitation, and reaction of CaS, respectively. Pure CaS is formed with high sulphur content or excessive calcium additions. Lastly, CaS and MnS can generate a solid solution by dissolving each other (Liu et al., 2018).

In an industrial setting, work done by (Ahlborg, 2001) discussed the negative effects of solid CaS inclusions on clogging at the caster. This work is further substantiated by S. Story when tracking the reject rate for final product quality based on the concentrations of CaS-rich inclusions as shown in Figure 2-24 (Story & Asfahani, 2013). As the area fraction of CaS-rich inclusions increased, the number of OD (Outside Diameter) quality rejections increased which means the amount of quality related issues increased. Additionally, the figure shows the CaS increases mould level fluctuations which are an indication of clogging during the cast (Story & Asfahani, 2013).

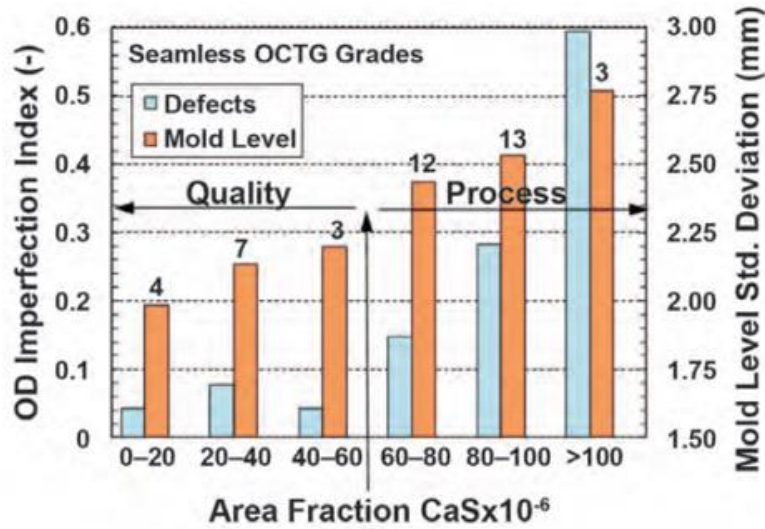


Figure 2-24. Area fraction of CaS compared to quality and caster processing issues (Story & Asfahani, 2013).

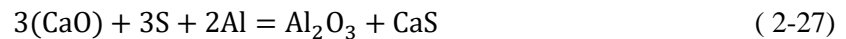
2.4.6 Application of Fundamentals in Industry – Modified Ca/Al Ratio

As mentioned previously, using a Ca/Al ratio from the bulk chemistry analysis is not practical in understanding the effectiveness of calcium treatment in an industrial setting. Using a Ca/Al ratio for individual inclusions may be more beneficial. However, this ratio has its limitations if sulphur level in the individual inclusion is not incorporated. Inclusions plotted on a Ca-S-Al ternary diagram for calcium modified inclusions clearly show that these inclusions are duplex in nature (Story et al., 2003) and therefore taking sulphur into account is important. A modified Ca/Al ratio was developed to account for this shown in Equation (2-26) (Story et al., 2003) where Ca, S and Al are the weight percentage of each element present in the inclusion analyzed. The value of 2 approximates the solubility of sulphur in liquid calcium aluminates (Story et al., 2003).

$$\frac{\text{Ca}}{\text{Al}} = \frac{\text{Ca} - (\text{S} - 2)}{\text{Al}} \quad (2-26)$$

Using steel samples taken from 14 heats made at Gary Works, Story et al. estimates that this ratio should be between 0.5 and 1.5 for the oxide portion of the inclusion to be liquid. Story estimates that the upper end of this range may cause erosion, roughly above 0.8, which places the inclusion towards the centre of the liquid region of the CA system. The study showed that stable casting was achievable with a ratio above 0.4, which, referencing the ternary diagram as well, is in the two-phase region of solid and liquid CA inclusions. Below 0.4 plugging occurred at the slide gate at various points during the cast, and heats below 0.2 plugged almost immediately (Story et al., 2003). This particular methodology can be used to describe the effectiveness of calcium treatment at the industrial partners process however, there are some limitations to this method which will be discussed in [Chapter 5.3.8](#).

A predictability study was conducted by Story to understand the optimal amount of calcium needed to avoid the excessive formations of CaS inclusions. This was done using thermodynamic calculations based on Equation (2-27) to predict the critical concentration of CaO at which CaS is favoured to form (Story & Asfahani, 2013).



Using the results from this study along with industrial data, the Ca/Al ratio was plotted in Figure 2-25 (Story & Asfahani, 2013). This figure shows that there is a good agreement between predicted and measured Ca/Al ratio at sulphur levels above 0.007 wt% or 70 ppm. Below this threshold Story et al. state that thermodynamic calculations underpredict the actual Ca/Al ratio. The limitation may be due to certain kinetic and mass balances that are more prevalent at lower S level which are not considered in this calculation. Story et al. propose two phenomena occurring at sulphur levels: localized desulphurization occurring at the steel-slag interface which may lower the effective sulphur level and the transient formation of CaS observed by Verma et al (Story & Asfahani, 2013; Verma et al., 2011a, 2011b). As a standard practice, more synthetic slag is added for lower sulphur heats.

Assuming consistent furnace slag carryover, more synthetic slag material results in further dilution of FeO + MnO. This dilution enhances the desulphurization capabilities of the slag.

A study conducted by (Verma et al., 2011b) shows that transient CaS forms directly after calcium additions which then reacts with Al₂O₃. Both these phenomena would increase the Ca/Al to a higher level than predicted. According to Story et al, high sulphur levels have better predictability, as it is theorized that CaS inclusions formed will immediately solidify. This is due to an inclusion composition change by CaO depletion and simultaneous addition of Al₂O₃ and CaS inclusions according to Equation (2-27) (Story & Asfahani, 2013).

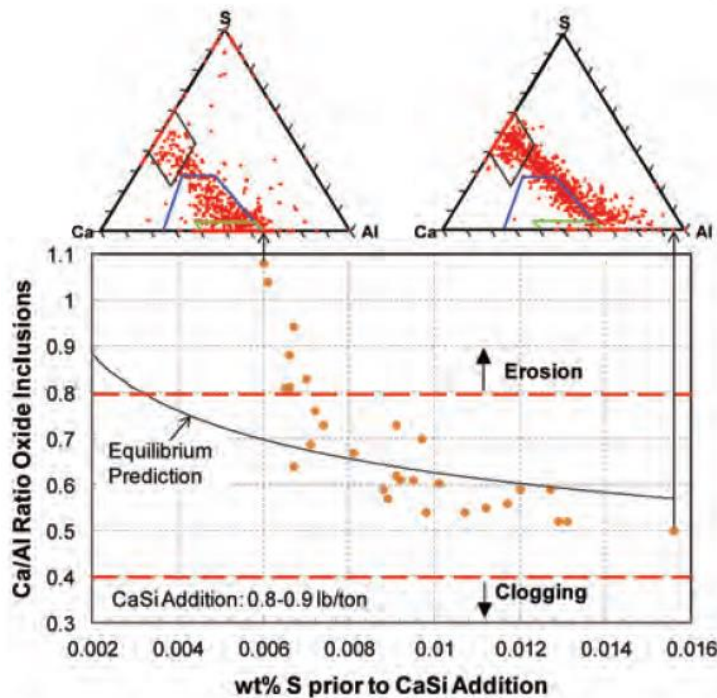


Figure 2-25. Predicted vs the actual effects of S on the Ca/Al ratio for oxide inclusions (Story & Asfahani, 2013).

In general, Story et al conclude that at lower sulphur levels (0.006% or lower) particular care must be taken to limit the amount of calcium added to avoid forming an inclusion

composition that will cause corrosion at the caster. At much higher level of sulphur (0.01 wt% or greater) the oxide Ca/Al ratio is limited by the early formation of CaS inclusions. This means any re-oxidation can easily reduce the ratio below the critical point of 0.4 leading to clogging at the caster (Story et al., 2003; Story & Asfahani, 2013).

3. Gap Of Knowledge

Steel cleanliness evaluation is a widely researched subject with thousands of published works that describe the criticality and fundamentals of controlling inclusion formation. Individual characteristic inclusions have been thoroughly researched for their precipitation mechanism, effects on production or quality, avoidance, and modification/removal techniques. These works are summarized well by several publications (Abraham et al., 2013; Cathcart, 2018; A. Costa e Silva, 2006; A. L. V. da Costa e Silva, 2018; Pretorius et al., 2015; L. Zhang & Thomas, 2003). While some debate still occurs for the reaction mechanism of certain inclusions, the major discrepancy is the ease of applying this work to industrial practice. Previous work (Ahlborg, 2001; Story et al., 2003; Story & Asfahani, 2013) has shown the applicability of experimental analysis techniques to industrial practice and while these have shown promise in correlating to casting behaviour, it is still unique to each individual process. Techniques from these works can be adopted but, at best, these are guidelines. This study investigates a tundish of eight calcium treated heats made at the industrial partners facility. The aim is to understand the effect of calcium on Al_2O_3 modification and its relation to caster behaviour which can help bridge the gap between experimental and industrial work for the industrial partner.

While work for in-process inclusion evaluation continues to be studied, the most effective and accurate cleanliness analysis techniques are done post processing using an SEM. Intense data gathering is required to accurately model the inclusion development given the variability in steel processing parameters. As automated inclusion assessment was previously unavailable, this study aims to provide the industrial partner with techniques to broaden their inclusion analysis capabilities and begin the process of modelling shop cleanliness.

4. Project Methodology

The aim of this study is to evaluate the effectiveness of calcium treatment on the modification of inclusions in an industrial setting. The steel grades chosen for this project are calcium-treated grades conducted at the industrial partners steelmaking facility and are based on customer criticality and caster clogging severity. For this study, 8 heats or steel ladles were tested. These heats were cast sequentially using the same tundish, stopper rod, and SEN. For context, this means that a poorly modified heat may affect subsequent heats cast in the same tundish.

The project methodology can be visualized in Figure 4-1 and includes the following steps. (1) Multiple samples of consecutive calcium treated steel grades were first collected during processing. (2) The chemistry of steel samples was determined by OES and LECO. (3) Process data for the individual ladles was collected through the in-house processing programs. Additionally, operator verbal comments were provided for any anomalies that may have occurred. (4) Once collected, samples were prepared for inclusion analysis by SEM. Tests were conducted using the industrial partner's in-house OES, LECO, and SEM. In part, the reason to keep the work in-house is to improve the industrial partners capabilities in inclusion analysis and provide recommendations for SEM parameters, data processing and eventually steel processing modifications. (5) SEM and EDS feature analysis was conducted after the parameters were set up according to procedure. The system completed the automated inclusion characterization including chemistry, size, and area. Ternary diagrams were also developed. (6) The raw data from the inclusion software was exported to Excel along with the ternary diagram. The inclusions were categorized further into soluble/insoluble phases using the ternary diagrams. (7) Finally, comparing the inclusion analyses to experimental work from literature and caster clogging behaviour. The following sections detail the procedure at each step of the process.

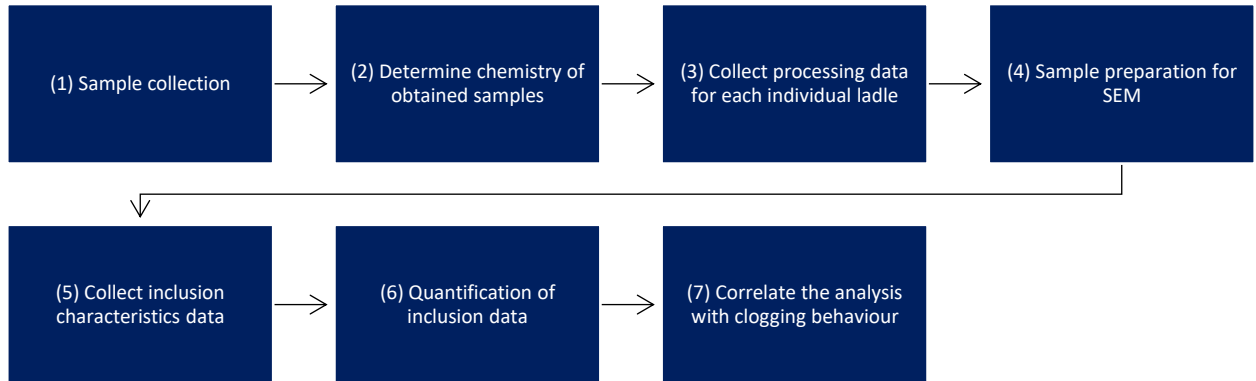


Figure 4-1. Project Methodology Steps.

4.1 Steel Chemistry Determination

The steel grades chosen for this project are calcium-treated grades produced at the industrial partners steelmaking facility and are based on customer criticality and caster clogging severity.

For this study, 8 heats or steel ladles were tested. These heats were cast sequentially using the same tundish, stopper rod, and SEN. For context, this means that a poorly modified heat may affect subsequent heats cast in the same tundish. After the surface is milled down, the lollipop samples are analyzed for chemistry using Optical Emission Spectroscopy (OES). OES provides a broad elemental analysis, including most light elements, such as carbon. An OES uses an electrical current to charge a steel sample that vaporizes a small sample area. When heated to 1000 degrees, the vaporized area emits a characteristic light in the form of plasma. This plasma passes into the internal spectrometer through a diffraction grading system that filters the light into different element-specific wavelengths. The concentration of said element is measured in a corresponding detector after the filtering system (Herman, 1996; Sanders, 2017).

The tail end of each lollipop sample is broken off and can be used for combustion (LECO) analysis of nitrogen, carbon, and sulphur at the current facility. Table 4-1 shows the aim chemistry for the grades tested.

Table 4-1. Grade chemistry aim (wt.%).

C	Mn	S	Si	Al	Ca (ppm)
0.06	0.55	<0.006	0.060	0.034	40

4.2 Scanning Electron Microscope (SEM)

4.2.1 SEM System

Electron microscopes utilize electrons as an energy source for illumination, which provides sophisticated visualization and characterization of a wide variety of samples, including steels. A schematic drawing of a typical SEM construction is shown in Figure 4-2 (Walock, 2012). The electron source in the most basic system is created by a tungsten wire, which is heated to a point where the thermal energy overcomes the work function of the source material. The electrons are focused in the electron column by magnetic lenses, and the final electron beam is rastered over the sample (Goldstein et al., 2018) in a vacuum. The resolution of the final SEM image relies on the electron source, instrument calibration, and operation parameters including the energy of the electron beam (also known as the voltage or keV). The resolution of SEM imaging is far superior in comparison to optical microscopy, where in most systems nanometre scale resolution is achievable.

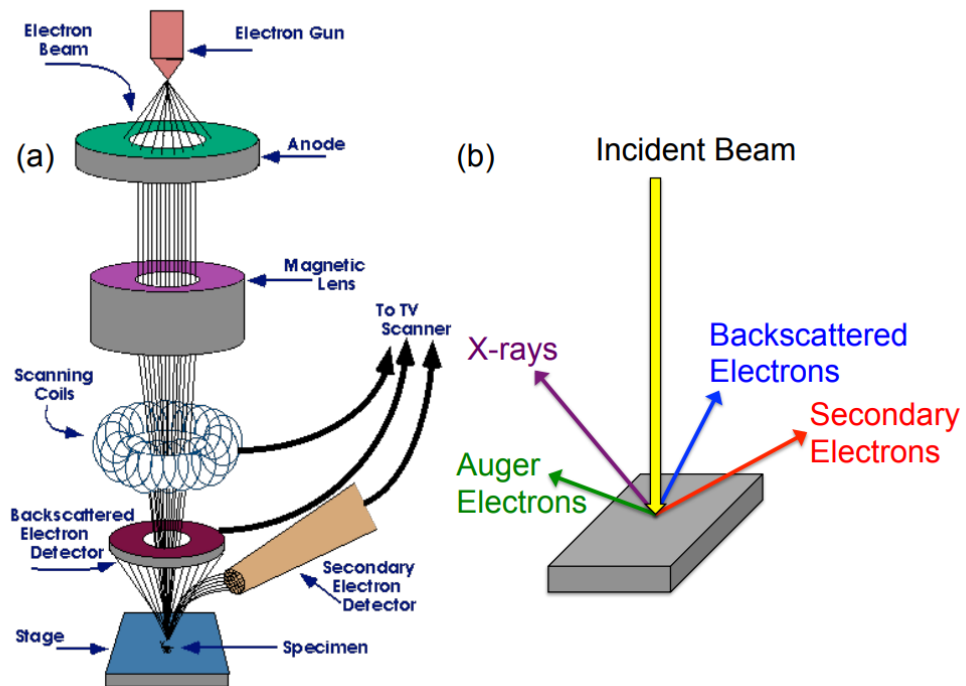


Figure 4-2. Schematic drawing of a typical SEM (Walock, 2012).

Upon electron beam interaction with the sample, a variety of detectable signals can be collected, providing structural, compositional, and chemical information. This study relied on three of the most common electron interactions in the SEM, secondary electrons (SE), backscatter electrons (BSE), and characteristic X-rays, which will be further described here. Although these signals provide information on relatively large samples, the interactions that yield SEM images and information occur on the atomic scale (Goldstein et al., 2018).

Secondary electrons are created as a result of a primary electron from the electron beam interacting with the electrons in the atoms of the sample. The primary beam ejects an electron from the atom, which is detected. SE imaging depicts sample morphology and topography. When utilizing SE imaging for inclusion analysis, the SEM operator uses this imaging mode to locate optimal areas on the sample to analyze, avoiding scratches, holes,

and slag entrapment. This practice ensures the inclusion run is smooth, timed correctly, and the data is valuable (Goldstein et al., 2018)).

BSE imaging is the result of a primary electron entering the sample and interacting with an atom in the sample. This interaction is not a physical relocation of electrons; however, the primary beam is reflected elastically through magnetic interactions with protons and other electrons. The electron reflection is dependent on the size of the nucleus, and thus related to the atomic number (Z) of the atom. Therefore, BSE imaging yields compositional information, whereby brighter regions of the final SEM image correspond to higher Z elements and darker regions correspond to lower Z elements. It is important to note that BSE electrons come from deep in the sample and require a polished surface for the most accurate analysis. Through the use of compositional contrast, the inclusions (usually oxides, carbides, and sulphides with low atomic numbers) are darker than the substrate, which is 90% iron (high atomic number). This helps locate the inclusion and gives the program a reference point to conduct an elemental analysis (Goldstein et al., 2018).

BSE imaging can be easily complimented with energy dispersive spectroscopy (EDS), which utilizes the generation of characteristic X-rays that provide confident element detection, also referred to as chemical information. Characteristic X-rays are emitted when primary electrons collide with the orbiting electron; they are ejected, leaving a hole in the orbit. For the atom to return to equilibrium, an electron from a higher valence must fill that hole, which is only achievable by the electron releasing a certain amount of energy that yields an X-ray. This characteristic X-ray energy is unique to specific elements and the energy shell in which the electron was replaced. These X-rays leave the sample and are detected by an EDS detector, which in conjunction with advanced software, converts the characteristic X-rays levels and intensities into elemental percentage values for the specific area of analysis. This information is used to determine the type of inclusion and group them into different categories (Goldstein et al., 2018).

4.2.2 Computer Controlled Scanning Electron Microscopy

One of the key issues with inclusion analysis is the total time required to receive a result. In the industrial setting, this issue is accentuated as the sample analysis is done after the steel is cast. Process or treatment modifications can only be conducted the next time that steel grade is scheduled for melting.

The CCSEM or Computer Controlled Scanning Electron Microscopy technique provides a rapid measurement of the inclusion size, shape, and chemistry by combining a SEM, an X-ray analyzer, and a digital scan generator that is computer controlled. The electron beam moves in “x, y” patterns over the sample area until it detects a feature that may be an inclusion by monitoring the back scatter signal. The computer directs the beam to pause at each point to compare the image intensity to a threshold point. If above the threshold point, this is considered an inclusion. This technique is known as “search and acquire”. Low grid point densities are used when searching to increase the area analyzed per unit of time. Once an inclusion is detected, the system switches to an acquire mode and creates a high grid point density on the detected inclusion, thus giving the morphology and chemistry (Ahlborg et al., 2003; Smith et al., 2004).

The industrial partner has a dedicated research lab at its Hamilton plant. The electron microscope installed at that facility has a computer-controlled SEM program called AZtech.

4.3 Sample Analysis

4.3.1 Sample Collection

There are multiple samples collected at different locations in the shop, the nomenclature is simplified to a few distinct names. The name, location, and purpose of the samples are summarized below. Additionally, the location of each sample is shown in Figure 4-3. Samples are all considered "liquid" as they are taken while the steel is in liquid form and then quenched in water immediately to preserve the structure. This also preserves the inclusions that are stable at steelmaking temperatures and reduces solidification type inclusions from forming. Due to process time constraints, it is difficult to take multiple samples during calcium treatment so at minimum, a sample is taken before and after. After the post Ca treatment sample is taken, the next samples are taken at the caster from the tundish.

Vacuum Degasser (VD) Before Calcium (Before Ca) – Use of secondary treatment station may depend on the steel chemistry or processing requirements. The degasser is the primary process for decarburization or reheating effectively. These samples are used to make the final chemistry of the steel. Alloy additions are available at the degasser only in bulk form. There may be multiple samples taken during the treatment, known as R1, R2, R3..., but the focus will be on the last sample taken at the degasser. This is considered the Before Ca sample if the next step in the process is to travel to the Argon Stirrer and proceed to Ca treatment.

Argon Stirrer Before Calcium (Before Ca), After Calcium (After Ca) – The LTS station can be used directly for treating calcium treated heats and the samples are designated as M1, M2, M3...Therefore, this station can have a before and after calcium treated sample as the treatment may only be conducted here.

Tundish 10/20 metres – These samples are taken at the caster and are the final liquid samples in the process. They are taken by operators once 10 metres and then 20 metres of slab is cast. These samples are known as C10 and F20 respectively in production.

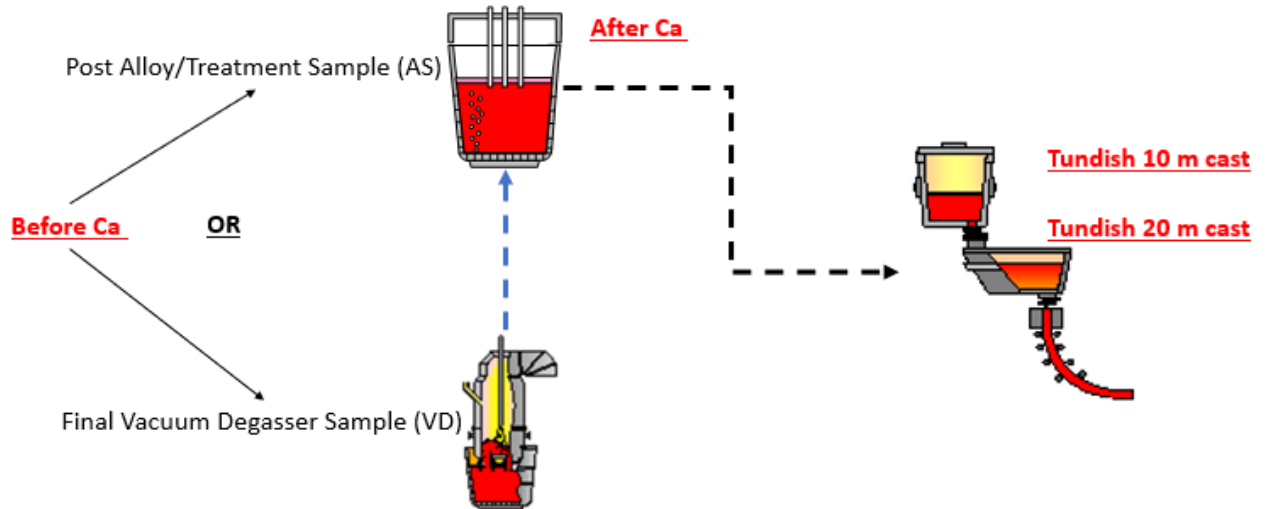


Figure 4-3. Sample location and nomenclature.

It should be noted that samples at the Vacuum Degasser and Argon Stirrer are taken by a machine which means consistent steel depth and exerted force. Samples taken at the caster are manually taken by an operator and can therefore have inconsistent depth and force.

Slag samples were also collected before and after calcium treatment when possible. Slag was collected in two ways: with a steel rod or a slag sampler. A steel rod with a known length is dipped into the ladle allowing the slag to stick to the rod. This method can be complicated if the slag is solid or too fluid. The slag sampler creates a puck of slag that can be directly analyzed in an X-ray machine however these samplers are not always readily available for use.

4.3.2 Sample Preparation Procedure for SEM Analysis

Samples are prepared for inclusions analysis in the industrial partners laboratory after they have been tested in production. The samples are consistent in size, shape, and weight. The dimensions of the samples used are shown in Figure 4-4 . For the analysis, the cross section of the sample is used. The identification of the sample is automatically labeled from the OES machine. Sample are prepared in the following sequence.



Figure 4-4. Lollipop sample dimensions

The first step is cutting the samples prior to mounting. They are cut using a Struers Unitom-5 metallographic cut-off machine. It is sometimes feasible to cut two samples at a time, but this is done with caution to avoid cut off blades from shattering apart. The samples are then mounted in a hot press using a Struers CitoPress-1. The mounting media using is a phenolic hot mounting resin with carbon filler designed to maintain edge retention. The media is also conductive to prevent imaging issues in the SEM. The identification of the sample is etched onto the resin. The mounted sample is shown in Figure 4-5 . After mounting, the samples are to be polished up to 6 samples at a time. They are polished in the following order of paper grit and total time:

- a. SiC paper #120 – 1 min

- b. MD-Piano #220 – 4 min
- c. MD-Allegro with 9-micron Diamond suspension – 4 min
- d. MD-Dac with 3-micron Diamond suspension – 4 min
- e. MD-Nap with 1-micron Diamond suspension – 2 min

Soapy water and ethanol are used to clean the sample surface before being placed in a desiccator prior to SEM testing.

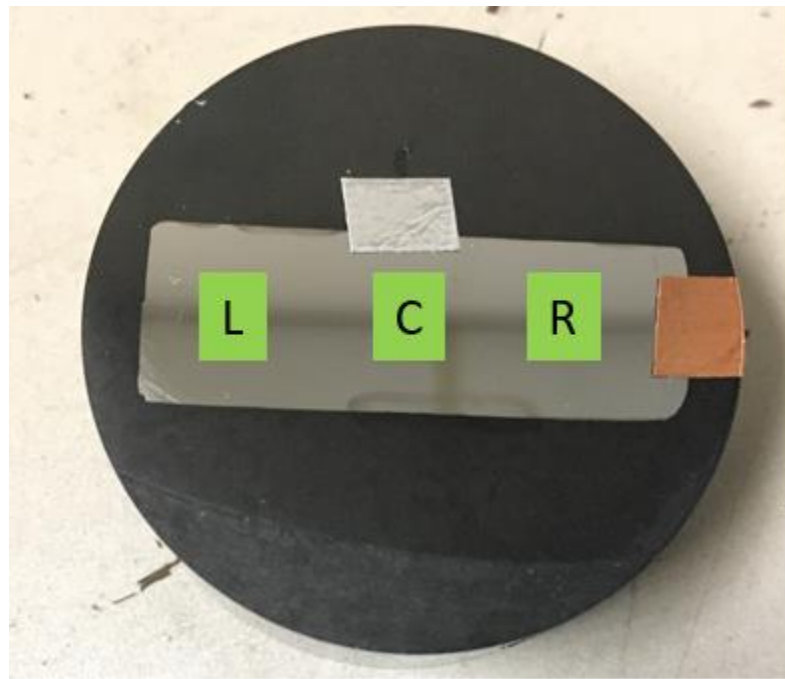


Figure 4-5. Polished and prepared sample. Including aluminum and copper tape for contrast and conductivity respectively.

The sample holder for the SEM is 50 mm in diameter. However, it is only capable of holding one mounted sample. This limitation significantly increases analysis time per steel ladle or heats with multiple samples. The sample is joined onto the holder using carbon tape to ensure conductivity. The sample itself has a strip of aluminum tape placed on one edge. This is used for contrast calibrations that will be discussed in the next section.

Additionally, strips of copper tape are affixed on the sample to connect the steel directly to the metal holder which improves conductivity and reduces charging effects.

4.3.3 SEM Parameters/Procedure for Inclusion Analysis

The SEM used is a JEOL JSM-6510 equipped with an Oxford Instrument EDS (Energy Dispersive X-ray Spectroscopy). Additionally, the software used to analyze and group the inclusions AZtech Feature and Steel Application.

Once the samples are prepped and ready to run in the SEM the following steps are taken for the complete inclusion analysis. The sample height is measured and inputted into the SEM to be used as a reference point for positioning. Once inserted in the holder slot, the SNS capture system is initiated which takes a photograph of the sample that can be used for positioning once in the chamber. After the sample is inserted in the chamber, the SEM is evacuated, and the electron beam can turn on. If the SEM has not been used in several hours, the beam is left on for 30-40 mins to stabilize before starting the analysis.

The sample is first set to the manufacturer's recommended working distance of 15mm. Then the SEM is set at 15KeV and spot size of 15mm. The area of interest is selected based on the top-down image taken by the SNS system. The selected area is purposefully done away from the centre line of the sample to avoid solidification inclusions or entrapped slag. This area is then magnified to 3000x to make smaller adjustments that improve the resolution.

Once these adjustments are done, the "Feature" program in the AZtech software is selected to prepare for the run. This analysis has a few parameters to set up before proceeding with the run. Iron, Carbon, and Oxygen are deconvoluted as these elements are abundant in the

sample and can skew the data. The threshold is set at 15,000 which reduces unclassified inclusions. Additionally, to reduce the number of inclusions the minimum size is set to 1-micron Equivalent Circular Diameter (ECD). The magnification for the run is set at 400x and the classification library is selected which is specific to the industrial partners inclusion classification parameters.

To run a specified area on the sample surface, it is divided into multiple fields, which can be analyzed in sequence or in random order. To reduce the run time, the number of inclusions per field is restricted to 200. Typically, the number of inclusions per field is much less than 200. If 200 is reached, the stage moves to the next field.

Once completed the next step is to set up the contrast to detect the inclusion. The EDS detector is inserted closer to the sample, taking care to avoid contact by observing the live infrared camera. Next the stage is moved to the point at which the aluminum tape meets the steel surface to begin brightness and contrast calibrations. The aluminum tape (low atomic number) is much darker compared to the iron matrix (high atomic number). Thus, providing a proper contrast between the bright iron matrix and the darker inclusion. This step is important as a reduction in contrast during the run can drastically affect the ability to pick up inclusions. The system was originally set to automatically recalibrate during the run every 30 minutes but after running multiple runs, it was safe to calibrate once during the entire run.

Once this calibration step is completed, a small area is selected and run as a test to ensure the settings are working well. This includes quality of the inclusions detected but most importantly the time taken to complete the area. Once satisfied, a 25 mm² area is selected off set from the centre and the run begins. The area selected is checked ahead time for any large voids or entrapped slag. Once the run is completed, the raw data is collected and

copied to Excel for further processing. Additionally, ternary diagrams generated from the program are also added to the Excel file.

4.4 Caster Behaviour Quantification

As previously discussed, caster clogging behaviour is based on a visual description of the stopper rod movement over the casting of a heat. In practice, this visualization is generalized to “Good Cast”, “Moderate Clogging”, “Severe Clogging” which is enough for in-process investigations/adjustments. However, this description becomes difficult to use when analyzing the calcium treatment effectiveness for an in-depth study.

To quantify this, the change in stopper rod height during the casting of individual heats was used. Changes in the stopper rod position can also be affected by cast speed and argon pressure. If these are constant, then it can be said with some certainty that the height changes were affected by clogging. For the calculation, the rod positions every 5 metres of steel cast was used to determine the overall movement of the stopper rod. This was done separately for each individual strand/mould at the caster.

4.5 Ternary Diagram Quantification

Complete and accurate calcium modification of every inclusion is not feasible in industry.. Each steel ladle may have significant differences in processing parameters and events, chemistry, mass, and total oxygen. Consistency and control are difficult to maintain as multiple variables affect the process.

To help understand the efficiency of calcium treatment, the chemistry of each inclusion can be plotted on a Ca-S-Al ternary diagram. Those plotted for this study were derived automatically from the AZtech program. After the raw data and graphs are transferred for

data processing to Excel, an overlaying diagram of boundaries are used to understand the ternary diagram clearer. These boundaries are for liquid oxides and were taken from multiple literature sources (Kumar et al., 2019; Pretorius et al., 2015; Story et al., 2003; Story & Asfahani, 2013).

Using industrial samples and processing data, Story et al. indicated that if the inclusion compositions are primarily concentrating on the right of the boundary, plugging or clogging may occur. To the left of the boundary refractory erosion may occur and so ideally the concentration should be primarily in the liquid oxide area. Figure 4-6 (Kumar et al., 2019) illustrates the boundary layers for liquid oxides. These boundary layers were then overlaid on ternary diagrams developed from the Aztec software.

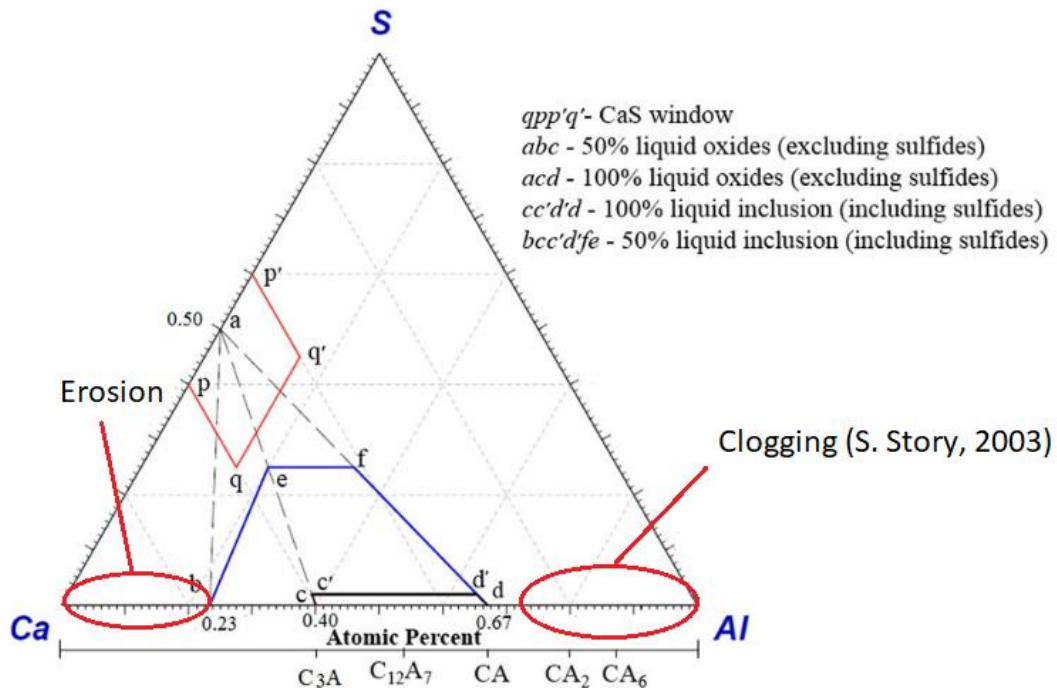


Figure 4-6. Ca-Al-S ternary diagram illustrating liquid oxide boundary layers, CaS window and ideal zones for calcium aluminate inclusions (Kumar et al., 2019).

From a macro-overview, these diagrams are a great visual indicator of the inclusion's characteristics. However, it is difficult to understand the level of modification when trying to compare it to the caster behaviour. Quantification is important in understanding the distribution for each inclusion phase. This will help understand the transformation of the inclusion count, density, and area fraction.

To quantify the data, criteria were created and used based on the liquid oxide boundaries noted in the diagram from literature. Although these criteria need additional work and cannot fully describe each area noted in the graph, it does paint a clearer picture.

As an example, Heat # 1 – After Ca will be used. The area fraction diagram is shown in Figure 4-7 along with the automated phase diagram in Figure 4-8. The ternary diagram for the Before Ca sample did not show anything visually and is therefore not shown in this example. The sample inclusions are mostly alumina which are concentrated on the bottom right corner of the ternary diagram.

For the After Ca ternary, it is easily seen that there is a large quantity of smaller, well modified inclusions inside the boundaries of the liquid oxides, however, this is not seen in the bar graph. This is because these smaller inclusions have a smaller total surface area than the under modified Al_2O_3 inclusions located at the bottom right corner of the ternary. The ternary shows these alumina inclusions as red colours indicating that they are greater than 2 micrometers in size.

From this example it is shown that the technique used to quantify the ternary diagrams gives a clearer picture on the effectiveness of calcium treatment. For this heat, it is shown that the calcium has begun to modify the alumina inclusions into smaller calcium aluminate inclusions. Most of the alumina inclusions have begun to modify, some turning into 50% liquid, some 100% liquid and some still unmodified. As the heat moves to the caster, there

is a large percentage of 100% and 50% modified inclusions which is reflected in the ternary diagram. This is indicating that the treatment is working well to modify the heat.

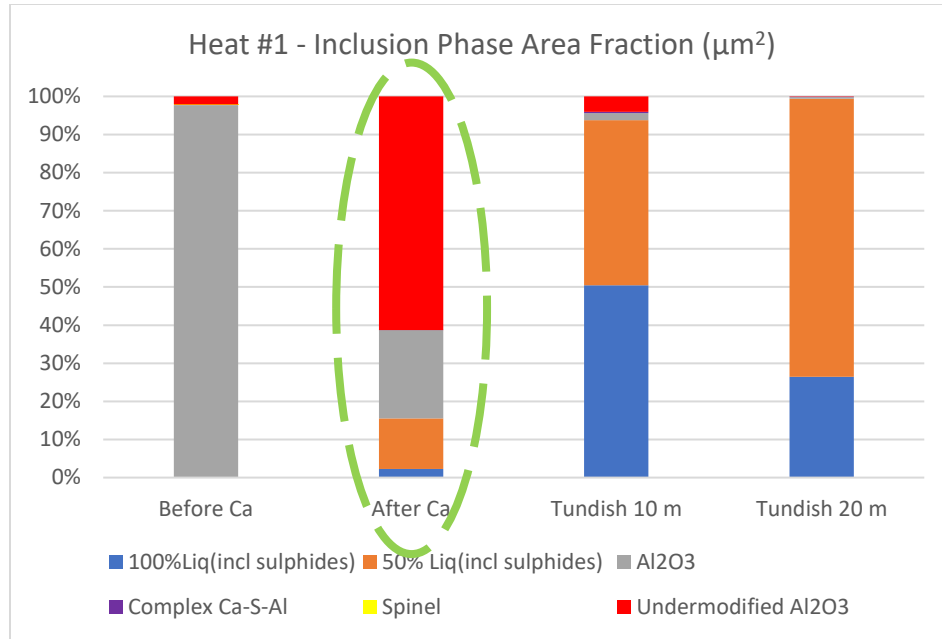


Figure 4-7. Inclusion area fraction percentage for heat #1

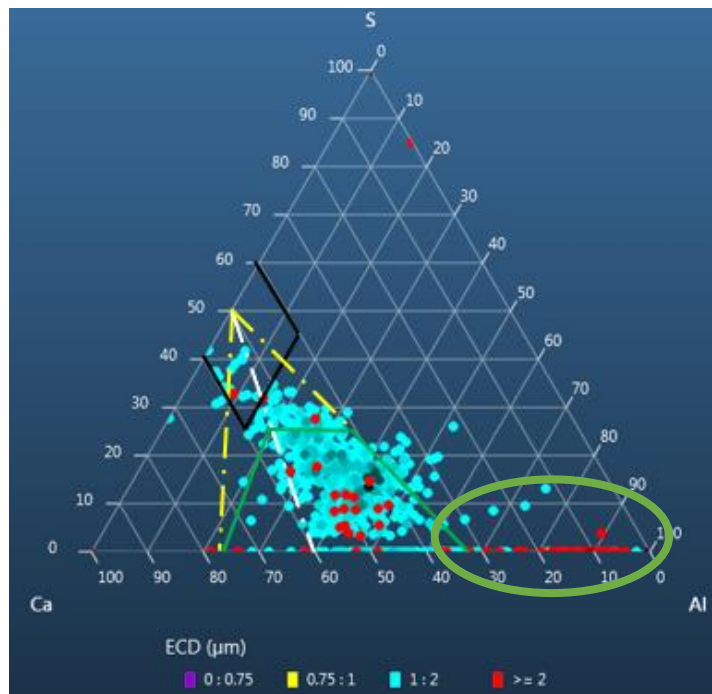


Figure 4-8. Ca-S-Al ternary diagram for Heat#1 – After Ca sample. Circled area shows significant portion undermodified alumina inclusions.

5. Results and Discussion

5.1 Determination of SEM Parameters

This section describes studies conducted to improve the SEM performance by optimizing the parameters to reduce total run time and quantity of unclassified inclusions per sample. All tests were conducted at the in-house SEM at the research lab and processed using statistical programs such as Excel and Minitab. The development of inclusion analysis at the industrial partners laboratory was in its early stages. Therefore, it was important to study the effects of SEM parameters on the number and quality of the inclusions detected.

5.1.1 Effects of Accelerating Voltage on Inclusion Characteristics

As the development of inclusion analysis at the industrial partners laboratory was in its early stages it was important to study the effects of a SEM parameters such as keV on the number and quality of the inclusions detected.

In the early stages of developing inclusion testing, a full run for a calcium treated sample took anywhere from 4 to 6 hours for a 3x3 mm area at 15 keV. A large proportion of these inclusion data sets consisted of solidification inclusions. The main solidification inclusion that was detected was MnS which should not form at the steelmaking temperatures these samples were taken at (formation temp of MnS is 1103°C) (Guo et al., 2016; Luo et al., 2011; Pretorius et al., 2015). The theory was that the beam was penetrating through the inclusions and analyzing the substrate of iron.

Conducting point analysis on the inclusions showed that inclusions had a large spike in iron energy levels with trace amounts of manganese and sulphur (Substrate). However,

since iron is deconvoluted, the program normalizes the manganese and sulphur, therefore grouping it as a Manganese Sulphide (MnS) inclusion.

In this study, samples were run at three different keV (10, 15, 20) on the exact same 3x3 area on the same sample. Each run was conducted right after each other without removing the sample from the chamber to ensure consistency in the process and repeatability using a set X and Y coordinate to mark the test area.

Table 5-1 compares the type and number of inclusions detected on a sample for a non-Ca treated sample. The results indicated that 15 and 20 keV had similar results and they were significantly different from the 10 keV results.

Two distinct observations can be made. The total number of inclusions and the percentage of MnS inclusions increased sharply with an increase in keV from 10 to 15/20 keV. A total of 64 or 28.4% of inclusions were MnS using the 10 keV setting compared to 399 or 79.6% for 15 keV and 472 or 84% for 20 keV. At this point in the inclusion study at the industrial partners facility, it was important to ensure that parameters were set up to create valid inclusion data and quantity. Having large quantities of MnS inclusions created a cause for concern related to data quality. This is reflected in small amounts of valid inclusions identified, such as Al_2O_3 , which should be the primary type of inclusion formed as this sample is aluminum killed and not calcium treated.

While running at 10 keV seemed to be the better option for analysis, it may not provide enough information due to the lower total inclusion count as seen in Table 5-1 with 10 keV having 219 inclusions and 15/20 having >500 each. For purposes of the project and the goal of reducing run time, the decision was made to keep the setting at 15 keV and work on other methods of reducing the number of unwanted/solidification inclusions (MnS).

Inclusion analysis work done by K. Gu on the same SEM showed a reduction in MnS or unclassified inclusions by modifying the threshold levels (Gu, 2020; K. Gu, personal communication, 2020) . The threshold was modified to 15,000 from 30,000. This improvement was made to the procedure which reduced the run time from 2-3 hours to 1-1.5 hours. Further studies were not conducted on this parameter due to time constraints.

Table 5-1. The comparison of inclusion type and count with respect to KeV setting.

Inclusion types	10 keV	10 keV Count	15 keV	15 keV Count	20 keV	20 keV Count
MnS	28.4%	64	79.6%	399	84.0%	472
No Classification	23.6%	53	2.4%	12	1.2%	7
Al ₂ O ₃	23.6%	53	6.4%	32	5.5%	31
Fe, O, C	13.8%	31	7.8%	39	4.3%	24
Spinel	4.9%	11	0.8%	4	0.9%	5
CaO.Al ₂ O ₃	2.7%	6	1.0%	5	0.4%	2
SiO ₂	0.4%	1	0.0%	0	0.2%	1
MnO	0.0%	0	0.8%	4	3.0%	17
Ti, Mn	0.0%	0	1.0%	5	0.5%	3
Total# Inclusions	219		500		562	

5.1.2 Effects of Analysis Area on Inclusion Characteristics

The objective of this study was to understand the homogeneity of the lollipop samples to validate testing one larger area of the sample. This would reduce run time and improve data quality.

Initial inclusion analysis on the SEM was performed on three separate areas of the sample. The selected areas were the left, centre, and right of the sample shown in Figure 4-5. When setting up for the run, image resolution had to be set up to ensure clear contrast between the brighter substrate and darker inclusion. This was done on a random area that was

selected by the operator, avoiding entrapped slag or holes. After 40+ runs were completed, the inclusion data showed that the number of inclusions significantly differed between the left, centre, and right areas of the sample. Typically, the side with the highest number of inclusions was used for the analysis instead of all three.

Work was done to compare the resolution of each area for the same sample. This involved manually checking some inclusions at a higher magnification. It was determined that the sample surface plane was not level across the cross section. This was due to inconsistent or uneven pressure during the polishing steps. As the SEM moved to analyze another area of the sample, the resolution was reduced, which subsequently reduced the number of inclusions detected. Consequently, it was imperative that a single larger area be selected for the run and that this area was used for setting up the initial contrast and resolution of the sample. Therefore, this study was conducted on two samples to determine the validity of analyzing one area (Melyashkevich, 2021).

The standard cross section of the sample that is normally analyzed for inclusions is 30 mm x 10 mm. Ten fields at 2 mm x 2 mm were examined with 5 fields along the centre line in the y-direction and 5 fields slightly below the centre line. The results are presented in the Figure 5-1 (Melyashkevich, 2021). The graphs indicated there is a consistent amount of inclusion quantity and types from left to right of centre for all the samples, with the exception of “M02 centre line at 0 mm” and “C10 of centre at (-)10 mm”. It should be noted that samples close to the centre typically detected higher numbers of inclusions which do not fall under a classification category. These are represented as porosity spots or areas of entrapped slag (Melyashkevich, 2021).

This study improved the reliability of the future analysis and improved the run time by selecting only one area on the sample.

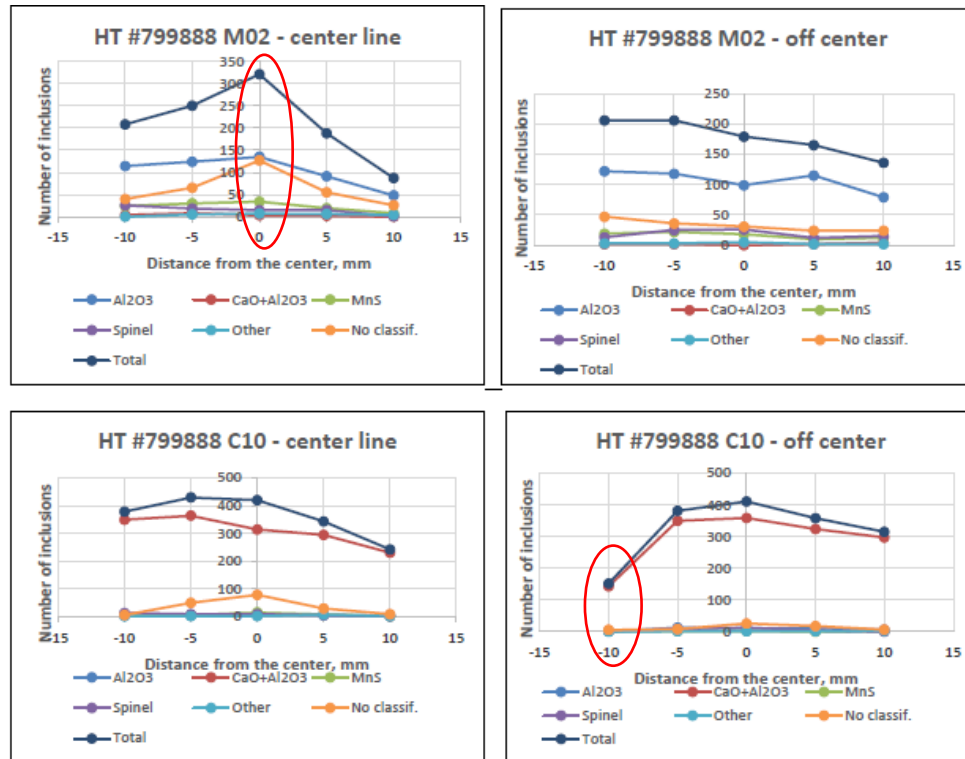


Figure 5-1. Inclusion count distribution for two samples. Circled are data points with significant discrepancies (Melyashkevich, 2021).

5.2 Results from 8 Sequentially Casted Heats

The following sections will describe the results of the selected calcium treated samples that are part of this study. These 8 heats were cast sequentially into one tundish and therefore have the same stopper rod ports and SENs. The analysis includes the inclusion type count, area fraction, density, and equivalent circular diameter to provide comprehensive data analysis and improve the conclusion.

Additional graphical data for population, area fraction, density and equivalent circular data is located in appendices [A](#), [B](#), [C](#) and [D](#) respectively.

5.2.1 Processing Parameters

Variation in process parameters is inevitable during industrial operations. It is important to incorporate such variations when studying the inclusion behaviour. Table 5-2 lists the treatment information for all 8 heats. Although these heats have the exact same aims for chemistry, temperature, and mass of liquid steel; limitations in process control creates variations in this data.

Table 5-2. Processing parameters for 8 heats studied

Heat	Treat Loc	BOF Blow Practice	Change in Temp Needed	Post Ca Stir (mins)	Total Stir Time (mins)
1	AS	-	0	5	21
2	AS	OB	0	5	20
3	AS	-	-20	5	23
4	VD/AS	-	+100	4	43
5	AS	OB	-20	3	20
6	VD/AS	-	+20	5	30
7	VD/AS	-	+10	5.5	28
8	AS	OB	-10	1.5	19

This grade of steel is normally designated to be treated at the AS however Heats 4,6 and 7 were treated at the VD as well due to reheating requirements. In Table 5-2, temperature adjustments are shown as positive/negative changes in degrees Celsius. This can affect the consistency of inclusion removal as the VD has a more vigorous stir compared to the AS. In this study, work was done to compare heats that were reheated to heats that were not. A concrete correlation on the effects of reheating could not be reached in part due to the additional stir time for Heats 4,6 and 7. For fair comparison, heats treated at the VD without reheating should be attained for future analysis.

At the furnace, there are variations in the oxygen blowing practice for these heats. Overblowing can contribute to inclusion formation by oxidizing the carryover slag,

reducing the aluminum recovery, and causing high temperatures which eventually need to be cooled using scrap. The optimal method of understanding, if too much or too little oxygen was added, is to observe the carbon and aluminum (Al) wt percent of the first sample. The process and steel grade have set Carbon and Aluminum ranges after processing at the BOF. If these values are significantly lower than predicted or compared to other heats of the same grade, then it can be deemed that the heats were overblown. Therefore, Heats 1, 3, 4, 6 and 7 were treated well while Heats 2, 5, 8 were overblown (OB). Potential reasons for overblowing a heat include imbalanced Fe inputs, variations in lance efficiency or slag condition, and temperature requirements.

Consistent control of ladle temperature was not maintained as heating and cooling requirements vary between Heats 3 to 8. As mentioned previously, heating is only done chemically using aluminum and oxygen, therefore introducing alumina later in the process. Rusty coolant scrap, used to reduce the temperature, can also oxidize the steel.

A post Ca treatment stir (rinse) is needed to allow the inclusion modifications to proceed and promote inclusion removal. However, these times vary between certain heats. Heats 1,2,3,4,6 and 7 have a rinse time greater than 4 mins while Heats 5 and 8 have under 3 mins. Standard procedures are not always followed as the operators are trying to make the connection at the caster. This can affect how well the modification occurs given that all heats are treated with the same amount of calcium. Subsequently, total stir time for the entire heat can vary. Heats 4,6 and 7 were treated at both the VD and AS leading to longer total stir times which are beneficial to floating out inclusions.

These variations are characteristic of the industrial steelmaking process. The effects on inclusions from these variations are important to understand for industrial purposes but are difficult to model without continuous and large quantities of data. Control is limited and

sometimes treatment that negatively affects the cleanliness of steel, such as overblowing or reheating, must be done to maintain production.

5.2.2 Inclusion Population

The change in total inclusion population, for all heats, is shown in Figure 5-2. Total number of inclusions between the heats varies between 120 and 275. There is no specific trend observed from the first heat to the eighth heat.. In general, the number of inclusions increases from Before Ca to After Ca. This is predictable as adding Ca creates many small inclusions such as C_xA_x , CaS and complex Ca-S-Al. As calcium modifies the inclusions and continuous stirring floats them out, the population should decrease as the heat is taken to the tundish for casting. This finding is consistent for all the heats except Heat 3 and agrees well with previous studies available in literature.

In the tundish, most heats see a decrease in inclusion population from Tundish 10 to 20, other than Heats 4 and 8 which increase slightly. Reoxidation may occur due to air exposure at the slag interface, inconsistent argon shrouding or leaks in the gasket. These factors will be part of future investigative efforts.

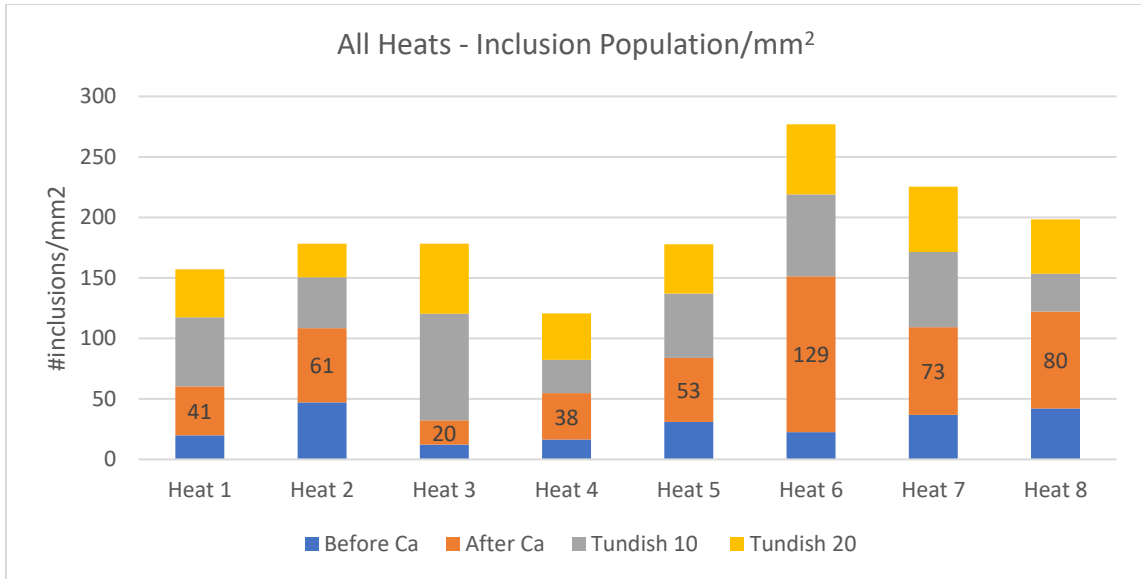


Figure 5-2. Inclusion population of production samples from all heats.

Figure 5-3 compares the density of inclusions detected in each sample for the 8 heats. Density is the area percentage of inclusions over the area of analysis. This is a good method to compare the steel cleanliness on a heat-by-heat basis. One key takeaway from this analysis is that the “Before Ca” samples for Heat 2, 5 and 8 have a significantly higher density of inclusions relative to the other heats. It is possible that this is the result of these heats being overblown in the furnace and therefore containing higher levels of dissolved oxygen and subsequently more alumina inclusions.

Similar to the inclusion population, the density of inclusions spikes after Ca treatment before decreasing at the caster. This decrease is in part due to floatation and agglomeration due to artificial and natural stirring occurring from the AS to caster.

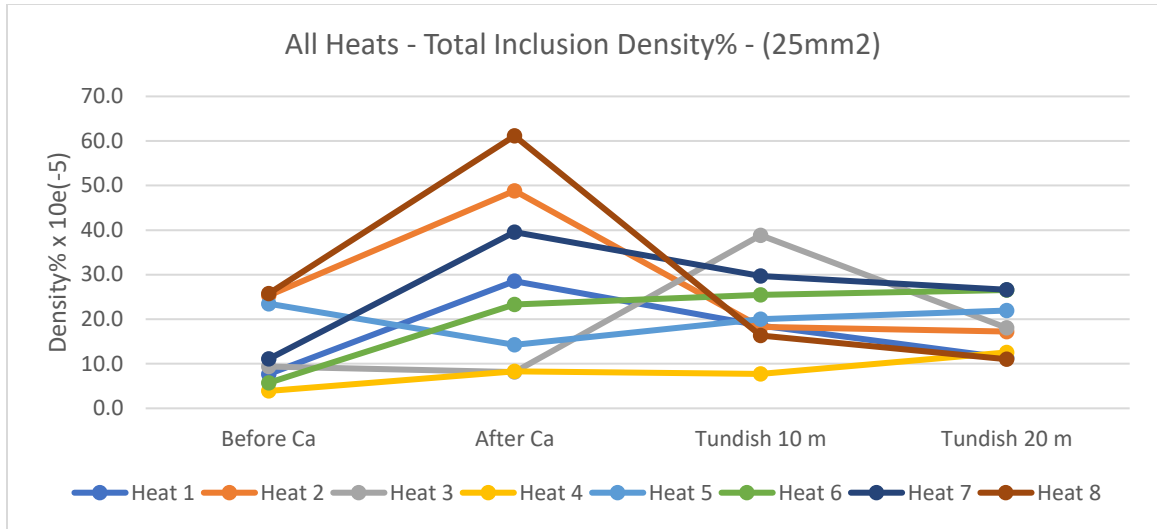


Figure 5-3. Inclusion density% of production samples from all heats

In conclusion, the population and density change give some idea into the transformation of inclusions through the process. From a macro perspective it can show the effects of processing as in the case of overblowing a heat. However, further analysis on inclusion composition will provide better understanding of effectiveness of Ca treatment on these heats.

5.2.3 Inclusion Population by Characteristic Type

The evolution of inclusion composition is studied to understand the effectiveness of Ca addition on the modification of inclusions. As discussed in [Chapter 4.6](#), ternary diagrams help understand the ratios of Ca/S/Al and determine the phase of the inclusion. The boundaries drawn on the diagram indicate if the inclusions are 100% liquid, 50% liquid, CaS, complex Ca-S-Al or under modified Alumina. These inclusion types were quantified using criteria developed through the study. Figure 5-4 shows this quantified data for Heat 1. The automatic classification system from the AZtech software was used for inclusions

that did not fall into the criteria. Additionally, classifications such as “No Classification” were removed to improve readability.

In all heats tested, Al_2O_3 inclusions are dominant in the “Before Ca” sample. This finding is expected since Al is the primary deoxidant in these heats and Al_2O_3 inclusions are formed as reaction products. In the “After Ca” samples, a significant portion of the inclusions are “50% Liquid” calcium aluminate inclusions which indicate that the modification of alumina has begun. “100% Liquid” inclusions are also present indicating a portion of the sample having the desired Ca/S/Al ratio. Additionally, there are small number of Al_2O_3 and under modified Al_2O_3 inclusions for all heats at this sample.

As the heats progresses to the caster, Heats 1,2,3,4,5 and 8 see a rise in “100% Liquid” inclusions, at the “Tundish 10m”, before falling in the final caster sample (Tundish 20m). This could be an indication of inclusions floating out (Geldenhuis & Pistorius, 2000). However, Heats 6 and 7 show different trend as the “100% Liquid” inclusion rise slightly at the Tundish 20m.

At the “Tundish 10m” sample, the portion of under modified alumina between each heat varies. Heats 1,5,7 and 8 have a portion (>3.0%) of under modified alumina inclusions relative to Heats 2,3,4, and 6 which are lower at (<1.0%). These inclusions can be detrimental to casting behaviour. This is an indication that the treatment was insufficient or of reoxidation occurring in the tundish. Reoxidation for Heat 1 is potentially a consequence of being the first heat in the tundish that is further discussed in [Chapter 5.3.6](#).

Between the Tundish 10 and 20m samples, there is a significant increase in the number of under modified alumina inclusions for Heat 3. The 10m sample had 4 while the 20m sample had 44. Other heats saw a decrease or small increase in the number of these inclusions. It

is possible that reoxidation occurred in the tundish during the casting of Heat 3, but further investigation is required to determine a root cause.

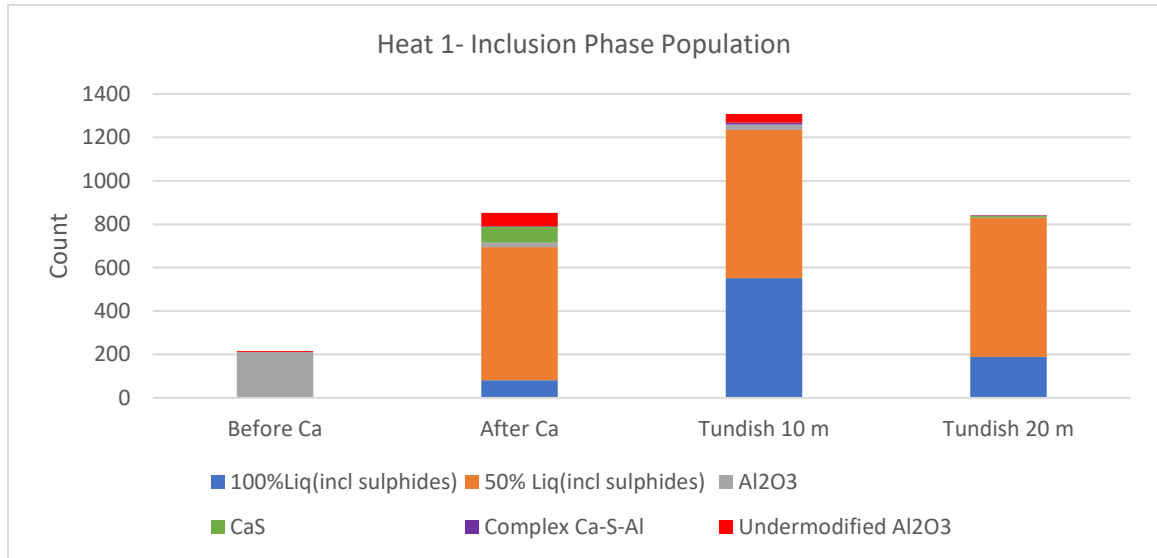


Figure 5-4. Heat 1 inclusion phase population for all samples based on ternary quantification.

5.2.4 Inclusion Area Fraction by Characteristic Type

Analyzing the total area fraction of the inclusions is an important part of understanding the effectiveness of calcium treatment. This is the area of each individual inclusion type (Al₂O₃, 100% Modified etc.) over the total area of valid inclusions. This analysis must be grouped with population to improve the conclusions made on the quality of treatment. For example, if the population of alumina particles is small but represents a significant portion of the total area fraction then this steel is not “modified well”. The area fraction also helps understand the change in phases as calcium treatment proceeds from alumina to under modified alumina to 50% or 100% liquid calcium aluminates. Once Ca is added, a large population of C_xA_x inclusions are formed and disperse through the steel. Although this is desired, the population itself does not show what percentage of the original alumina inclusions have had enough treatment time to be considered properly modified.

Figure 5-5 compares the fraction of the number of each inclusion type for all samples in Heat 1 while Figure 5-6 compares the area fraction of each inclusion type for all samples in Heat 1. The two samples to focus on are the “After Ca” and “Tundish 10 m”. When observing the population percentages, in Figure 5-5, for the After Ca sample, there is a large spike in the “50% Liquid” samples. This is an indication that most inclusions have begun achieving the ideal Ca/S/Al ratio based on the ternary diagram. From a processing standpoint, this sample marks the last point in the process where artificial (Argon lance) stirring occurs and so this sample should have predominantly modified inclusions. However, the area fraction, seen in Figure 5-6, for this sample tells a different story. Under modified inclusions cover the largest area fraction followed by alumina. This indicates that the modification process has begun but the total area fraction of harmful inclusions is significantly larger. This is an indication that stir time may not have been enough after the calcium was added. Similar patterns are observed for Heats 2 to 8. Heat 3 has distinct levels of CaS inclusions present in the area fraction diagram for this sample which could be evidence of transient CaS phases as discussed in [Chapter 2.4.5](#).

As the heats move to the caster (“Tundish 10m” sample), further modification takes place and increases the area fraction of well modified inclusions. However, as discussed in the previous chapter Heats 1,5,7 and 8 show a portion of under modified alumina and alumina. Additionally, Heat 3 sees a 19.7% increase in area fraction of under modified alumina inclusions, from the Tundish 10 to 20 m sample which as discussed may be due to reoxidation in the tundish. These inclusions can be detrimental to casting behaviour by building and clogging at the SEN.

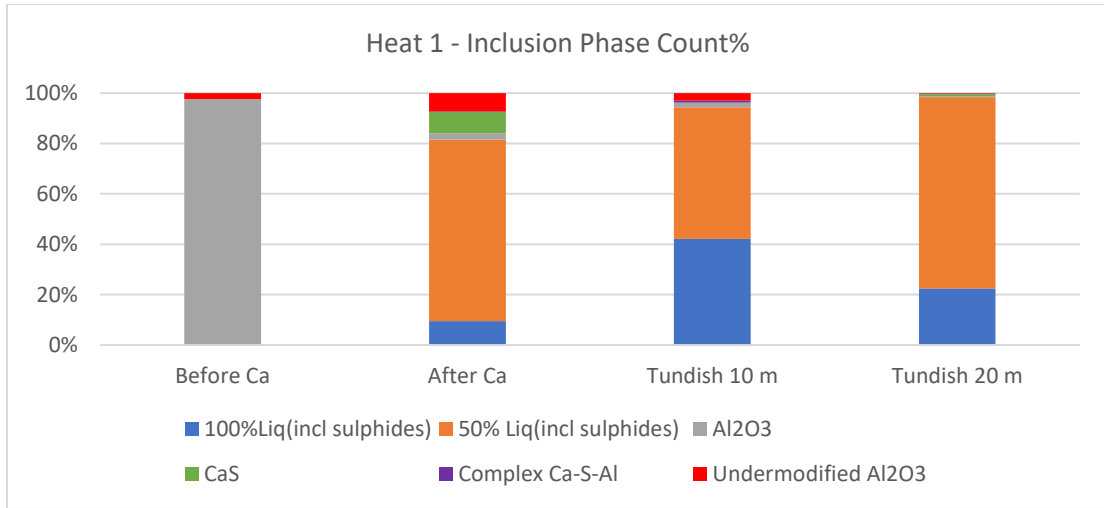


Figure 5-5. Fraction of the number of each inclusion type for all samples in Heat 1

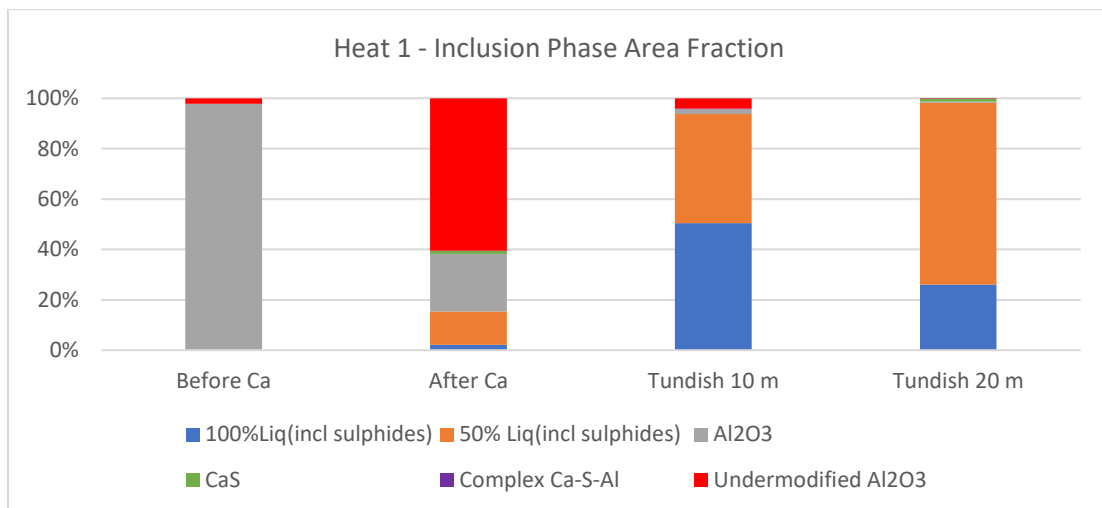


Figure 5-6. Area fraction of each inclusion type for all samples in Heat 1.

5.2.5 Inclusion Density by Characteristic Type

Density by individual inclusion type helps understand how well the heat is treated/modified. As an example, Figure 5-7 will be used to describe the importance of density for individual inclusion types.

Going forward, for clarity purposes, under modified alumina and alumina inclusions will be added together and shown in the graphs as both inclusions can contribute to clogging behaviour.

This specific sample type (“Tundish 10m”) was used as an example, as at this point in the casting process, the steel should, in theory, be considered properly modified and clean to ensure a smooth cast. Heat 3 has the highest total density among all other heats; however, it consists primarily of desirable inclusions i.e., 50 and 100% liquid inclusions. Heat 5 has a higher proportion of under modified alumina and alumina ($3.41\% \times 10^{-5}$) inclusions although low in total density. Therefore, although Heat 3 has a larger density of inclusions, it is less detrimental to the casting behaviour than Heat 5.

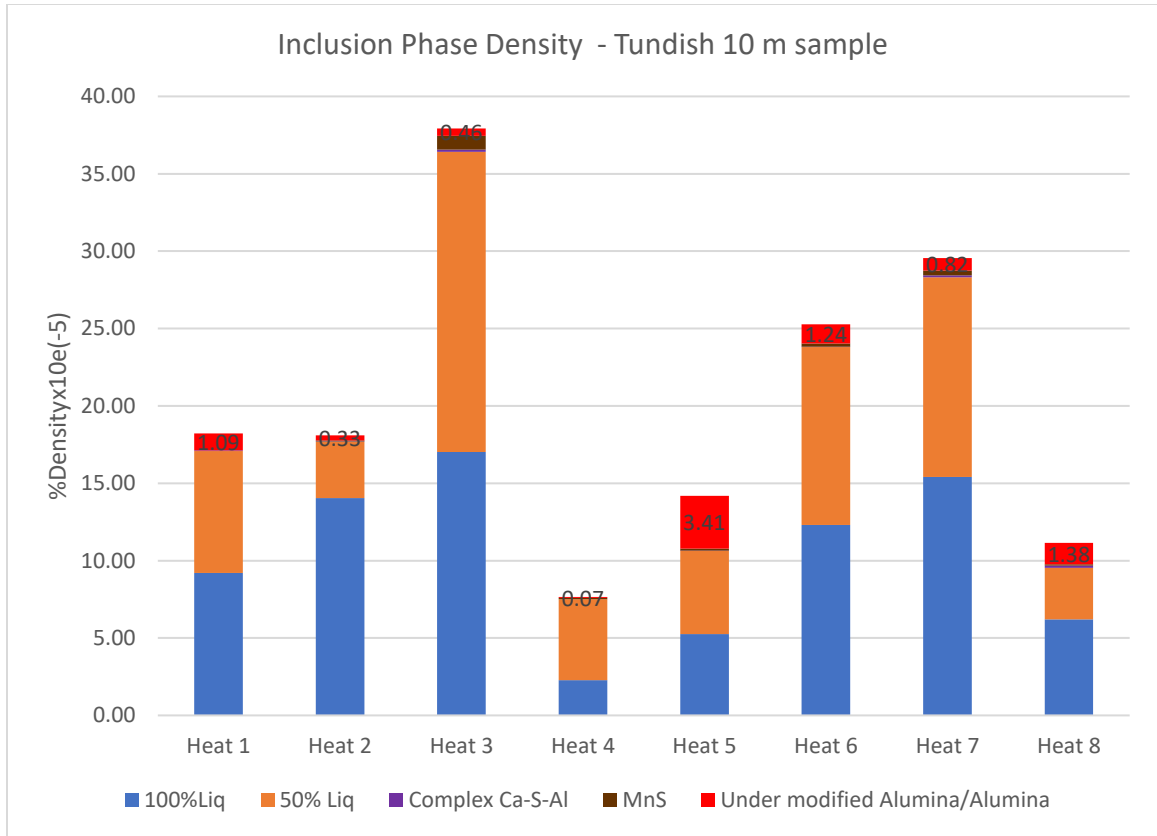


Figure 5-7. The density of various inclusion types detected in Tundish 10m samples for all heats.

Density calculations are useful to compare heat cleanliness between themselves. For determining how clean the steel is, total density is not as valuable as the density of individual types as seen with Heats 3 and 5.

5.2.6 Inclusions Size (ECD) – Equivalent Circular Diameter

The inclusion size distribution is another parameter for determining steel cleanliness. The diameter of an inclusion can assist in identifying how inclusions agglomerate and start to float up into the slag. As discussed in [Chapter 3.3.2](#), the straightforward way to remove inclusions is to float them out through artificial and natural stirring. Larger agglomerated

inclusions are easier to float through Stokes Law (A. L. V. da Costa e Silva, 2018; Zheng & Zhu, 2016).

The diameter transformations for Heats 1, 2, 3 and 7 are shown in (Figure 5-8, Figure 5-8, Figure 5-9, Figure 5-11, respectively). For Heat 1, the “After Ca” sample shows a spike in the population of smaller inclusions (1- 1.5 microns) and then as the heat moves to the tundish, the smaller inclusions grow, and agglomerate and their population starts to decrease as larger inclusions increase. Heat 3 has a small population of small inclusions in the “After Ca” sample which then sharply increase in the tundish 10 and 20 m sample.

These patterns do not follow for the remaining heats as Heat 2 and later in the sequence Heat 7 see a sharp decrease in the number of smaller inclusions at the tundish. Other heats shown in the [Appendix D](#) portray the same pattern as Heat 2 and 7.

The reasons for the difference in Heat 1 are potentially due to being the first heat on the tundish. When this ladle opens at the caster, it pours into an empty tundish which must be filled to ~35 tonnes before casting begins. As it fills, the turbulent movement of the steel allows added exposure to the air which may oxidize the steel forming newer and smaller inclusions. Additionally, the turbulence may disturb loose spray refractory material before stabilizing. These can create or add more inclusions to the steel which may explain the comparatively large quantity of small inclusions in Heat 1.

For Heat 3, the conclusion for the pattern is unknown but there are a few potential reasons. As discussed previously, the “After Ca” sample showed significantly lower quantities of inclusions relative to the other samples so this sample may not be representative and may have been taken too early or improperly. Furthermore, as seen in the population, area fraction and density data the “Tundish 10m” sample for Heat 3 has primarily desirable inclusions. However, between the “Tundish 10” and “20m” samples, there is a sharp increase in undesirable inclusions.

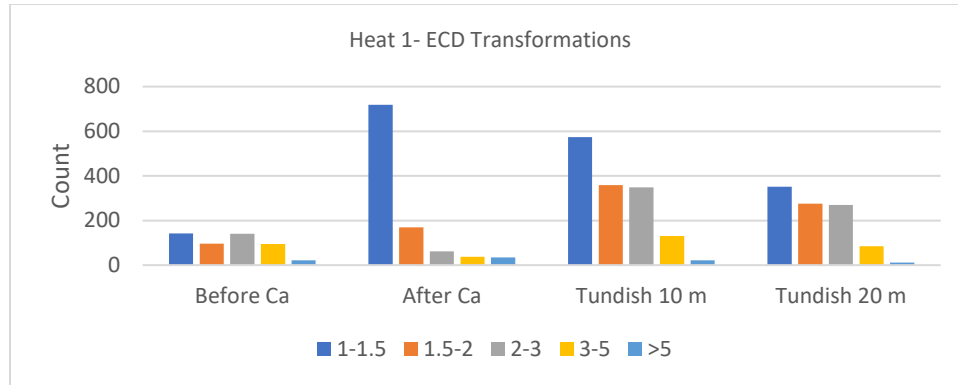


Figure 5-8. Heat 1 ECD transformations for all samples. Showing a slow drop in inclusion size

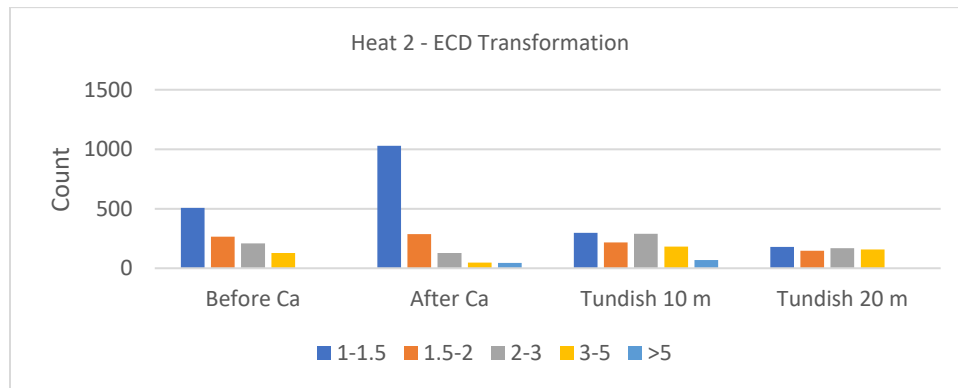


Figure 5-9. Heat 2 ECD transformations for all samples. Shows a sharp drop in inclusion size at the Tundish 10m

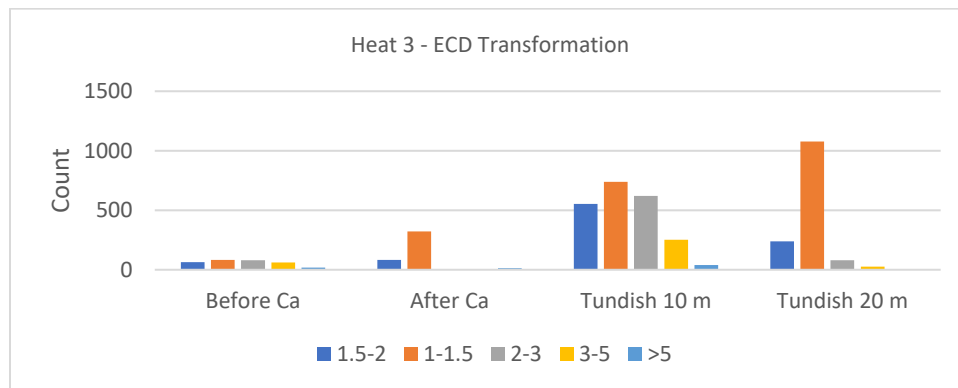


Figure 5-10. Heat 3 ECD transformations for all samples. Shows an increase in small inclusions at the Tundish 10 and 20m

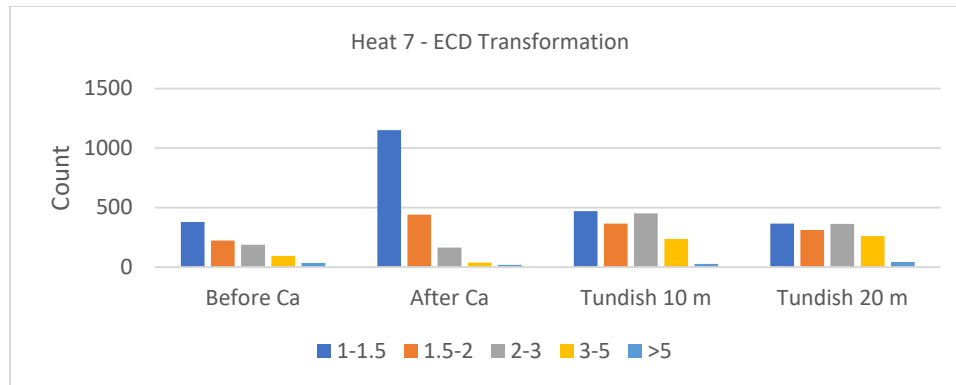


Figure 5-11. Heat 7 ECD transformations for all samples. Similar to Heat 2, it shows sharp drop in inclusions size at the Tundish 10m

This analysis shows the natural floatation and agglomeration of inclusions through the process. This analysis can also portray potential oxidization later in the process which was indicated by a rise in smaller inclusions. It would be valuable to add additional data to this analyse to see if these patterns emerge and help further investigative efforts.

5.2.7 Slag Sample Analysis

Slag components such as FeO and MnO play a major role in the formation of alumina further down the process through reoxidation. As discussed in [Chapter 3.1.5](#), slag samples from heats 1, 2, 3, 5, and 8 were taken before and after Ca treatment. Figure 5-12 compares the total FeO and MnO slag components of three samples from these heats. The “Start” sample indicates the beginning of general treatment of the heat. Unfortunately, due to shop conditions and timing, operators were not able to take slag samples for the remaining heats. For all heats available, the total FeO and MnO decrease over the addition of Ca and general processing of the heat.

Although the FeO and MnO components are high at the beginning of the heat, it is unclear if this played a part in the development of alumina inclusions. Ideally additional data is needed and will be one of the focuses for future studies.

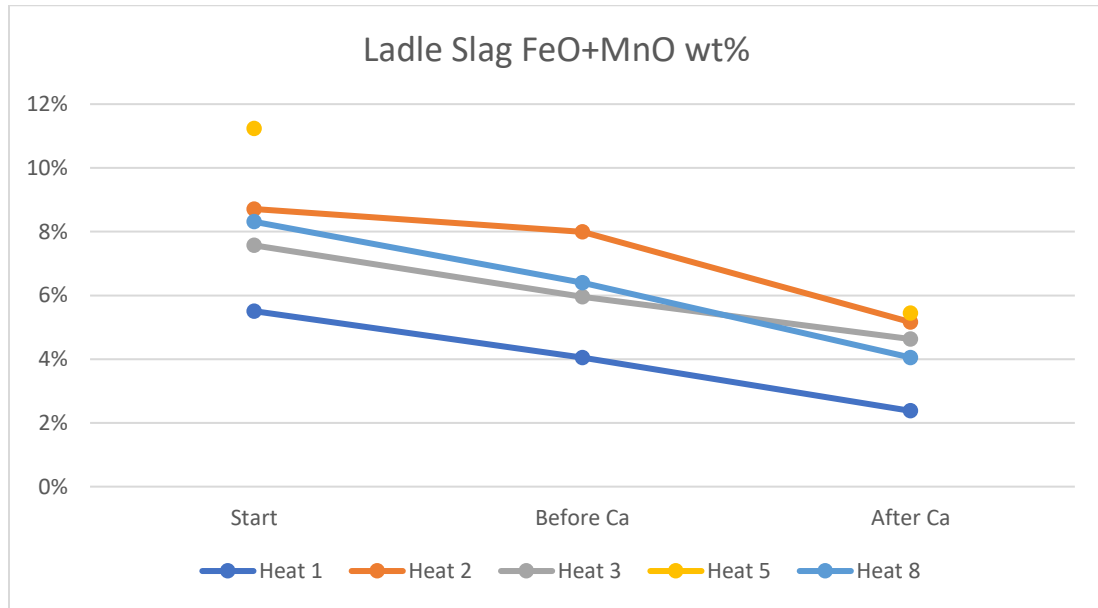


Figure 5-12. Ladle slag FeO+MnO wt% transformation before and after Ca treatment.

5.2.8 Modified Ca/Al Ratio Results

The modified Ca/Al ratio for individual inclusions incorporates a sulphur component due to the duplex nature of calcium aluminate inclusions. The inclusions data from every sample, after calcium treatment, incorporated this modified ratio (Equation (2-26)) and was plotted in a box plot showing the shifts in value through the casting process. This is shown in Figure 5-13.

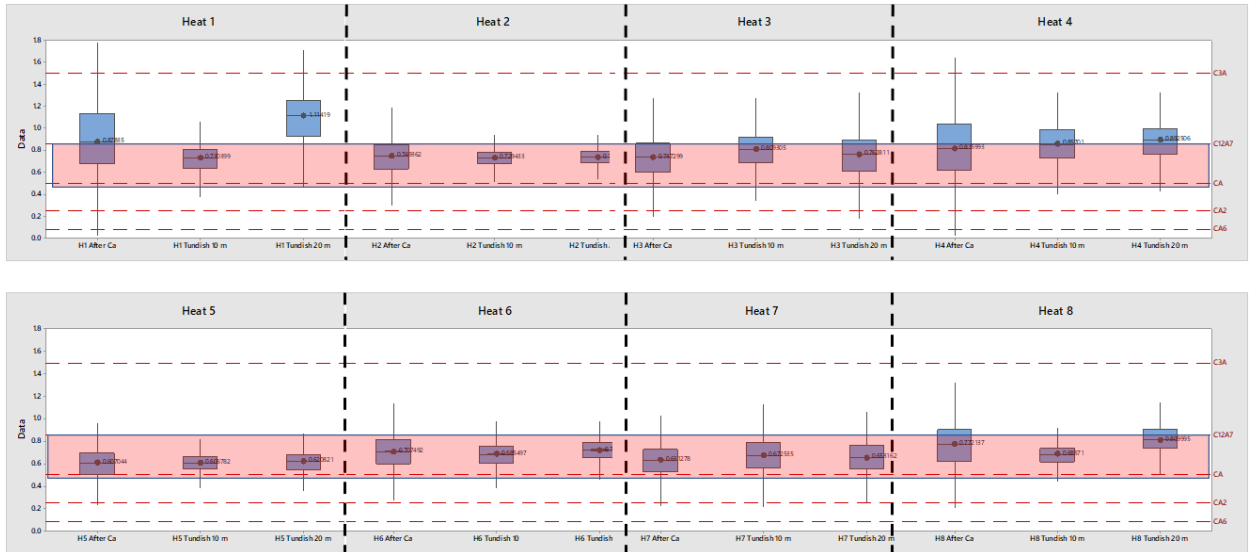


Figure 5-13. Modified Ca/Al ratio for all heats after calcium treatment. Red dashed lines represent C_xA_x ratios.

The ratios noted in the Y-axis are the ratio of Ca content to Al content of the different C_xA_x types found in the CaO-Al₂O₃ phase diagram. In CaO·Al₂O₃, there are two Al atoms for every one Ca atom. So, for example, C₁₂A₇ is $\frac{C_{12}}{A_{7*2}} = \frac{12}{14} \cong 0.85$. The ideal area highlighted on the boxplot corresponds to the areas noted in [Chapter 3.3.4](#) or Figure 2-21. These areas are where C_xA_x are liquid/semi-liquid in nature noting sufficient modification and eventually smooth casting.

As discussed in [Chapter 5.7.6](#), the first heat of the tundish depicts different behaviours compared to other heats. This is due to the tundish filling procedure as the steel interacts with air and loose refractory particles break up and are entrained in the liquid. Heats 2 to 4 and 6 to 8 are primarily in the ideal zone with Heat 5 shifting towards non-ideal areas. This can be an indication of insufficient modification, however, this heat itself did not clog but could affect subsequent heats in the tundish

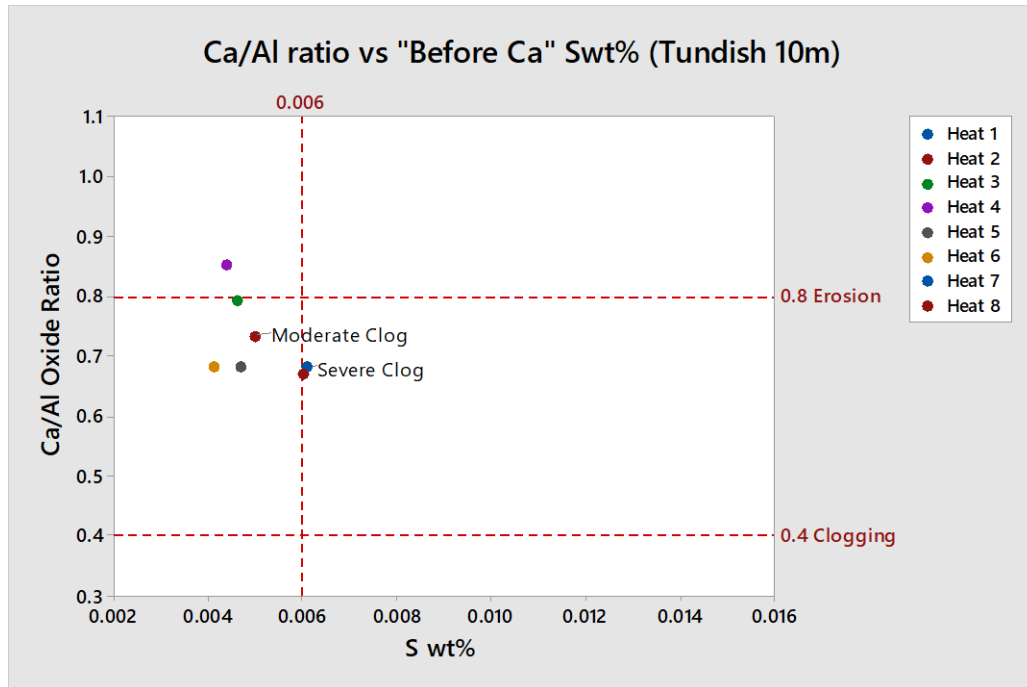


Figure 5-14. Relationship between Ca/Al ratio and the pre-Ca treatment S wt% for all heats.

Figure 2-25 describes the effects of the pre-Ca treatment sulphur wt% and Ca/Al ratio on the caster processing. As discussed in [Chapter 2.4.6](#) work done by Story et al describes the difficulty in using this relation for sulphur levels less than 0.007 wt%. These levels can cause the oxide Ca/Al ratio to be higher than predicted by equilibrium calculations (Story & Asfahani, 2013; Verma et al., 2011a, 2011b). However, Story et al mentions that at these low sulphur levels, care must be taken to limit the amount of CaSi wire added. The Ca/Al ratio increases rapidly as sulphur decreases which can produce inclusions that erode the caster pouring system (Story & Asfahani, 2013). It is then possible that Heat 3 and 4, with the highest Ca/Al ratios, may have formed corrosive inclusions and potential refractory erosion. This was not the case as described in the following chapter.

These methods of analyzing the effectiveness did not show anything that stood out. There are a few factors at play that may affect this type of analysis. The sample is taken to represent a large quantity of steel and therefore it would be ideal to test additional samples

of the same heat at different points during the cast. Furthermore, additional samples with varying sulphur levels can help paint a broader picture of its effects in the casting process. The ideal Ca/Al ratio has a large range. The range in the diagram conveys a typical steelmaking temperature, however, samples are sometimes taken at specific temperatures below or above the typical value. These methods require additional refining and will be part of future investigative efforts.

5.2.9 Correlating Population, Area Fraction, and Density to Clogging behaviour.

Some amount of clogging occurs in every tundish as inclusion particles build up at the SEN, thereby raising the average stopper rod height slowly. The current indications of clogging are based on visual quantification of the stopper rod behaviour as described in [Chapter 3.2.4](#) and [Chapter 5.5](#). Normalizing the stopper rod data by taking the average height over the course of the cast helps understand the clogging behaviour. This was done by taking the stopper rod height at every 5 meters of steel cast including height at the start. As is the purpose of this study, it is important to correlate the inclusion data to the corresponding clogging behaviour. This will help understand the effectiveness of the current treatment methods and what can be done to help improve the process.

The following graphs compare the stopper rod positions to the population, area fraction and density of the “Tundish 10m” sample for all heats in sequence. The stopper rod trends are shown for both strands as the facility have a dual strand caster. The tundish feeds both strands (two SENs) simultaneously. The “Tundish 10m” was used as at this point in the cast, the steel should be considered clean for casting purposes. [Appendix E](#) has the same comparison for the “Tundish 20m” sample. The numerical data points shown for each bar graph display the “under modified alumina/alumina” inclusions. Displayed on the graph are the heats that visually showed moderate (Heat 2), or severe (Heat 7) clogging behaviour

based on the techniques used in [Chapter 2.3.4](#). Along with Heat 1, all other heats were considered a good cast.

Figure 5-15 shows the inclusion types count for the heats in sequential order. Heat 1 has 63 “under modified alumina/alumina” inclusions but shows a low stopper rod-height comparatively. The reason for minimum clogging is likely due to this being the first heat on the tundish and it therefore has new SENs with fully opened ports. The following heat (Heat 2) does have a higher stopper rod height although having a much lower count at 13 “under modified alumina/alumina” inclusions. This may be an indication of a previous heat affecting a subsequent heat. Heat 1 may have begun building the clog at the SEN which eventually affected Heat 2.

Past that, Heat 3 has a large quantity of total inclusions (1800+) but shows a decline in the average stopper rod height compared to the previous heat. This is a good example of quality and not the quantity of inclusions present in the steel. Most inclusions in this sample have been properly modified, with only 10 “under modified alumina/alumina” inclusions, which have allowed for a smoother casting process. This low stopper rod height is maintained until Heat 5 where 72 “under modified alumina/alumina” inclusions were detected. Heats 5,6, and 7 have a significant portion of “under modified alumina/alumina” which is reflected in the rise in the average height for both strands until the severe clogging event at Heat 7. Heat 8 sees a drop in rod position although there are a significant number of “under modified alumina/alumina” inclusions (40) which is likely due to operators releasing the previous heat’s clog through O2 lancing, flushing and general wariness of clogging potential for Heat 8.

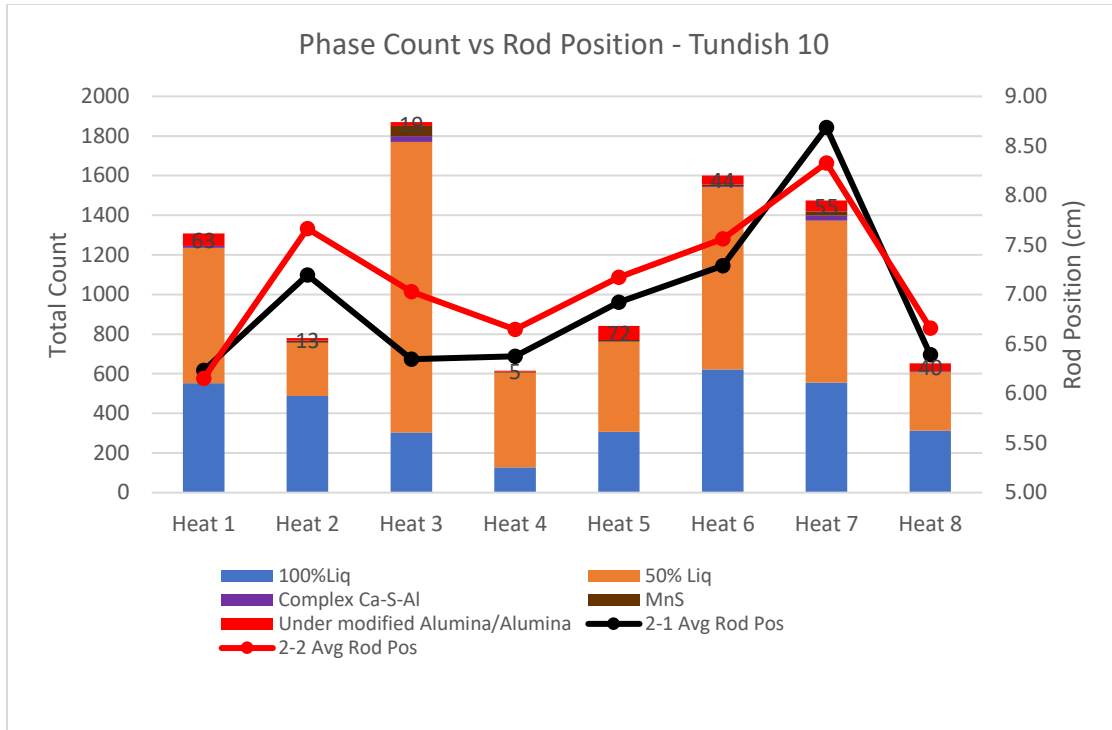


Figure 5-15. Tundish 10m inclusion phase population vs caster rod position for all heats.

As discussed in Chapters 5.3.4 and 5.3.5 density and area fraction graphs, shown in Figure 5-16 and Figure 5-17, can help validate the inclusion count.

Heat 2 had a low count value (13) for “under modified alumina/alumina”, similar to Heat 3 and 4, however the density ($0.33\% \times 10^{-5}$) and area fraction (1.8%) of said inclusions are higher comparatively. This, along with “under modified alumina/alumina” from Heat 1, may also play a part in Heat 2 having a slightly higher stopper rod height. Heats 1,5,6,7 and 8 have significant density and area fraction amounts for “under modified alumina/alumina” with Heat 5 having the highest overall, at $3.41\% \times 10^{-5}$ and 17.1% for both categories respectively.

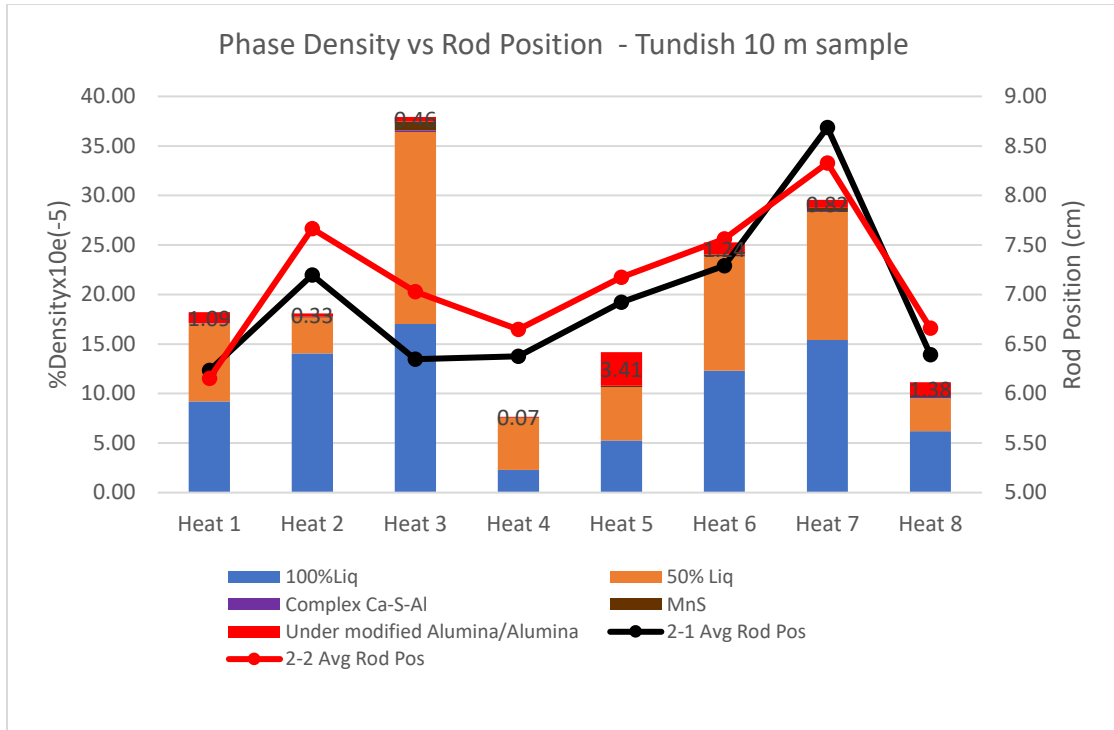


Figure 5-16. Tundish 10m inclusion phase density vs caster rod position for all heats

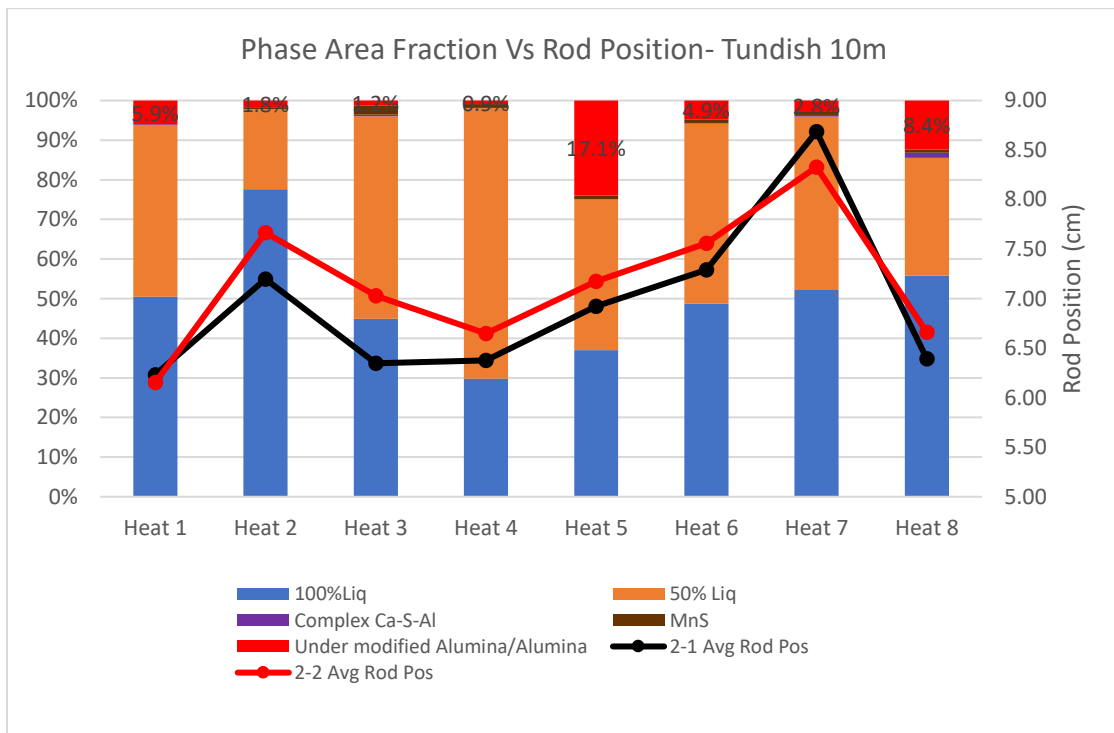


Figure 5-17. Tundish 10m inclusion phase area fraction vs caster rod position for all heats

Using these techniques has helped validate the hypothesis that “under modified alumina/alumina” affected the casting behaviour. These techniques can be used, with additional data, to help model the clogging potential at the facility. With added data, processing parameters such as alloying, temperature adjustments or stir efficiencies can be isolated to understand their effects.

6. Summary and Conclusions

Calcium treatment can be used to modify inclusions to a semi liquid/liquid state which can improve castability, yield and production pace. Understanding the effects of such treatment on castability in an industrial setting is the focus of this study. In this work, 8 heats, or ladles, of calcium treated steel were sampled throughout the process and analyzed for inclusion behaviour using an automated SEM. Additionally, SEM processing parameters and data processing techniques were developed to improve the quality and time of data analysis. These heats were compared to the casting behaviour to determine a correlation between the inclusion modification and its subsequent clogging behaviour. The following results were obtained from this study:

- This study will provide the industrial partner the techniques to expand their inclusion analysis capabilities.
- SEM parameter studies for KeV and sample homogeneity were conducted which improved the total inclusion analysis run time and quality of data.
- Ternary diagram techniques developed from this study improved the interpretation of the inclusion data making it easier to compare to castability on a heat-by-heat basis
- By using the average stopper rod height, smaller changes in clogging behaviour were noticeable and improved the analysis.
- The severity of clogging was not directly affected by the total number of inclusions in the sample. The Tundish 10m sample for Heat 3 had the highest population (88 incl/mm²) but showed minimal clogging behaviour while the same sample for Heat 5 displayed lower inclusion population (53 incl/mm²) and some clogging behaviour.
- Combining inclusion type population and area fraction percentages improves the understanding of the effectiveness of calcium treatment. For Heat 1 After Ca sample, a large quantity (68.8%) of 50% liquid calcium aluminates is seen, however, the area fraction shows that only a small proportion of alumina had begun modification.

- The inclusion density can help describe the difference in steel cleanliness between individual heats, however a greater density does not necessarily mean dirtier steel. Heat 3 had the highest total density ($39 \times 10^{-5}\%$) but had predominantly desirable inclusions while Heat 5 had a low total density ($20 \times 10^{-5}\%$) but a large percentage of undesirable under modified alumina.
- For heats, other than Heat 1 and Heat 3, the tundish samples show a sharp decrease in smaller sized inclusions and an increase in larger ones. This can be due to agglomeration allowing larger inclusions to float into the slag. Heat 1 is the first heat and therefore as the tundish fills the steel experiences a longer period of air exposure, compared to subsequent heats, therefore oxidizing and forming new inclusions. The steel flow may also disturb loose refractory particles as it fills.
- Heat 3 displayed potential reoxidation in the Tundish between the 10m and 20m sample. The 10 m sample showed primarily desirable inclusions which corresponded well with the clogging behaviour. The Tundish 20m displayed a significant gain in undesirable inclusions but subsequently did not negatively affect the clogging behaviour. Further investigation is required.
- Using these analysis techniques, the “Tundish 10m” sample for Heats 5,6,7 showed evidence of under modified alumina/alumina inclusions which steadily increased the average stopper rod height eventually leading to a severe clogging event at Heat 7. Heats 2,3 and 4 showed minimal “under modified alumina/alumina” and subsequently lower average stopper rod height. Heat 8 had a significant portion of “undermodified alumina/alumina” inclusions but did not show signs of severe clogging due to operators releasing the clog on the previous heat.
- The study for these 8 heats found that the calcium modification was inconsistent which was reflected in the subsequent clogging behaviour. This is in part due to the processing inconsistencies when this steel was made.

7. Future Work

As discussed in the previous chapter, there is a significant amount of additional work that needs to be conducted to improve the effectiveness of the analysis. The process is complex and multiple variables can affect the inclusion behaviour.

- This study modified the SEM parameters to improve the run time and quality of data. Further work can be done on reducing the post processing time by implementing the methods directly in the AZtech feature analysis software.
- The modified Ca/Al ratio was useful in observing bulk modification of the inclusions and their location in the ideal ratio range. However, the ideal ratio covers a significant range of temperature values and therefore should be broken down further due to the changes in liquid steel temperature during processing.
- The effects of reheating on the inclusion behaviour were studied but did not show a clear trend. This may be due, in part, to the reheated heats being processed at the VD where the stir is vigorous and longer. To reduce variability, heats treated at the VD with and without heating should be sampled.
- A steel cleanliness report, specific to the industrial partners process, can be developed based on improving the data quantity. This can be used for process investigations. This information would include general statistics on desirable and undesirable inclusions that affect clogging.
- Use the techniques developed from this work to model inclusion formation and improve the predictability of clogging behaviour.
- For all future work cases discussed, increased data quantity can isolate processing variables that are not controllable such as reheating, alloying, stir rates or slag practices etc.
 - Samples can be taken after every 5 meters cast to understand reoxidation effects or the continuous modification and agglomeration of inclusion

particles during the cast. Likewise, at the VD or AS, additional samples can be taken during the process and isolate for variables.

- Although additional sampling can be helpful to understanding the inclusion behaviour, for practicality reasons, it is also important to understand the validity of samples currently taken as standard practice. Other than modelling, this project aims to provide investigative techniques for clogging that occurs in the process. Therefore, being able to confidently use the samples available, after the fact, is important to acknowledge.

A. Inclusion Type Population

The following graphs describe the inclusion type population for Heats 2 to 8.

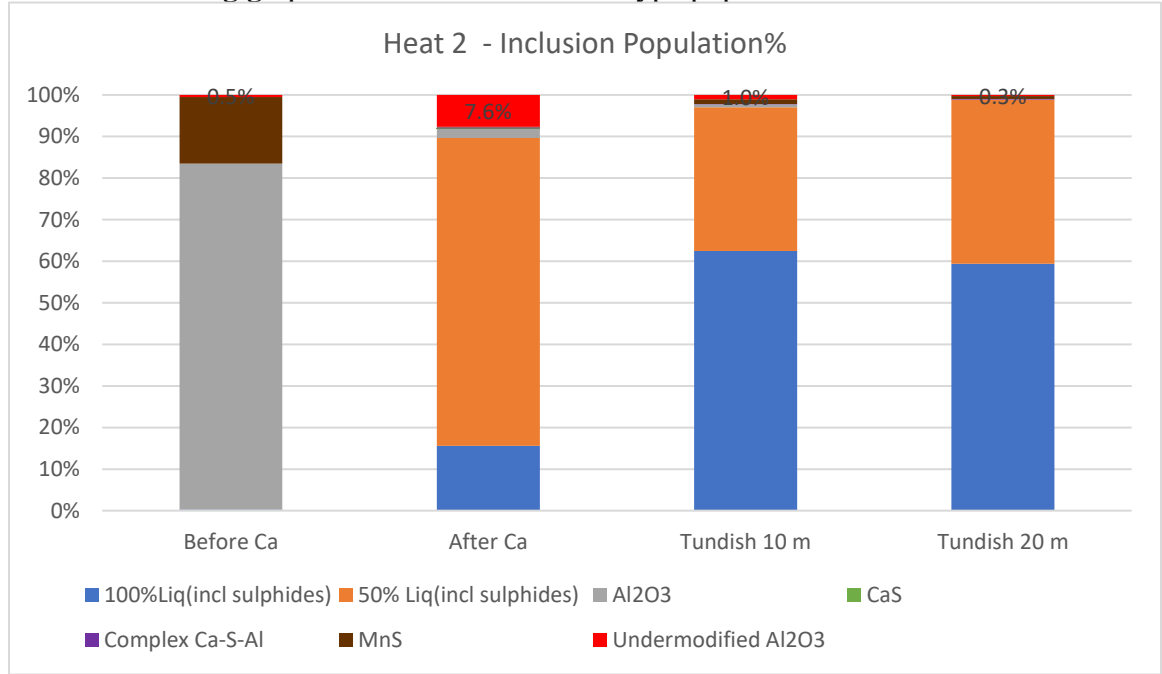


Figure A-1. Heat 2 inclusion phase population for all samples based on ternary quantification

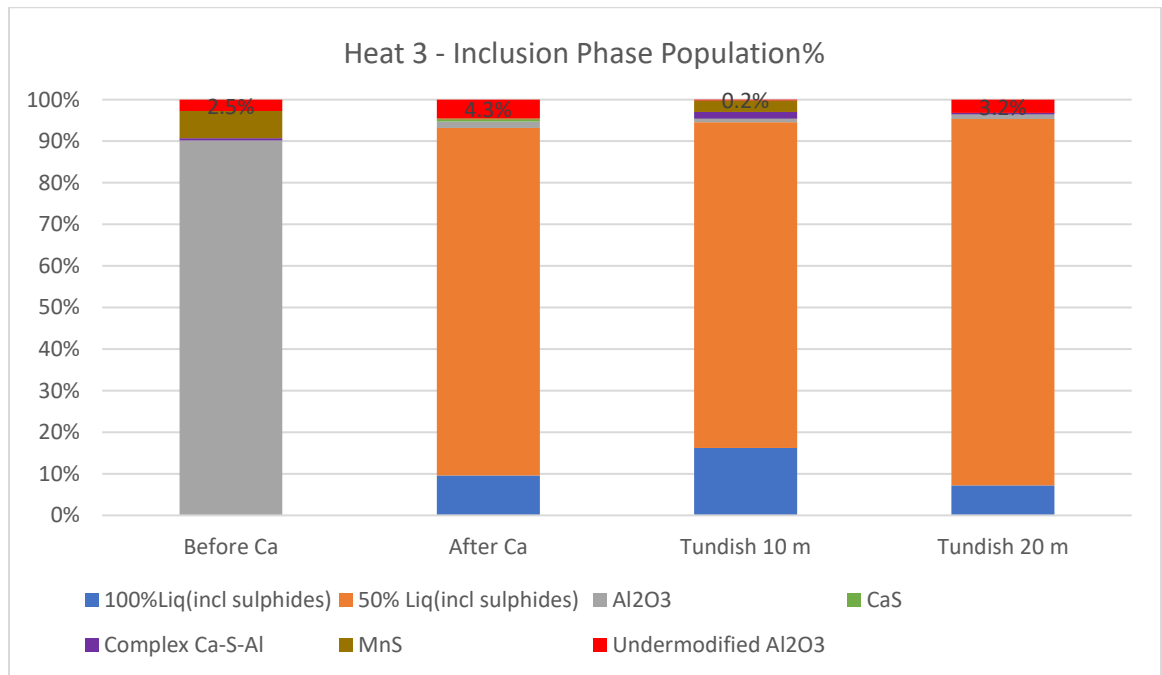


Figure A-2. Heat 3 inclusion phase population for all samples based on ternary quantification.

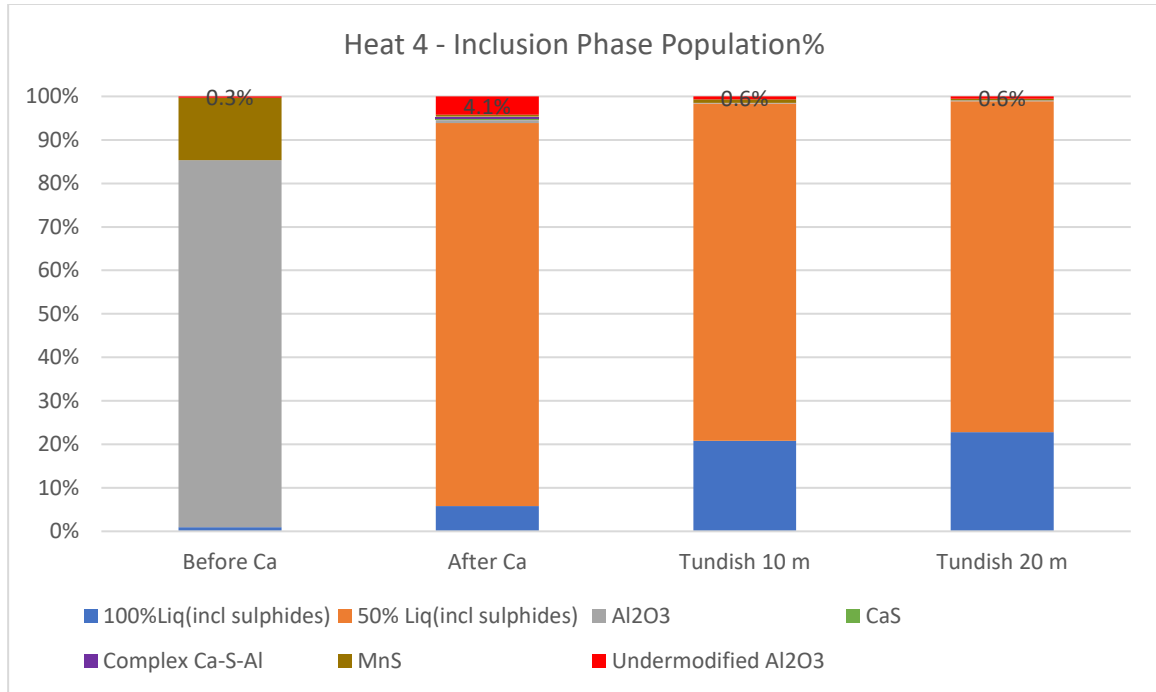


Figure A-3. Heat 4 inclusion phase population for all samples based on ternary quantification.

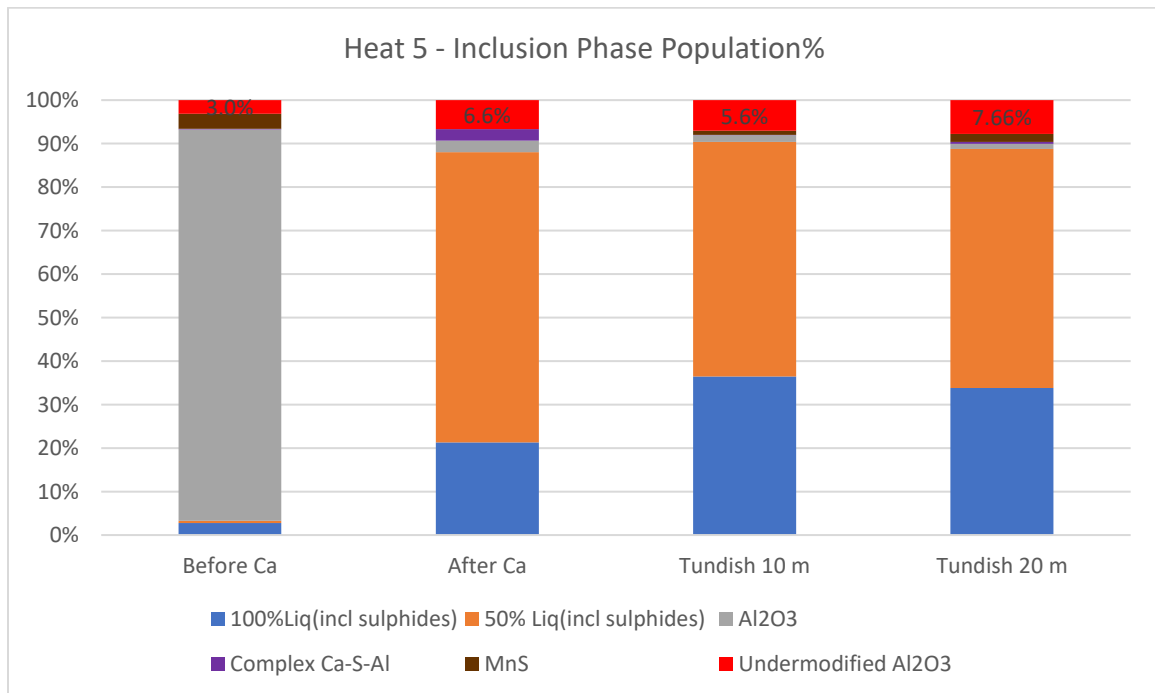


Figure A-4. Heat 5 inclusion phase population for all samples based on ternary quantification.

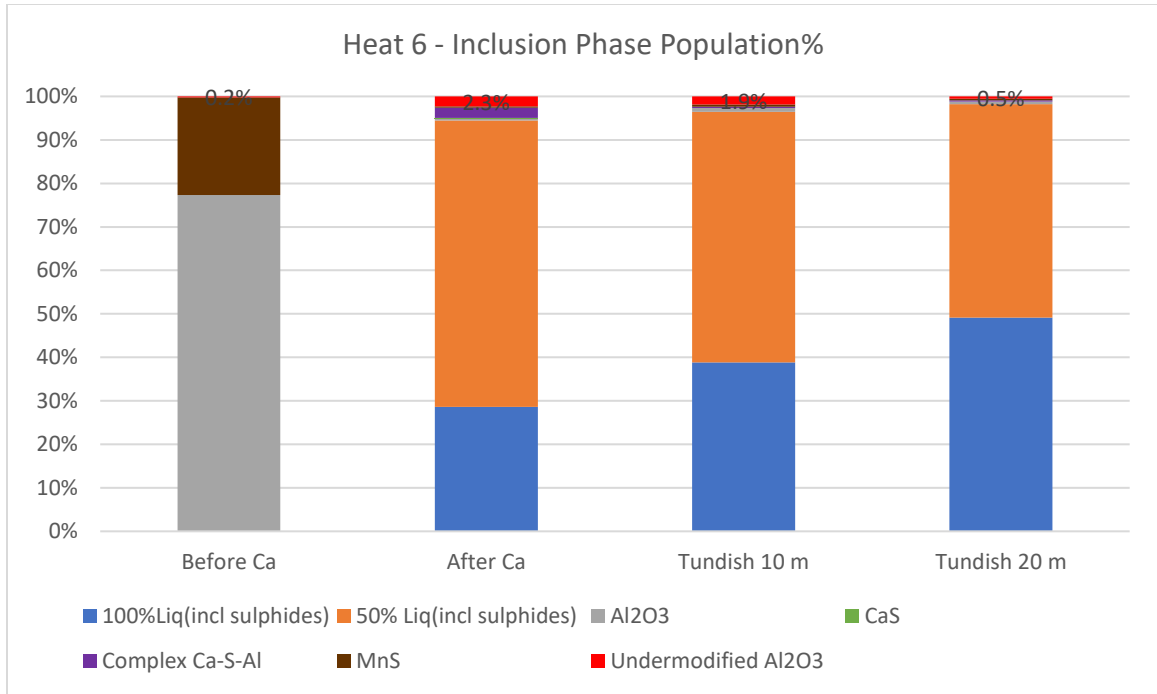


Figure A-5. Heat 6 inclusion phase population for all samples based on ternary quantification.

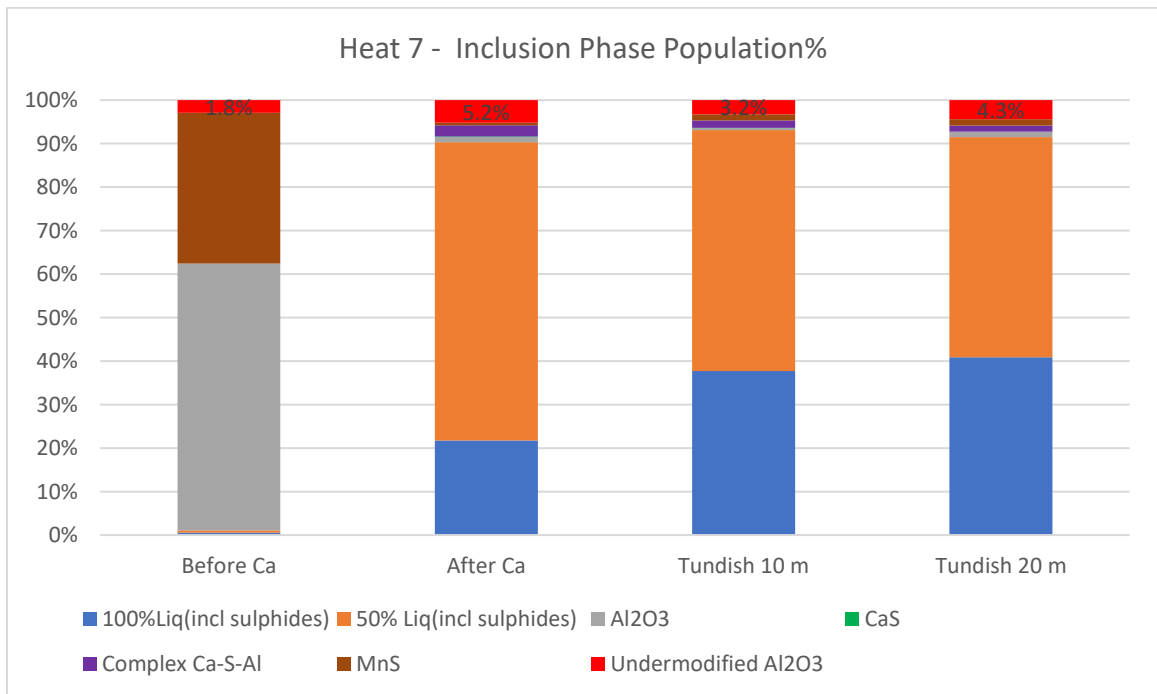


Figure A-6. Heat 7 inclusion phase population for all samples based on ternary quantification.

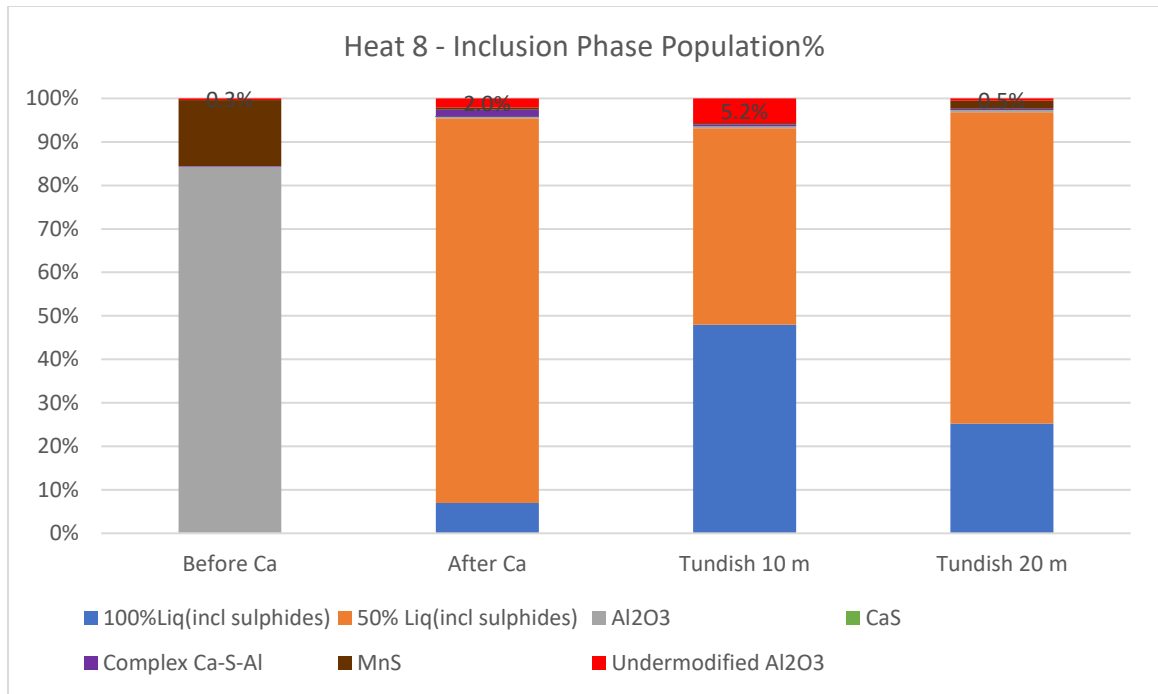


Figure A-7. Heat 8 inclusion phase population for all samples based on ternary quantification.

B. Inclusion Phase Area Fraction

The following graphs describe the inclusion phase area fraction for Heats 2 to 8.

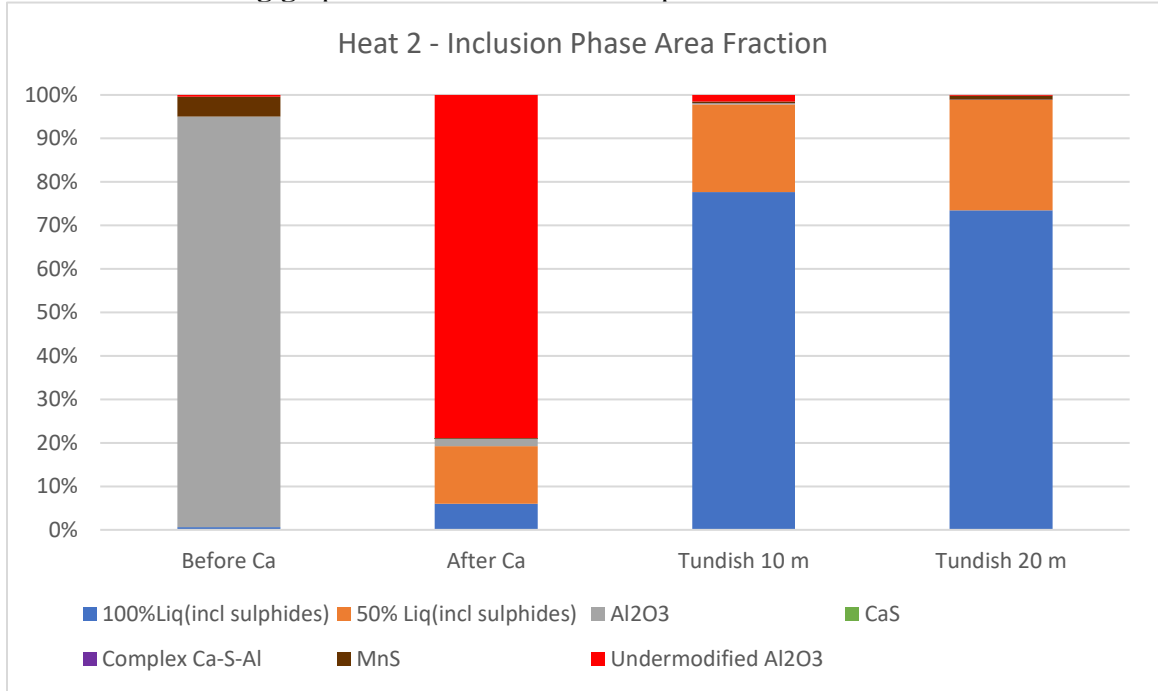


Figure B-1. Area fraction of each inclusion type for all samples in Heat 2

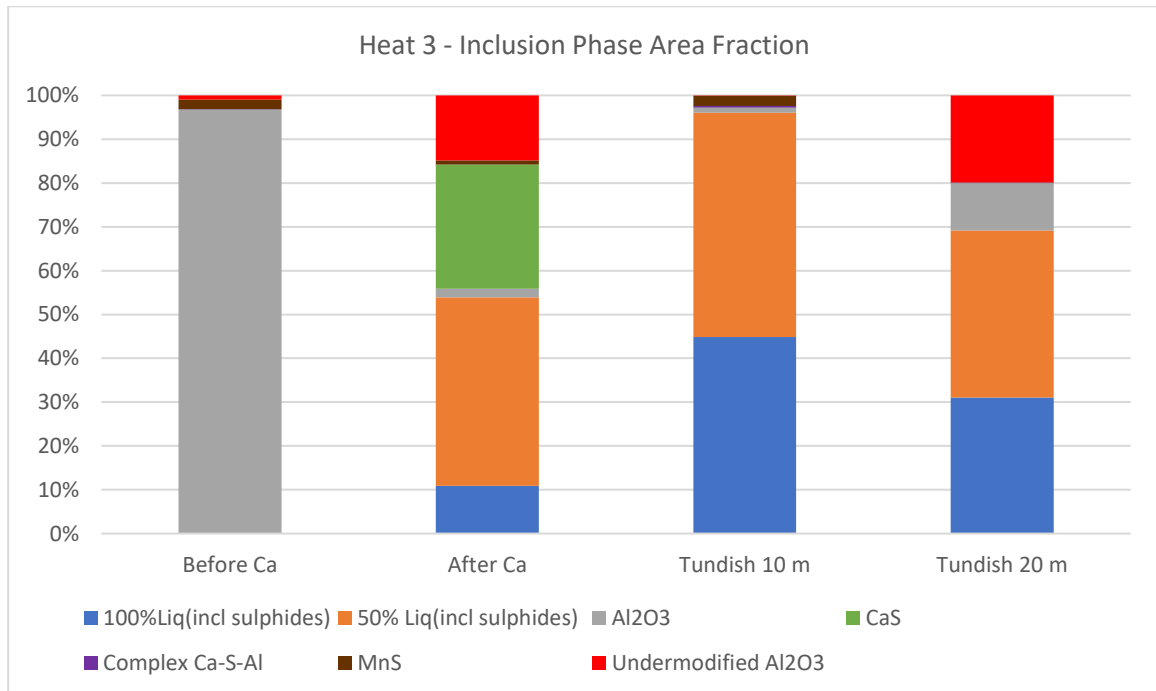


Figure B-2. Area fraction of each inclusion type for all samples in Heat 3.

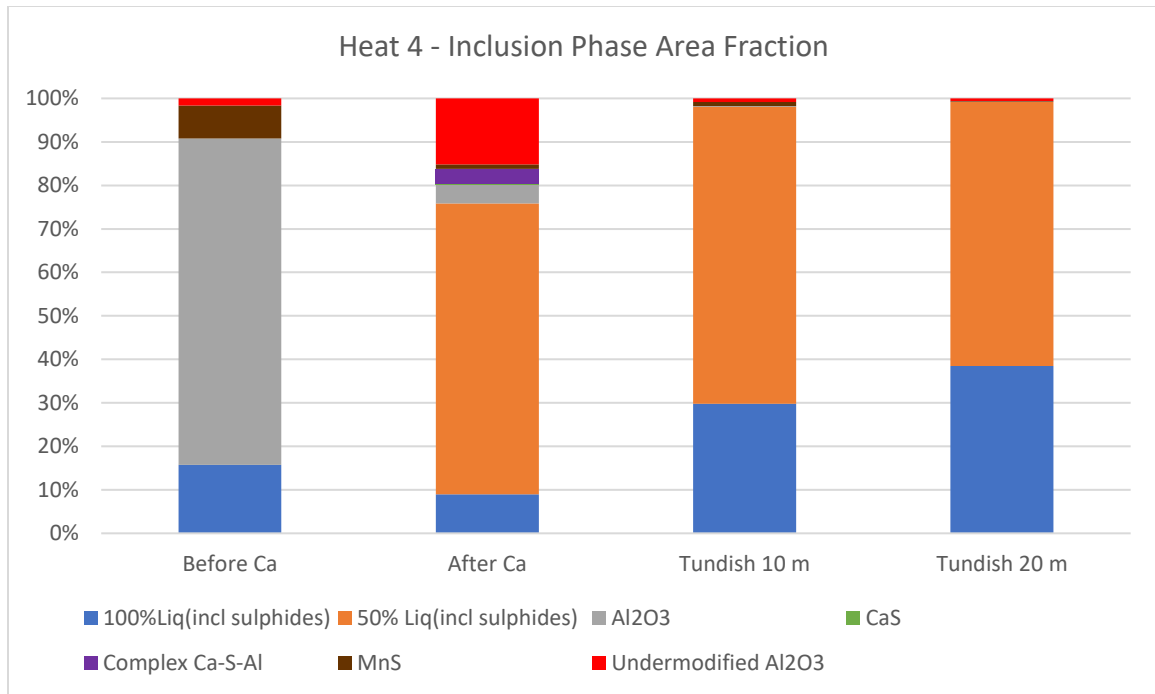


Figure B-3. Area fraction of each inclusion type for all samples in Heat 4.

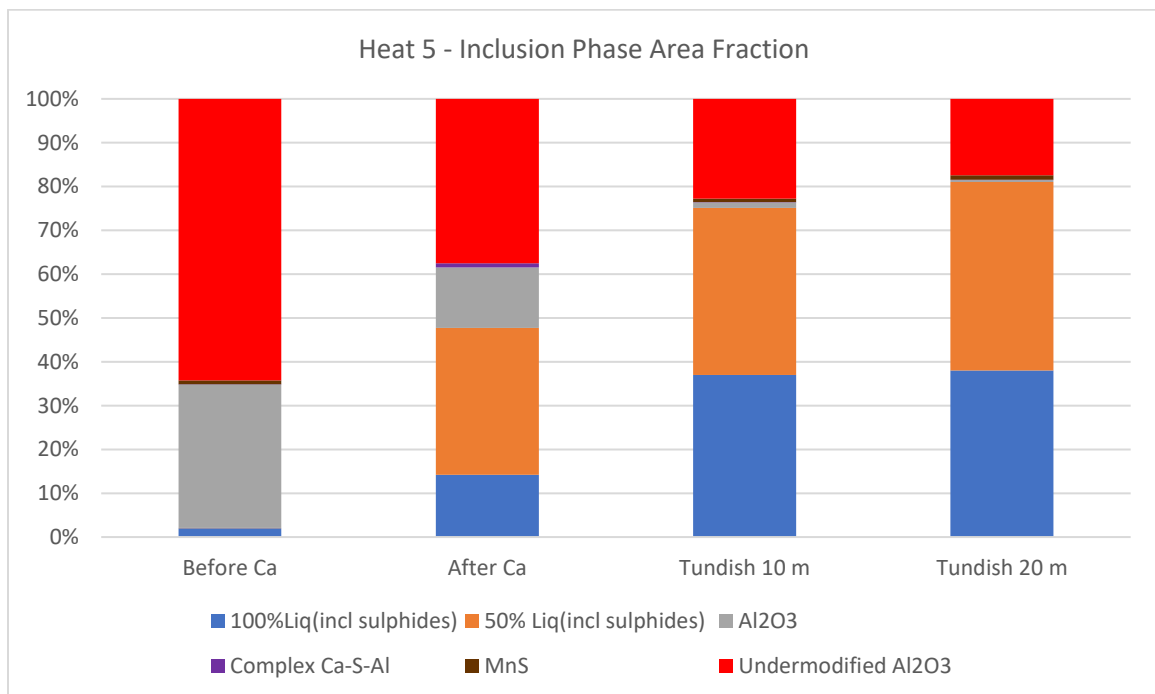


Figure B-4. Area fraction of each inclusion type for all samples in Heat 5.

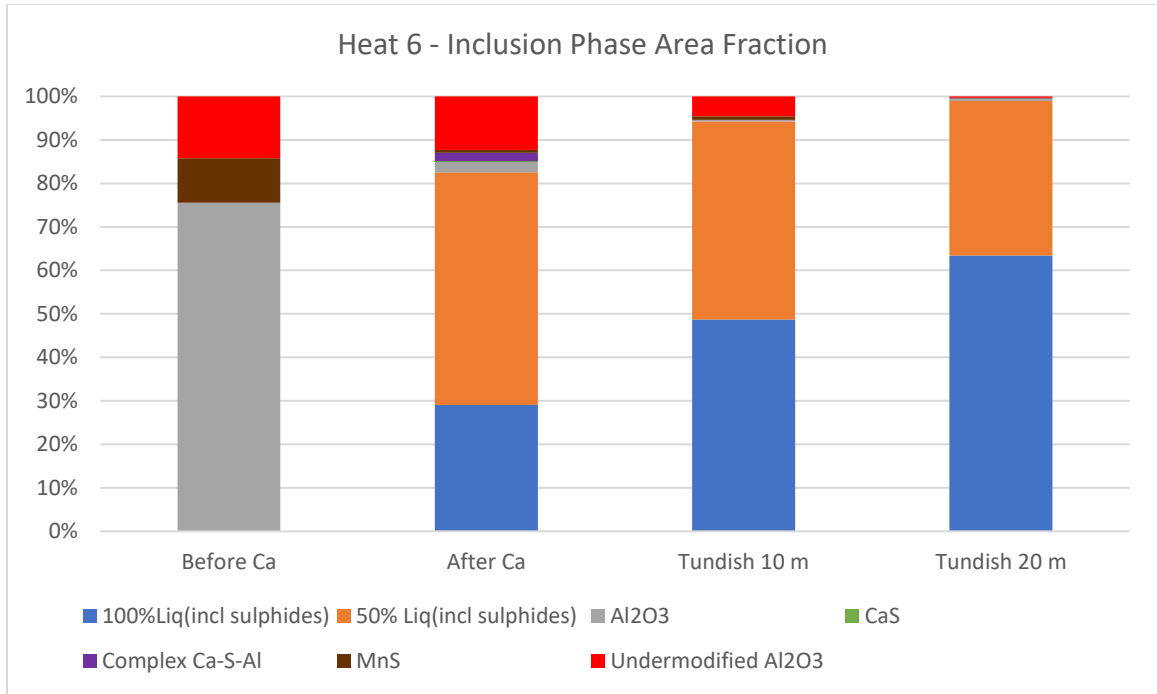


Figure B-5. Area fraction of each inclusion type for all samples in Heat 6.

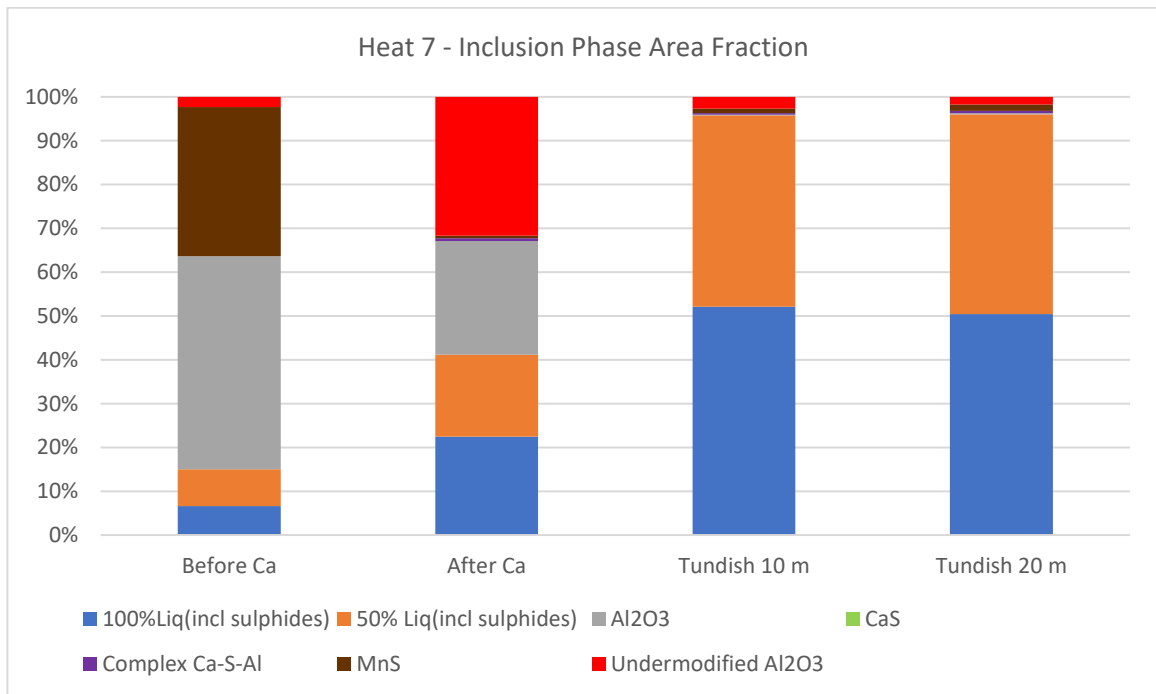


Figure B-6. Area fraction of each inclusion type for all samples in Heat 7.

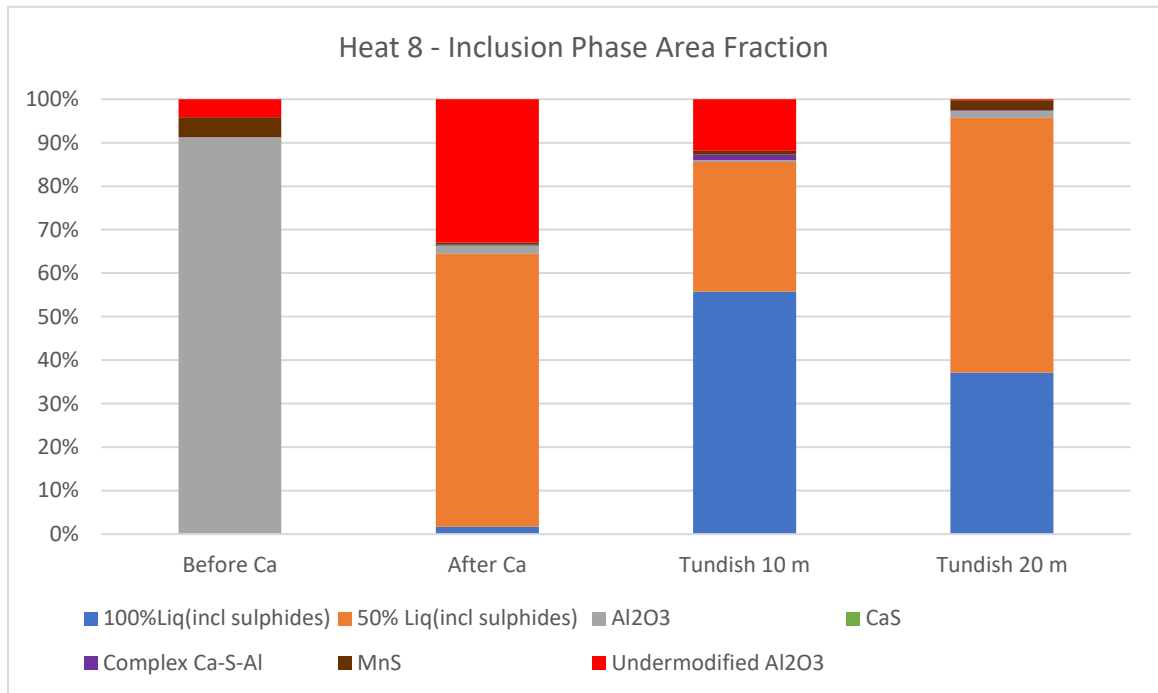


Figure B-7. Area fraction of each inclusion type for all samples in Heat 8.

C. Inclusion Phase Density

The following graphs describe the inclusion phase density for Heats 1 to 8.

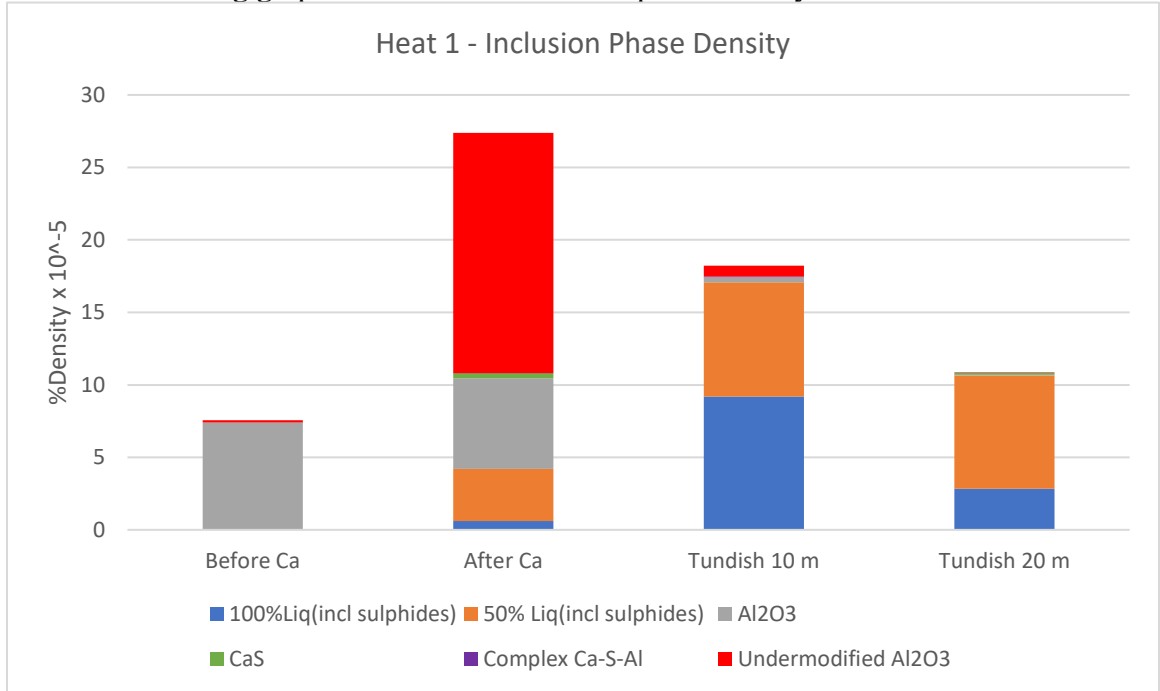


Figure C-1. Density of each inclusion type for all sample in Heat 1.

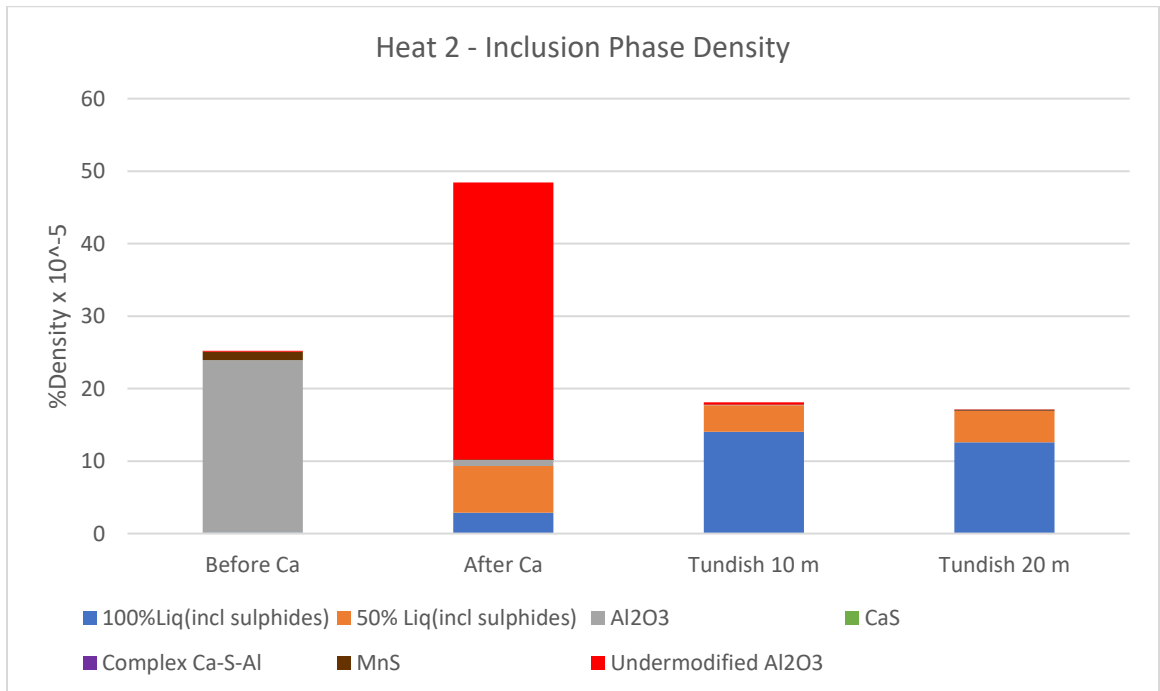


Figure C-2. Density of each inclusion type for all sample in Heat 2.

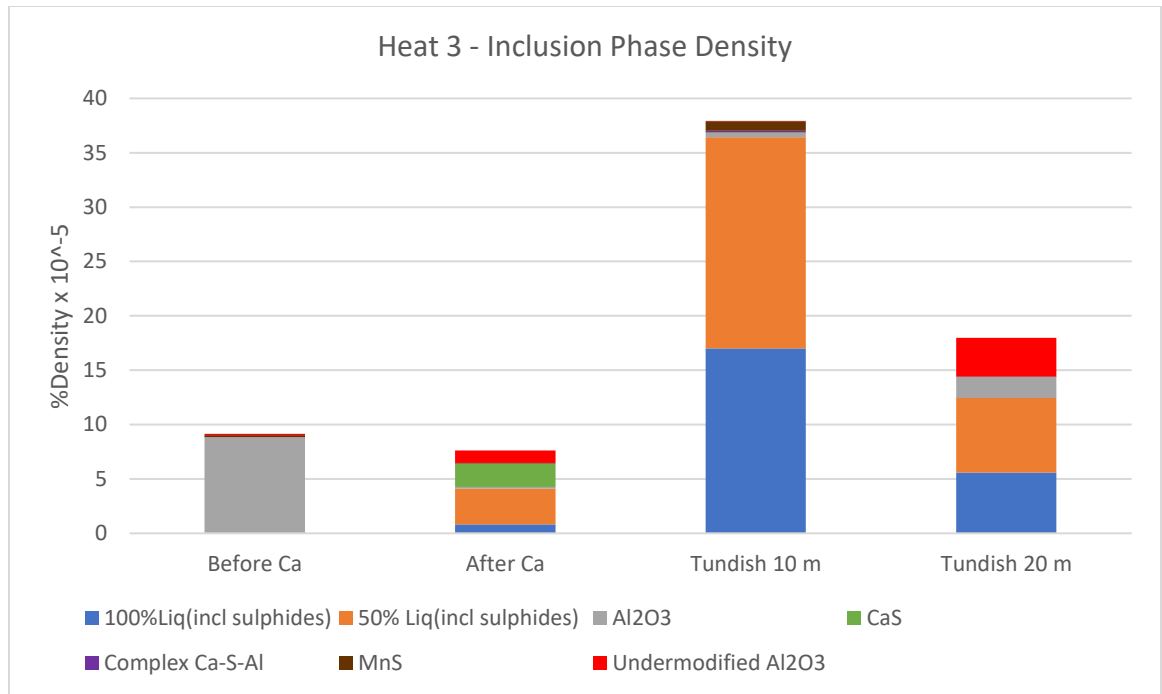


Figure C-3. Density of each inclusion type for all sample in Heat 3.

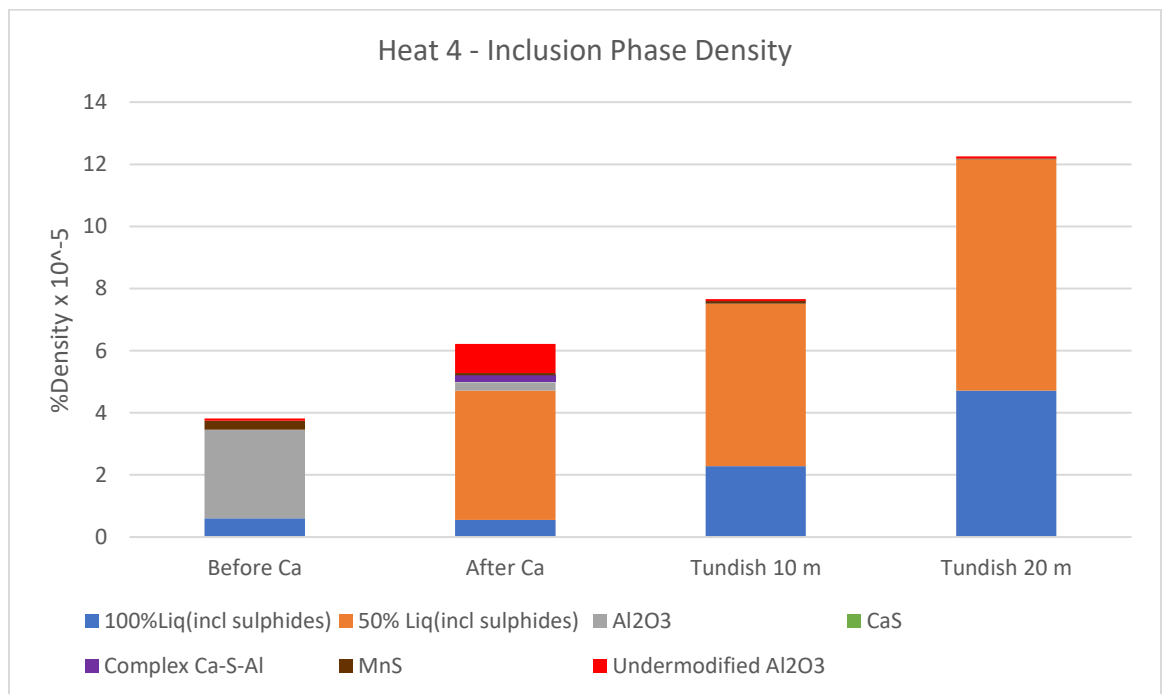


Figure C-4. Density of each inclusion type for all sample in Heat 4.

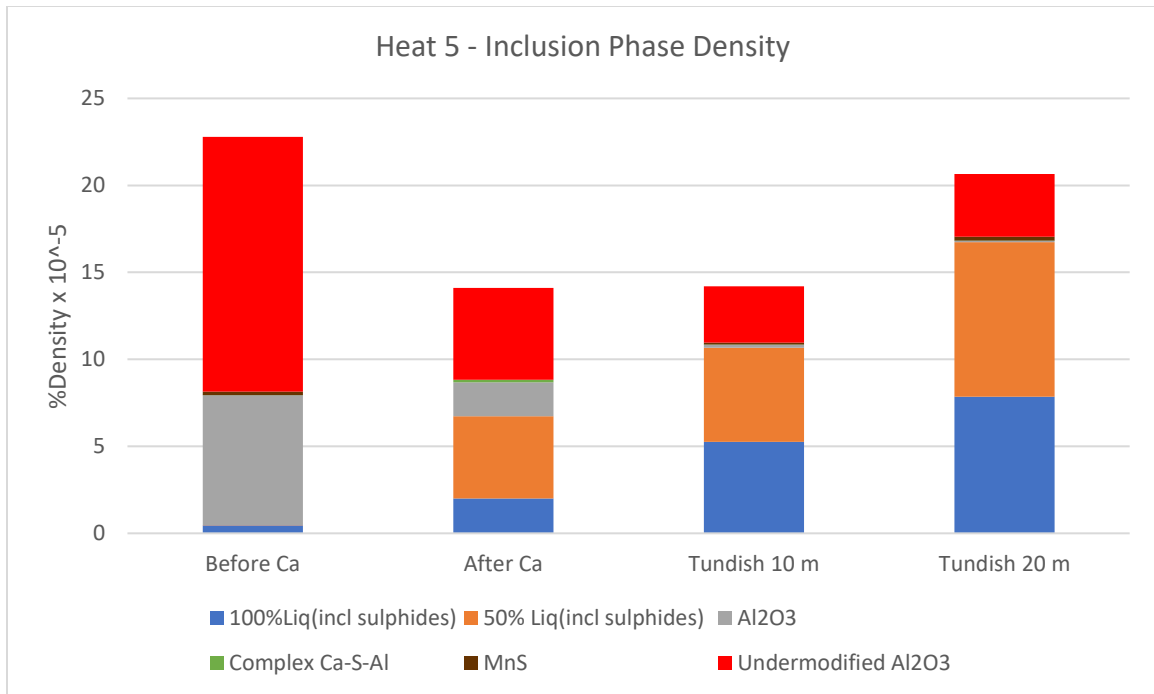


Figure C-5. Density of each inclusion type for all sample in Heat 5.

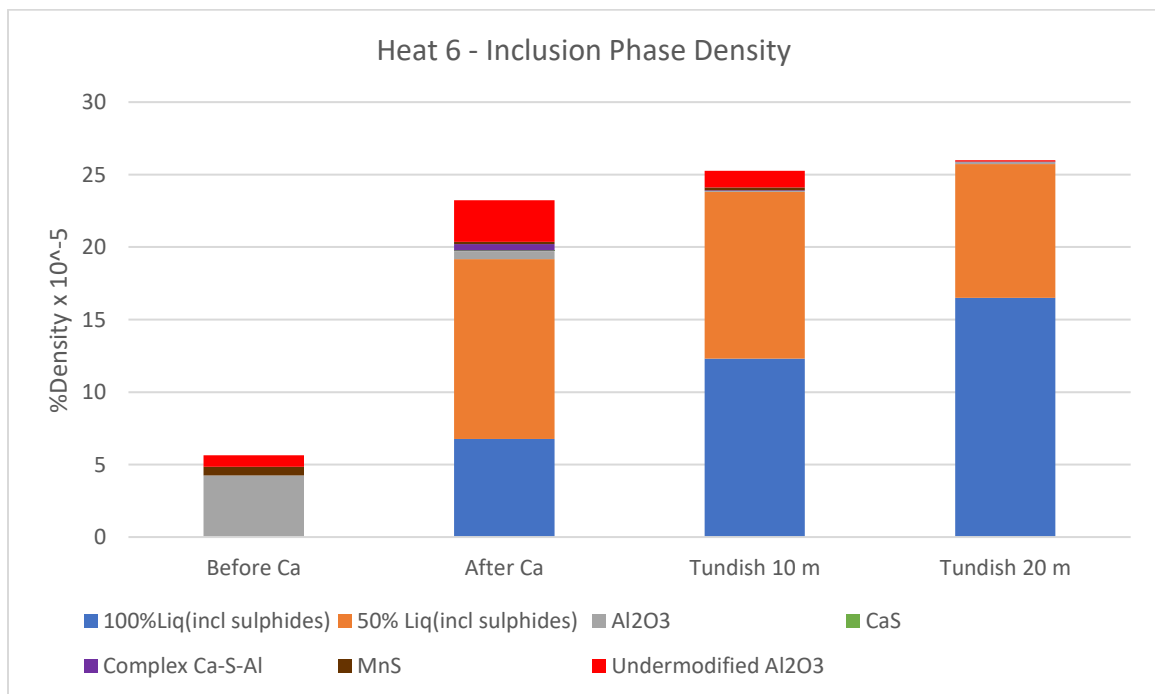


Figure C-6. Density of each inclusion type for all sample in Heat 6.

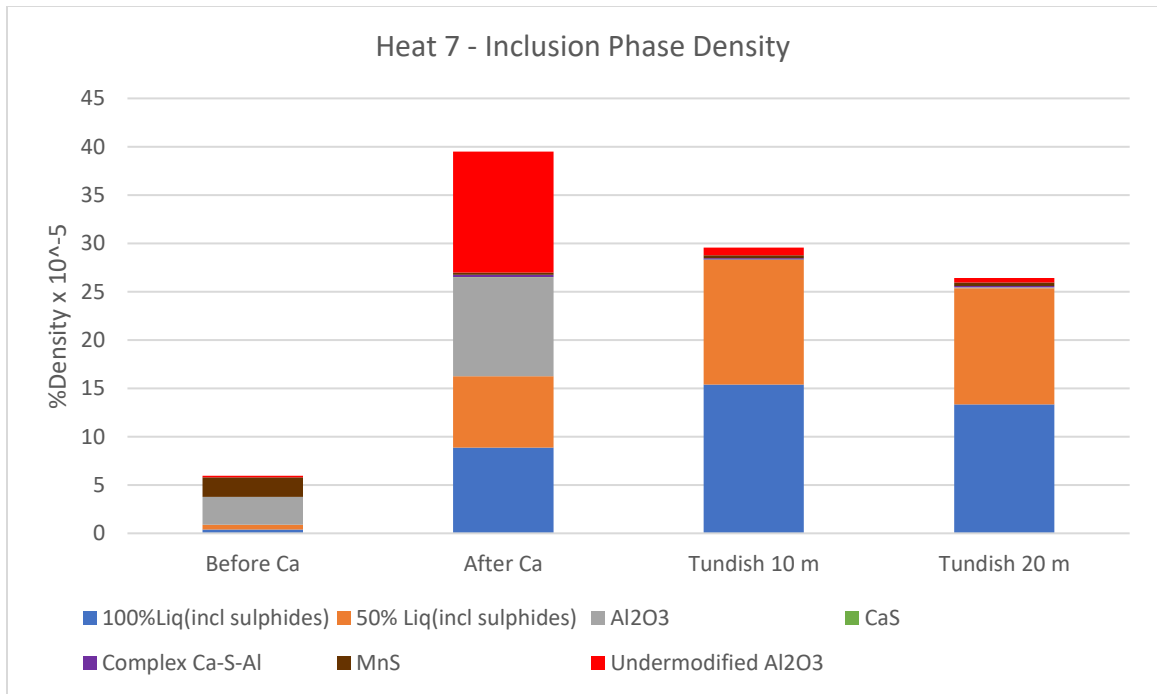


Figure C-7. Density of each inclusion type for all sample in Heat 7.

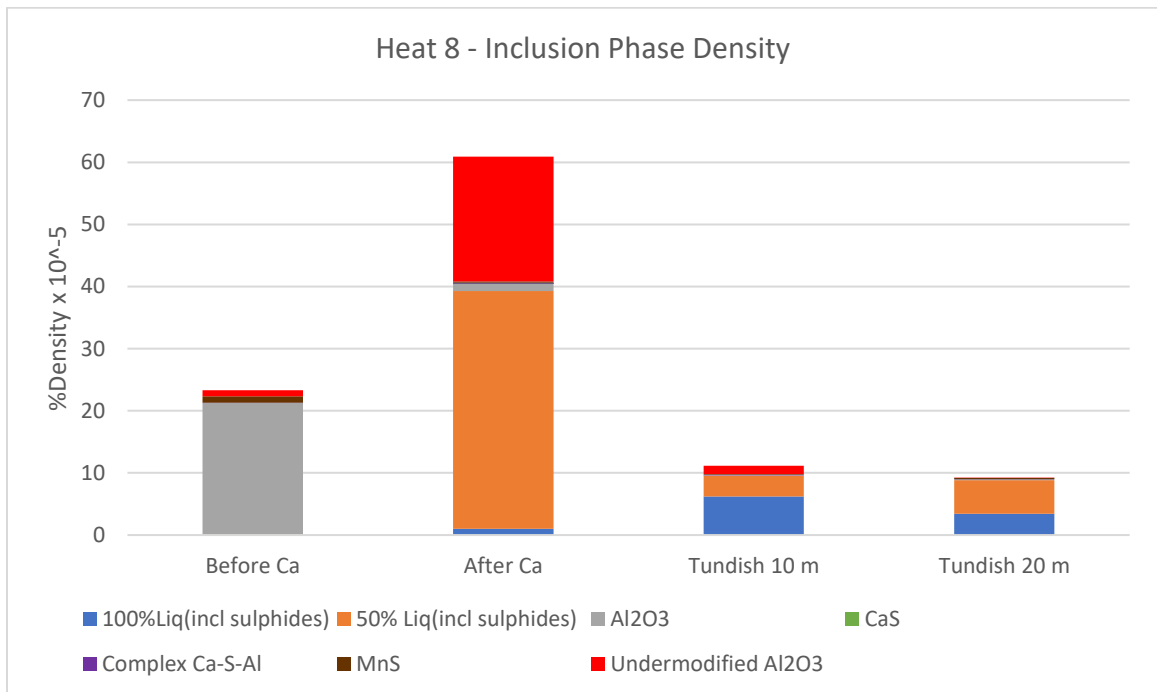


Figure C-8. Density of each inclusion type for all sample in Heat 8.

D. Inclusion Size (ECD) – Equivalent Circular Diameter

The following graphs describe the change in ECD for Heats 4,5,6 and 8.

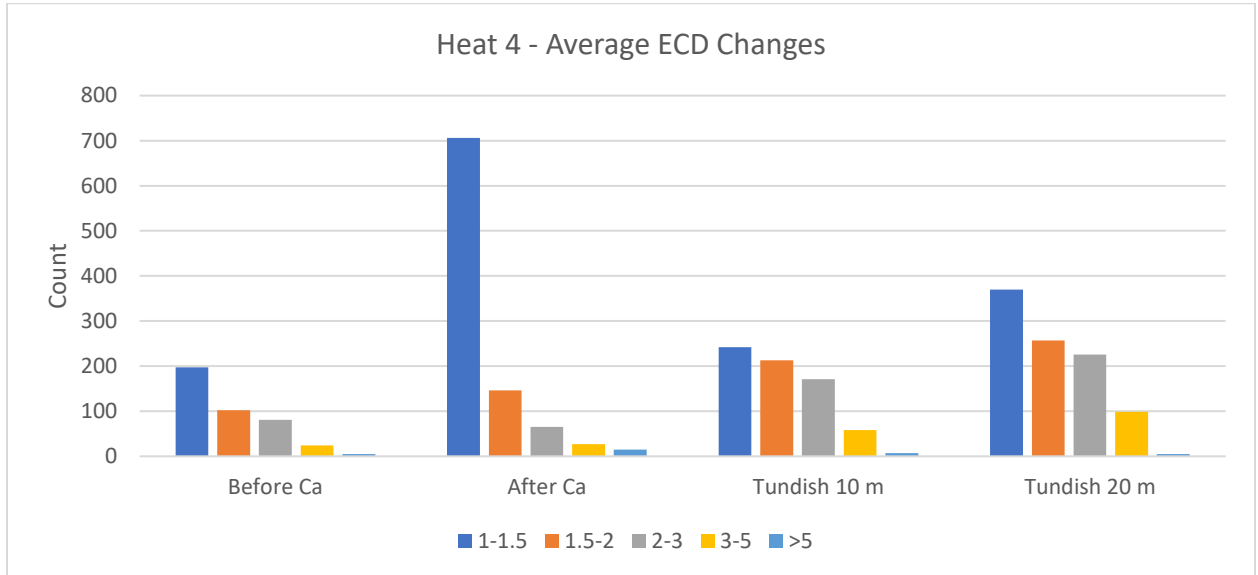


Figure D-1. Change in inclusion diameter for all samples for Heat 4.

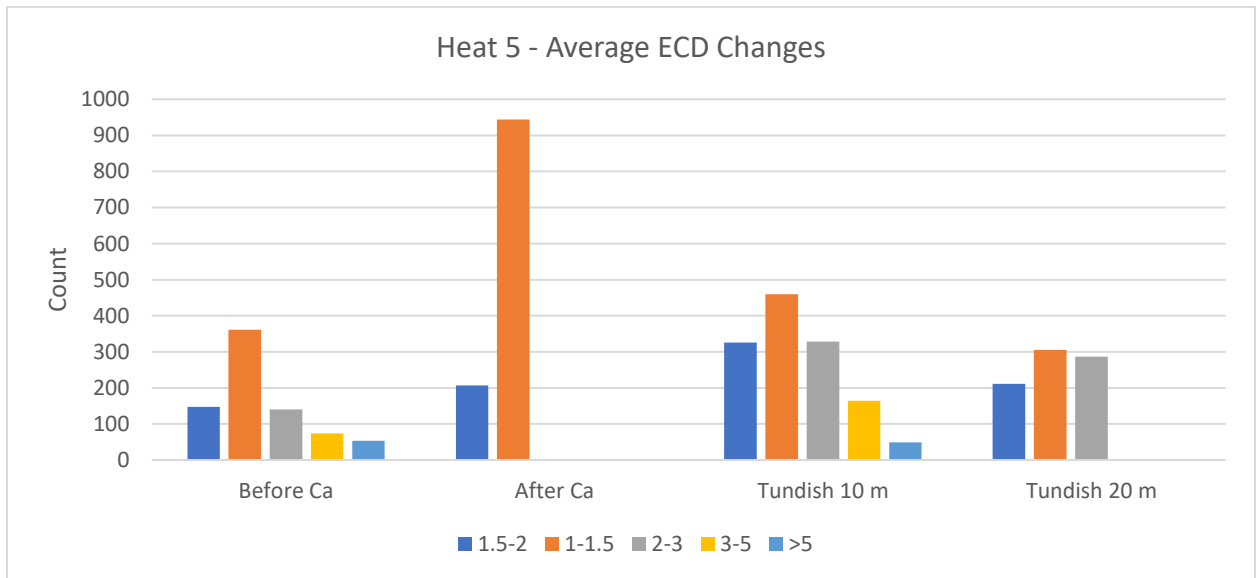


Figure D-2. Change in inclusion diameter for all samples for Heat 5.

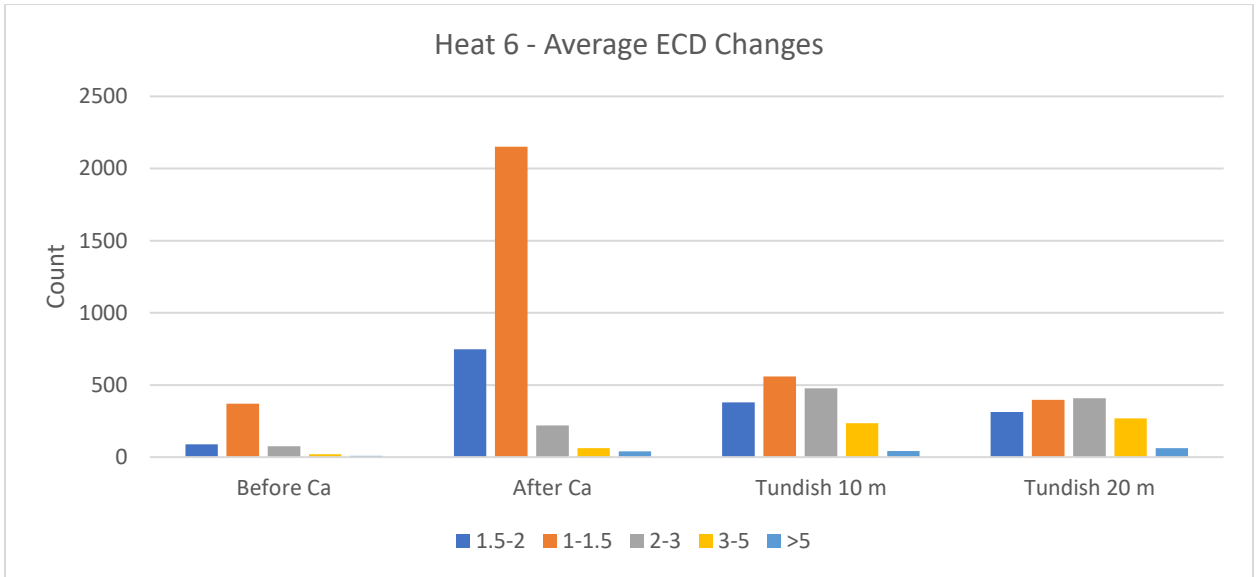


Figure D-3. Change in inclusion diameter for all samples for Heat 6.

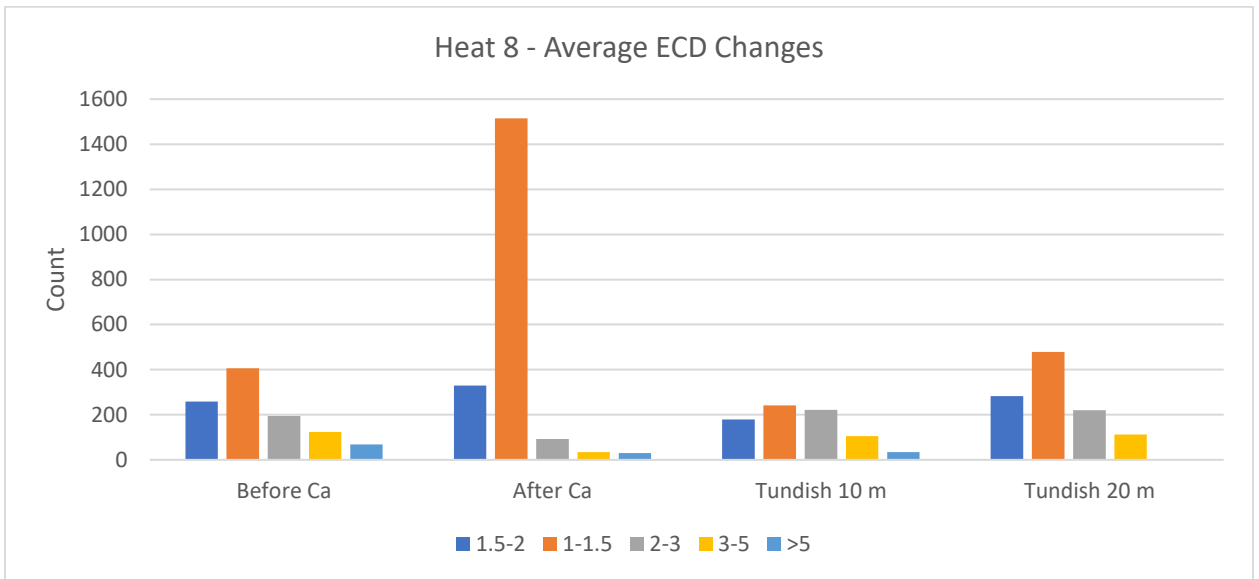


Figure D-4. Change in inclusion diameter for all samples for Heat 8.

E. Tundish 20 m Population, Density and Area Fraction v Rod Position

The following graphs describe the population, density, and area fraction versus the caster rod position for the tundish 20 m sample.

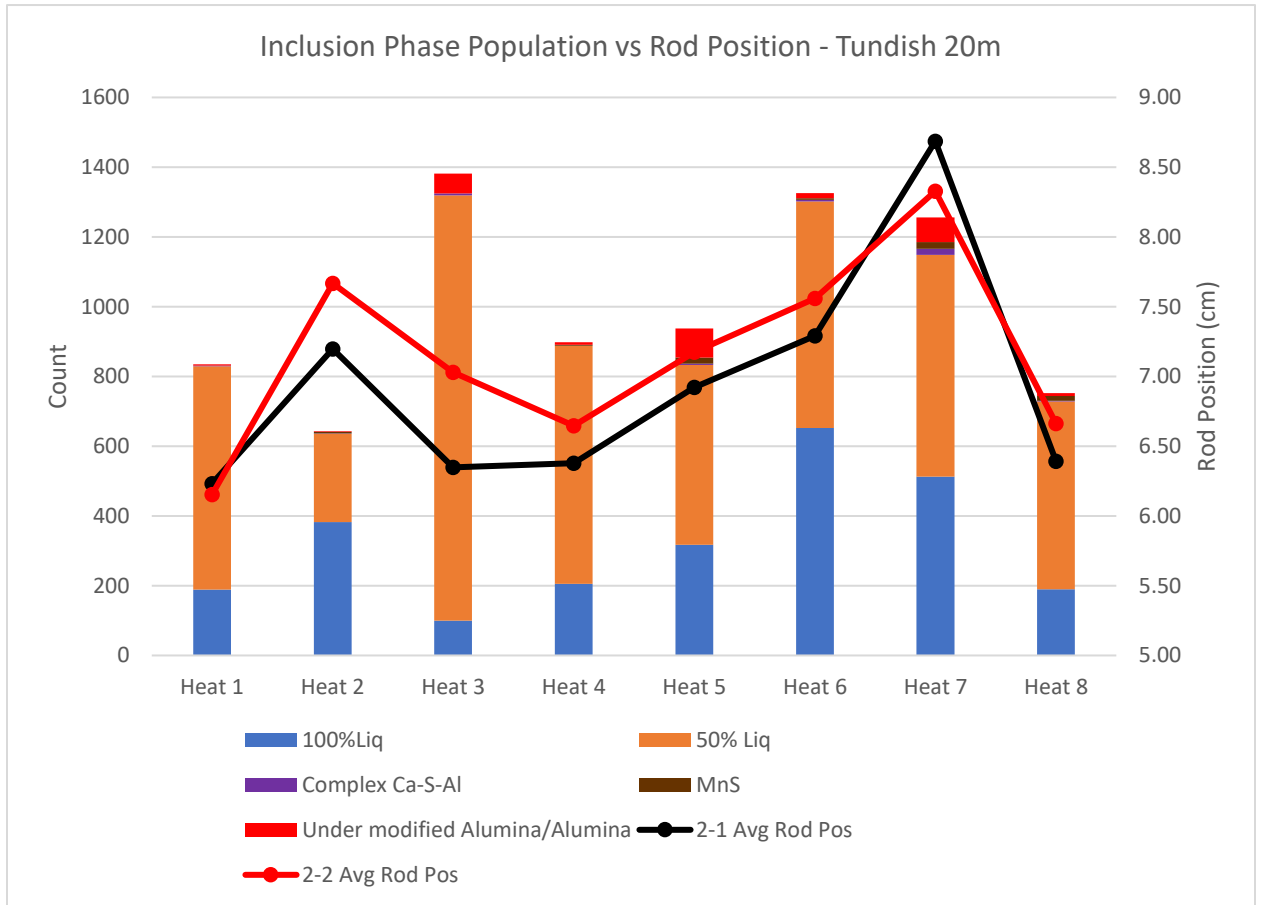


Figure E-1. Inclusion count v caster rod position for Tundish 20 m.

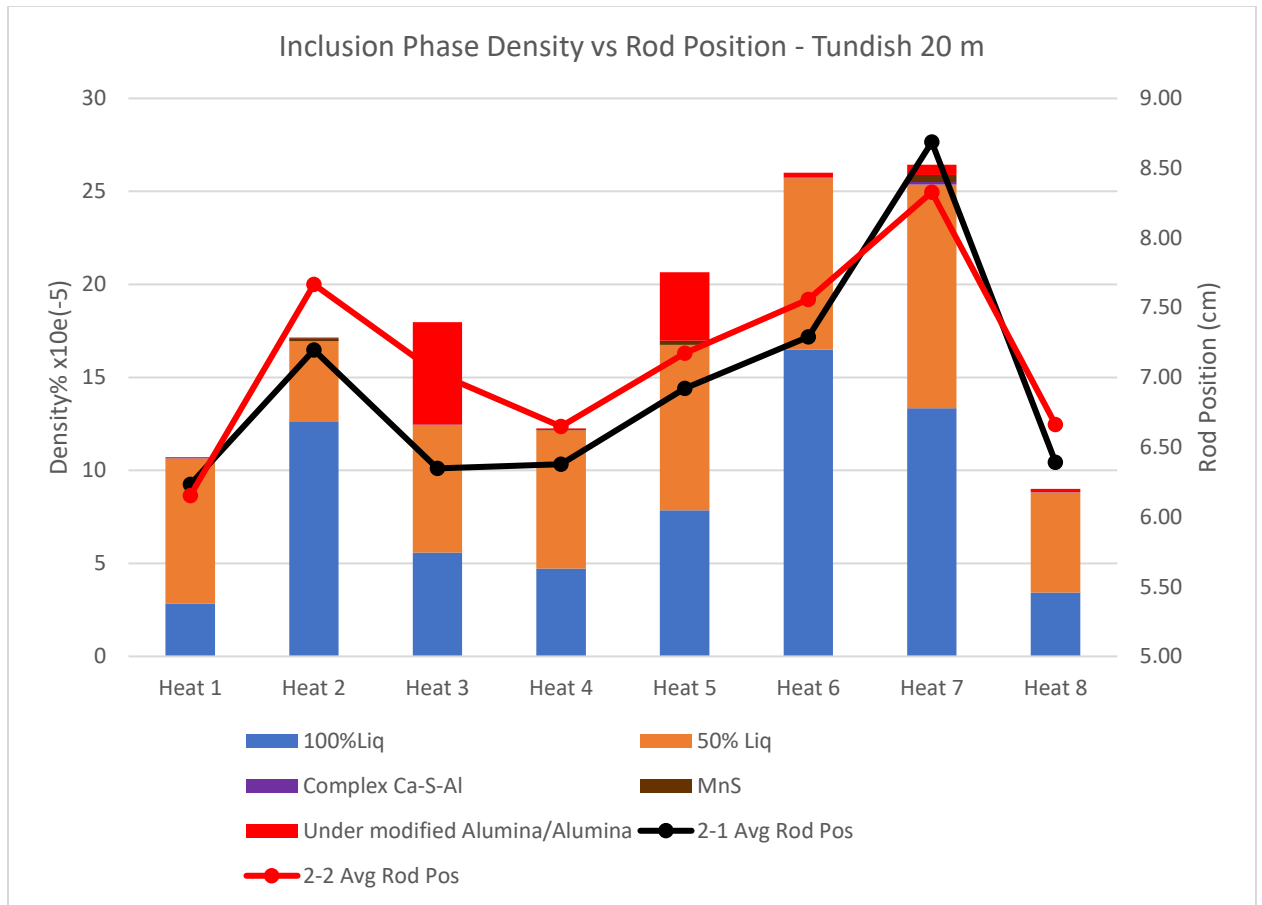


Figure E-2. Inclusion density v caster rod position for Tundish 20 m.

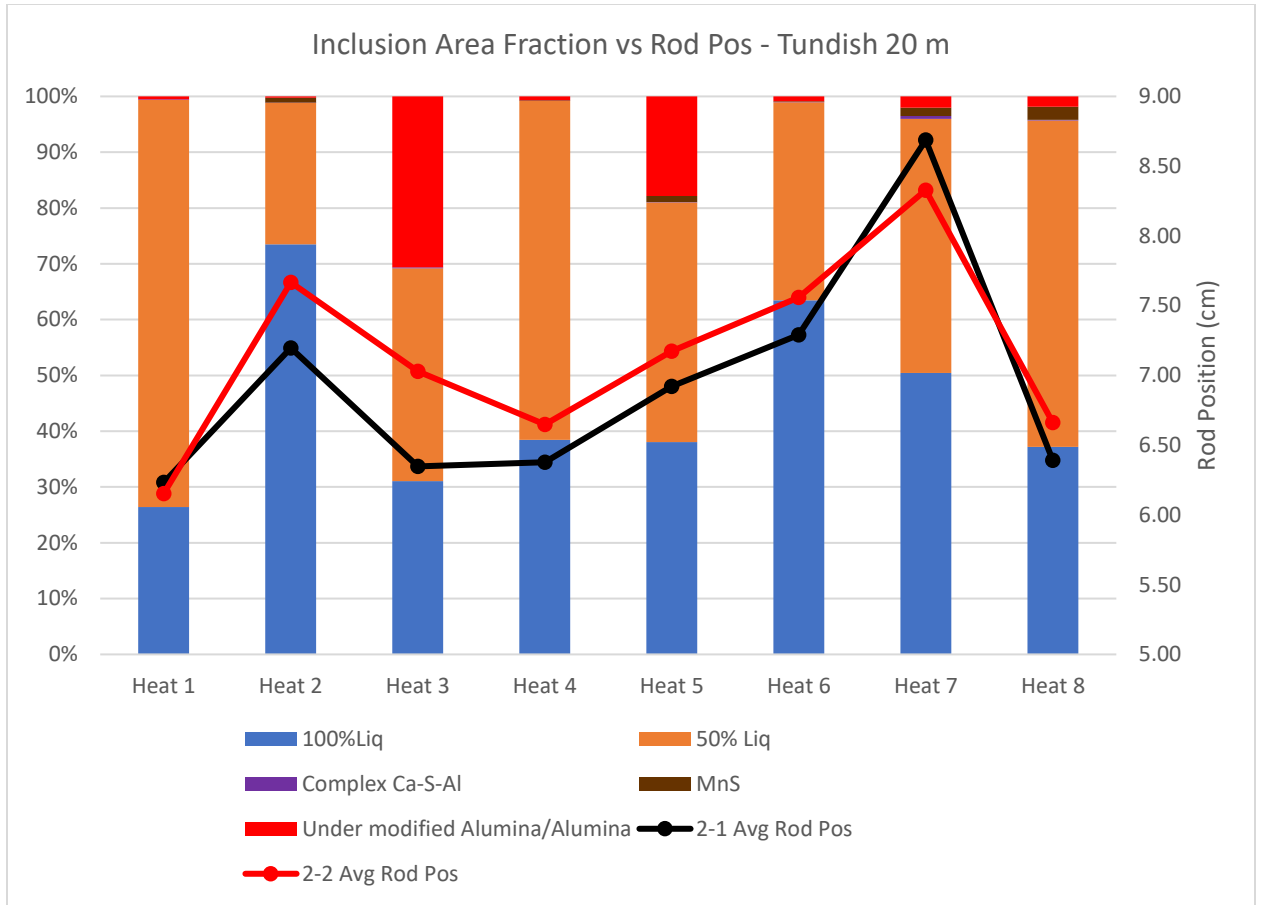


Figure E-3. Inclusion area fraction v caster rod position for Tundish 20 m.

References

- Abdelaziz, S., Megahed, G., El-Mahallawi, I., & Ahmed, H. (2009). Control of Ca addition for improved cleanness of low C, Al killed steel. *Ironmaking & Steelmaking*, 36(6), 432–441. <https://doi.org/10.1179/174328109X401578>
- Abraham, S., Bodnar, R., & Raines, J. (2013). *Inclusion Engineering and the Metallurgy of Calcium Treatment*. 1243–1257.
- Ahlborg, K. (2001). Seven Ways to Shut Down the Caster. *Steelmaking Conference Proceedings*, 84, 861–869.
- Ahlborg, K., Bieniosek, T. H., & Tucci, J. H. (1993). Slag Making Practices at the LTV Steel-Cleveland Works. *76th Steelmaking Conference Proceedings*, 469–473.
- Ahlborg, K., Cleveland, I., Avenue, E., Fruehan, R. J., Potter, M. S., Group, R. L., & Road, H. (2003). Inclusions in Aluminum-Killed Steel with Varying Calcium Additions. *Conference Proceedings*, 18.
- Baochen, H., Rong, Z., Yiqiang, Z., Runzao, L., Wenhe, W., Qiang, L., & Guangsheng, W. (2018). Research on Selective Oxidation of Carbon and Aluminum with Introduction of CO₂ in RH Refining of Low-Carbon Steel Process. *Metallurgical and Materials Transactions B*, 49, 3544–3551.
- Behrens, H., & Webster, J. (2018). *Sulfur in Magmas and Melts: Its Importance for Natural and Technical Processes*.
- Bell, C., Cathcart, C., Barbera, R., Vokes, R., & Spoelstra, J. (2021). *Interview with BOSCO Operations* [Discussion].

- Braun, T. B., Elliott, J. F., & Flemings, M. C. (1979). The clustering of alumina inclusions. *Metallurgical Transactions B*, 10(2), 171–184.
<https://doi.org/10.1007/BF02652461>
- Cathcart, C. (2018). *Clean Steel Assessment*. AISTech 2018.
- Chakraborty, S., & Hill, W. (1994). Reduction of Aluminum Slivers at Great Lakes No.2 CC. *77th Steelmaking Conference Proceedings*, 77, 389–395.
- Choudhary, S. K., & Ghosh, A. (2008). Thermodynamic Evaluation of Formation of Oxide–Sulfide Duplex Inclusions in Steel. *ISIJ International*, 48(11), 1552–1559.
- Costa e Silva, A. (2006). Thermodynamic aspects of inclusion engineering in steels. *Rare Metals*, 25(5), 412–419. [https://doi.org/10.1016/S1001-0521\(06\)60077-6](https://doi.org/10.1016/S1001-0521(06)60077-6)
- Costa e Silva, A. L. V. da. (2018). Non-metallic inclusions in steels – origin and control. *Journal of Materials Research and Technology*, 7(3), 283–299.
<https://doi.org/10.1016/j.jmrt.2018.04.003>
- Cramb, A. W. (1998). High Purity, Low Residual and Clean Steels. *Brimacombe Continuous Casting Course Notes*, 1, 16–42.
- da Rocha, V. C., Pereira, J. A. M., Yoshioka, A., Bielefeldt, W. V., & Vilela, A. C. F. (2017). Evaluation of Secondary Steelmaking Slags and Their Relation with Steel Cleanliness. *Metallurgical and Materials Transactions B*, 48(3), 1423–1432.
<https://doi.org/10.1007/s11663-017-0935-7>
- Dekkers, R., Blanpain, B., & Wollants, P. (2003a). Crystal growth in liquid steel during secondary metallurgy. *Metallurgical and Materials Transactions B*, 34, 161–171.
- Dekkers, R., Blanpain, B., & Wollants, P. (2003b). *Steel Cleanliness at Sidmar*. 197–209.

- Dekkers, R., Blanpain, B., Wollants, P., & Haers, F. (2002). Non-Metallic Inclusion in Aluminium Killed Steels. *Ironmaking & Steelmaking*, 29 (6), 437–444.
- Emi, T. (1994). Theoretical and Process Study on Steelmaking and Steel refining. *8th China Steelmaking Conference Proceedings*, 8–10.
- Gaskell, D. R. (2008). *Introduction to the Thermodynamics of Materials* (5th ed., Vol. 1). CRC Press.
- Geldenhuis, J. M. A., & Pistorius, P. (2000). Minimisation of calcium additions to low carbon steel grades. *Ironmaking & Steelmaking*, 27, 442–449.
<https://doi.org/10.1179/030192300677769>
- Goldstein, J. I., Newbury, D. E., Michael, J. R., Ritchie, N. W. M., Scott, J. H. J., & Joy, D. C. (2018). *Scanning Electron Microscopy and X-Ray Microanalysis*. Springer New York. <https://doi.org/10.1007/978-1-4939-6676-9>
- Gu, K. (2020). *Discussion On SEM Parameters (internal)* [Personal communication].
- Gu, K. (2020). *Inclusion Analysis on the Effects of Reheating* [Unpublished report for internal use only].
- Guo, Y., He, S., Chen, G., & Wang, Q. (2016). Thermodynamics of Complex Sulfide Inclusion Formation in Ca-Treated Al-Killed Structural Steel. *Metallurgical and Materials Transactions B*, 47(4), 2549–2557. <https://doi.org/10.1007/s11663-016-0685-y>
- Guozhu, Y., Jonsson, P., & Lund, T. (1996). Thermodynamics and Kinetics of the Modification of Al₂O₃ Inclusions. *ISIJ International*, 36, S105–S108.

- Herman, I. (1996). Optical Emission Spectroscopy. *Optical Diagnostics for Thin Film Processing*.
- Higuchi, Y., Numata, S., Fukagawa, S., & Shinme, K. (1996). Inclusion Modification by Calcium Treatment. *ISIJ International*, 36, S151–S154.
- Hille, K. F., Papay, N., Genma, N., & Miller, M. L. (1991). Slag Control Techniques for high quality steel. *74th Steelmaking Conference Proceedings*, 74, 419–422.
- Hiroyasu, I., Mitsutaka, H., & Shrio, B.-Y. (1997). Assessment of Al Deoxidation Equilibrium in Liquid Iron. *Tetsu-to-Hagane*83, 83, 773–778.
- Ji, Y., Liu, C., Lu, Y., Yu, H., Huang, F., & Wang, X. (2018). Effects of FeO and CaO/Al₂O₃ Ratio in Slag on the Cleanliness of Al-Killed Steel. *Metallurgical and Materials Transactions B*, 49(6), 3127–3136. <https://doi.org/10.1007/s11663-018-1397-2>
- Kang, Y., Sahebkar, B., Scheller, P. R., Morita, K., & Sichen, D. (2011). Observation on Physical Growth of Non-metallic Inclusion in Liquid Steel During Ladle Treatment. *Metallurgical and Materials Transactions B*, 42(3), 522–534. <https://doi.org/10.1007/s11663-011-9497-2>
- Karoly, G., Ghazally, S., Tardy, P., Harcsik, B., & Jozsa, R. (2012). *Decreasing the nozzle clogging tendency in low-silicon Alkilled mild steels at ISD Dunaferr Co.* 8 th International Conference on Clean Steel, Budapest, Hungary.
- Kaushik, P., & Yin, H. (2012). *Thermodynamics, engineering and characterization of inclusions in advanced high strength steels.* 8 th International Conference on Clean Steel, Hungary.

- Kiessling, R. (1968). *Non-metallic inclusions in steels*. The Iron and Steel Institute.
- Kohatsu, I., & Brindley, G. W. (1968). *Zeitschrift fuut Physikalische Chemie Neue Folge*, 60, 79–89.
- Kor, G. J. (1990). *Proceedings of Elliott Symposium*. 400–417.
- Kor, G. J., & Glaws. (1998). *Fundamentals of Iron and Steelmaking* (11th ed.).
- Kumar, B., Mishra, S., Rao, M. B. V., & Roy, G. G. (2019). Experimental investigation of recovery and efficiency of calcium addition through cored wire in steel melt at Visakhapatnam Steel Plant. *Ironmaking & Steelmaking*, 46(5), 454–462.
<https://doi.org/10.1080/03019233.2017.1405147>
- Lindon, P. H., & Billington, J. C. (1969). Oxide Formation and Separation During Deoxidation of Molten Iron with Mn-Si-Al Alloys. *Transactions of the Metallurgical Society of AIME*, 245, 1775–1784.
- Liu, Y., Zhang, L., Zhang, Y., Duan, H., Ren, Y., & Yang, W. (2018). Effect of Sulfur in Steel on Transient Evolution of Inclusions During Calcium Treatment. *Metallurgical and Materials Transactions B*, 49(2), 610–626.
<https://doi.org/10.1007/s11663-018-1179-x>
- Lu, D., & Irons, G. A. (1994). *Ironmaking & Steelmaking*, 21, 362–371.
- Lu, D., Irons, G. A., & Lu, W. K. (1988). Proc. First Int. Calcium Treatment Symp. *The Institute of Metals*, 23–30.
- Lu, D., Irons, G. A., & Lu, W. K. (1991). Calculation of CaS and MnS activities and their application to calcium treatment of steel. *Ironmaking & Steelmaking*, 18(5), 342–346.

- Luo, Y., Zhang, J., Liu, Z., & Xiao, C. (2011). In situ observation and thermodynamic calculation of MnS in 49MnVS3 non-quenched and tempered steel. *Acta Metallurgica Sinica*, 24, 326–334.
- Melyashkevich, I. (2021). *Distribution Study for Aztech Feature* [Unpublished report for internal use only].
- Mu, W., Dogan, N., & Coley, K. S. (2017). Agglomeration of Non-metallic Inclusions at Steel/Ar Interface: In-Situ Observation Experiments and Model Validation. *Metallurgical and Materials Transactions B*, 48(5), 2379–2388.
<https://doi.org/10.1007/s11663-017-1027-4>
- Oltmann, H. G., Pretorius, E. B., & Schart, B. T. (2015). Analytical Techniques to Assess Cleanliness in Ca Treated Steel. *Clean Steel 9*. Proceedings of the 9th International Conference on Clean Steel, Budapest.
- Park, J. H., Lee, S.-B., & Kim, D. S. (2005). Inclusion control of ferritic stainless steel by aluminum deoxidation and calcium treatment. *Metallurgical and Materials Transactions B*, 36(1), 67–73. <https://doi.org/10.1007/s11663-005-0007-2>
- Pretorius, E. B., Oltmann, H. G., & Schart, B. T. (2015). *An Overview of Steel Cleanliness From an Industry Perspective*. 34.
- Ren, Y., Zhang, L., & Li, S. (2014). Transient Evolution of Inclusions during Calcium Modification in Linepipe Steels. *ISIJ International*, 54(12), 2772–2779.
<https://doi.org/10.2355/isijinternational.54.2772>
- Ruby-Meyer, F., & Willay, G. (1997). Rapid Identification of Inclusions in Steel by OES-CDI Technique. *La Revue de Métallurgie-CIT*, 367–378.

- Sanders, W. (2017). *What is Optical Emission Spectroscopy?* [https://hha.hitachi-hightech.com/en/blogs-events/blogs/2017/10/25/optical-emission-spectroscopy-\(oes\)/](https://hha.hitachi-hightech.com/en/blogs-events/blogs/2017/10/25/optical-emission-spectroscopy-(oes)/)
- Schober, M. (2013). The Story of the Linz-Donawitz process. *Voestalpine*.
<https://www.voestalpine.com/group/static/sites/group/.downloads/en/press/2012-broschuere-the-linz-donawitz-process.pdf>
- Smith, S. M., Fruehan, R. J., Casuccio, G. S., Potter, M. S., Lersch, T. L., & Group, R. J. L. (2004). *Application of Rapid Inclusion Identification and Analysis*. 10.
- SMS Siemag Standards Office. (2011). Classification of Defects in Materials: Standard Charts and Sample Guide. *SMS GmbH*.
- Story, S., & Asfahani, R. (2013). *Control of Ca-Containing Inclusion in Al-Killed Steel Grades*. 86–99. <http://digital.library.aist.org/download/PR-TN1013-1.15851.pdf>
- Story, S., Piccone, T., Fruehan, R. J., & Potter, M. (2003). *Inclusion Analysis to Predict Casting Behavior*. AISTech.
- Tabatabaei, Y., Coley, K. S., Irons, G. A., & Sun, S. (2018a). A Multilayer Model for Alumina Inclusion Transformation by Calcium in the Ladle Furnace. *Metallurgical and Materials Transactions B*, 49(1), 375–387.
<https://doi.org/10.1007/s11663-017-1120-8>
- Tabatabaei, Y., Coley, K. S., Irons, G. A., & Sun, S. (2018b). Model of Inclusion Evolution During Calcium Treatment in the Ladle Furnace. *Metallurgical and Materials Transactions B*, 49(4), 2022–2037. <https://doi.org/10.1007/s11663-018-1266-z>

- Tapia, V. H., Morales, R. D., Camacho, J., & Lugo, G. (1996). The influence of the tundish powder on steel cleanliness and nozzle clogging. *79th Steelmaking Conference Proceedings*, 79, 539–547.
- Tiekink, W., Santillana, B., Boom, R., & Kooter, R. (2008). Calcium: Toy, tool or trouble? *Iron and Steel Technology*, 5 (9), 184–195.
- Torga, G., Gonzalez Atchabahaian, D., & Scoccia, J. (2011). Development and application of a quantitative tool to assess casting behavior. *AISTech Conference Proceedings*, 7.
- Tsai, H. T., Sammon, W. J., & Hazelton, D. E. (1990). *Characterization and Countermeasures for Sliver Defects in Cold Rolled Products*. 73, 49–59.
- Turkdogan, E. T. (1984). Recent Developments in the Physical Chemistry of Steelmaking. *Perspectives in Metallurgical Development*, 49–60.
- Turkdogan, E. T. (1996). *Fundamentals of Steelmaking*. The Institute of Materials.
- Turner, P. (2016). *EAF CELOX Measurements and Application Considerations*.
- Turpin, M. L., & Elliott, J. F. (1966). Nucleation of Oxide inclusions in Iron melts. *IRON STEEL INST J*, 204(3), 217–225.
- Valdez, M., Shannon, G., & Sridhar, S. (2006). The Ability of Slags to Absorb Solid Oxide Inclusions. *ISIJ International*, 46(3), 450–457.
- Van Ende, M.-A., Guo, M., Dekkers, R., Burty, M., Van Dyck, J., Jones, P., Blanpain, B., & Wollants, P. (2009). Formation and Evolution of Al–Ti Oxide Inclusions during Secondary Steel Refining. *ISIJ International*, 1133–1140.

- Verma, N., Lind, M., Pistorius, P., & Fruehan, R. (2010). *Iron and Steel Technology*, 7(7), 189–197.
- Verma, N., Pistorius, P. C., Fruehan, R. J., Potter, M., Lind, M., & Story, S. (2011a). Transient Inclusion Evolution During Modification of Alumina Inclusions by Calcium in Liquid Steel: Part I. Background, Experimental Techniques and Analysis Methods. *Metallurgical and Materials Transactions B*, 42(4), 711–719. <https://doi.org/10.1007/s11663-011-9516-3>
- Verma, N., Pistorius, P. C., Fruehan, R. J., Potter, M., Lind, M., & Story, S. R. (2011b). Transient Inclusion Evolution During Modification of Alumina Inclusions by Calcium in Liquid Steel: Part II. Results and Discussion. *Metallurgical and Materials Transactions B*, 42(4), 720–729. <https://doi.org/10.1007/s11663-011-9517-2>
- Verma, N., Pistorius, P., Fruehan, R., Potter, M., Oltmann, H., & Pretorius, E. (2012). Calcium Modification of Spinel Inclusions in Aluminum-Killed Steel: Reaction Steps. *Metallurgical and Materials Transactions B*, 43. <https://doi.org/10.1007/s11663-012-9660-4>
- Walock, M. (2012). *Nanocomposite coatings based on quaternary metalnitrogen* [PhD]. Arts et Métiers ParisTech.
- Wang, R., Bao, Y., Li, Y., Li, T., & Chen, D. (2017). Effect of slag composition on steel cleanliness in interstitial-free steel. *Journal of Iron and Steel Research International*, 24(6), 579–585. [https://doi.org/10.1016/S1006-706X\(17\)30088-2](https://doi.org/10.1016/S1006-706X(17)30088-2)

- Wang, X., Li, Q., Huang, F., Yang, J., & Kang, X. (2012). *Control of B type non-metallic inclusions in linepipe steel plates*. 8 th International Conference on Clean Steel, Budapest.
- Wang, Y., Sridhar, S., & Valdez, M. (2002). Formation of CaS on Al₂O₃-CaO inclusions during solidification of steels. *Metallurgical and Materials Transactions B*, 33(4), 625–632. <https://doi.org/10.1007/s11663-002-0042-1>
- Wasai, K., & Kusuhira, M. (1999). Thermodynamics of nucleation and supersaturation for the aluminum-deoxidation reaction in liquid iron. *Metallurgical and Materials Transactions B*, 30 (6), 1065–1074.
- Wasai, K., & Mukai, K. (2002a). Observation of inclusion in aluminum deoxidized iron. *ISIJ International*, 42.5, 459–466.
- Wasai, K., & Mukai, K. (2002b). Thermodynamic Analysis on Metastable Alumina Formation in Aluminum Deoxidized Iron Based on Ostwald's Step Rule and Classical Homogeneous Nucleation Theories. *ISIJ International*, 42(5), 467–473.
- Wilson, A. D. (1984). Applications, Microstructure, and Properties of Low Sulfur Plate Steels. *Proceedings of the Low-Sulfur Steel Symposium*, 27–39.
- World Steel in Figures 2021*. (2021). <https://worldsteel.org/wp-content/uploads/2021-World-Steel-in-Figures.pdf>
- Wu, L. (2011). [PhD]. Royal Institute of Technology.
- Xiao, G., Dong, H., Wang, Q., & Hui, W. (2011). Effect of sulfur content and sulfide shape on fracture ductility in case hardening steel. *Journal of Iron and Steel Research International*, 18, 58–64.

- Xu, Jianfei, Huang, F., & Wang, X. (2016). Formation Mechanism of CaS-Al₂O₃ Inclusions in Low Sulfur Al-Killed Steel After Calcium Treatment. *Metallurgical and Materials Transactions B*, 47, 1217–1227.
- Yang, W., Duan, H., Zhang, L., & Ren, Y. (2013). Nucleation, Growth, and Aggregation of Alumina Inclusions in Steel. *JOM*, 65(9), 1173–1180.
<https://doi.org/10.1007/s11837-013-0687-z>
- Yang, W., Zhang, L., Wang, X., Ren, Y., Liu, X., & Shan, Q. (2013). Characteristics of Inclusions in Low Carbon Al-Killed Steel during Ladle Furnace Refining and Calcium Treatment. *ISIJ International*, 53(8), 1401–1410.
<https://doi.org/10.2355/isijinternational.53.1401>
- Zeynep Yildirim, I., & Prezzi, M. (2011). *Chemical, Mineralogical, and Morphological Properties of Steel Slag*.
- Zhang, L. (2002). *Evaluation and Control of Steel Cleanliness* □ review. 85th Steelmaking Conference Proceedings.
- Zhang, L., & Cai, K. (2001). Experimental and Theoretical Study on the Cleanliness of Steel. *84 Steelmaking Conference Proceedings*, 84, 275–291.
- Zhang, L., & Thomas, B. G. (2003). State of the Art in Evaluation and Control of Steel Cleanliness. *ISIJ International*, 43(3), 271–291.
<https://doi.org/10.2355/isijinternational.43.271>
- Zhang, T., Liu, C., Mu, H., Li, Y., & Jiang, M. (2018). Inclusion evolution after calcium addition in Ti-bearing Al-kill steel. *Ironmaking & Steelmaking*, 45(2), 187–193.
<https://doi.org/10.1080/03019233.2016.1251749>

Zheng, S., & Zhu, M. (2016). Modelling Effect of Circulation Flow Rate on Inclusion Removal in RH Degasser. *Journal of Iron and Steel Research International*, 23(12), 1243–1248. [https://doi.org/10.1016/S1006-706X\(16\)30183-2](https://doi.org/10.1016/S1006-706X(16)30183-2)